Stellingen

behorende bij het proefschrift
Man–Machine Aspects of Remotely Controlled Space Manipulators,
Jan Frans Tonnis Bos

1. In tegenstelling tot het "Crossover Model" voorspelt het "Optimal Control Model" niet of een systeem onbestuurbaar is voor de mens. (Dit proefschrift, hoofdstuk 2)

2. Behalve voor het verbeteren van de drie–dimensionale perceptie zijn referentielijnen ook nuttig om onjuiste informatie van hoeksensoren te detecteren. (Dit proefschrift, hoofdstuk 9)

3. In het geval van het uitvoeren van de insert–taak in de End–Effector control mode dient het point–of–resolution variabel te zijn: Indien het point–of–resolution halverwege de tip van de End–Effector en de opening van het gat wordt gekozen behoeven er alleen orientatiecommando's te worden gegeven om uit een jamming situatie te geraken. (Dit proefschrift, hoofdstuk 2)

4. In de End–Effector control mode dient de opgelegde maximum snelheid van de End–Effector onafhankelijk te zijn van de richting. (Dit proefschrift, hoofdstuk 7)

5. In het informatica-onderwijs dient niet alleen aandacht te worden geschonken aan het leren ontwikkelen van software. Juist het leren *documenteren* van de ontwikkelde software verdient meer aandacht.

6. Ervaringen van een jeugdcommissielid bij een tennisclub wijzen uit dat de voornaamste functie van het hek om een tennisbaan is om de tennissende kinderen tegen de ouders te beschermen.

7. De britse houding ten aanzien van de europese eenwording kan misschien wel het beste gekarakteriseerd worden door het feit dat het vasteland Europa wordt genoemd.

8. Men dient bij voorkeur bij een andere groep te promoveren dan waar men zijn universitaire graad heeft behaald. Daardoor behouden zowel de promovendus als de promotor een frisse kijk op het onderzoek.

9. Goed onderzoek beantwoordt ten minste één vraag, maar levert tevens vele nieuwe vragen op.

10. De hogere werkdruk in de gezondheidszorg heeft tot gevolg dat de verpleegkundige op de hulpvraag van de patient al weglopende zegt dat hij eraan komt.

11. Gezien het feit dat de spelregel uit het zaalvoetbal die lichamelijk contact verbiedt niet ook in het veldvoetbal ingevoerd wordt, mag men zich afvragen of de FIFA wel echt de spelverruwing wil aanpakken.

Man–Machine Aspects
of
Remotely Controlled
Space Manipulators

Man–Machine Aspects
of
Remotely Controlled
Space Manipulators

PROEFSCHRIFT

ter verkrijging van de graad van doctor
aan de Technische Universiteit Delft,
op gezag van de Rector Magnificus, prof. drs. P.A. Schenck,
in het openbaar te verdedigen ten overstaan van
een commissie aangewezen door het College van Dekanen
op dinsdag 17 december 1991 te 16.00 uur

door

Jan Frans Tonnis Bos,

geboren te Groningen,
doctorandus in de Wiskunde.

Dit proefschrift is goedgekeurd door de promotor

prof.dr.ir. H.G. Stassen,

en de toegevoegd promotor

dr.ir. A. van Lunteren.

Preface

Contents

iv

Notation

COP	: center of projection
DOF	: degrees-of-freedom
EE	: End–Effector
ESA	: European Space Agency
EVA	: extravehicular activities
FOV	: field of view
HERA	: Hermes Robot Arm
HO	: human operator
HSFP	: HERA Simulation Facility Pilot
KBB	: knowledge based bahaviour
MIMO	: multi–input–multi–output
MMI	: man–machine interface
MTFF	: Man Tended Free Flyer
OCM	: Optimal Control Model
OCDM	: Optimal Controller Decision Model
ORU	: Orbit Replaceble Unit
POR	: point of resolution
RBB	: rule based behaviour
ROV	: remotely operated vehicles
SBB	: skill based behaviour
SISO	: single–input–single–output
2D	: two–dimensional
3D	: three–dimensional
f	: perspectivity parameter
D	: inertia matrix
dX	: incremental cartesian position change
Δ	: differential transformation matrix
θ_i	: angle joint i
$\dot{\theta}_i$	: angular velocity joint i
$\ddot{\theta}_i$	: angular acceleration joint i
$\dot{X}_s$	: End–Effector velocity setpoints
A_i	: transformation matrix between link i-1 and link i
a_n	: normal distance between link n-1 and link n

α_n : twist angle between link n–1 and link n
P_{stop} : stopping distance
T : torque vector
T_i : $A_1 \cdots A_i$
T_6^s : required (new) T_6 matrix
T_{stop} : stopping time
T_{pred} : prediction time horizon
T_{min} : minimal prediction time horizon

Chapter 1

Introduction

1.1 Background

In the near future an increase in space activities is foreseen, for instance the construction and use of a space station. A space station will be used for research activities and the production of very high quality materials. These products cannot be manufactured on Earth, because the specifications cannot be met due to the influence of gravity. For the construction of a space station, and for the supply of materials, transport facilities are necessary. The American Space Shuttle project [Covault, 1981a, 1981b] has shown that the concept of a spacecraft in combination with a robot arm is sound. The European Space Agency (ESA) has ordered the construction of a spacecraft (Hermes) and of the Hermes Robot Arm (HERA), see Fig. 1.1.

Our research concerns the design of a Man–Machine Interface (MMI) for a space manipulator. The design criteria concern the safe and efficient use of the manipulator.
Space manipulators are quite different from present days robots acting on Earth. For a manipulator on Earth the mass of a load is mostly very small compared to its own mass, whereas for a space manipulator the mass of a load can exceed its own mass many times. Therefore, the size and construction of a manipulator on Earth is such that it may be considered to be totally stiff, whereas a space manipulator will be flexible. Furthermore, a robot on Earth is designed for high speed and strongly repetitive tasks, whereas the speed of a space manipulator will be very limited and the tasks are less repetitive.
To obtain realistic characteristics of a space manipulator in this study, the specifications of HERA are used.

The total length of HERA (Fig. 1.2) will be about 11 meter, it will consist of seven joints, two links and two End–Effectors. There is an End–Effector at each end of the manipulator, so that each end can be used as base or as manipulating device. In this way the manipulator is able to "walk" to another working area. During operation one joint of the End–Effector which is used as base, will be fixed. The total mass is about 230 kg, depending on the tools

1
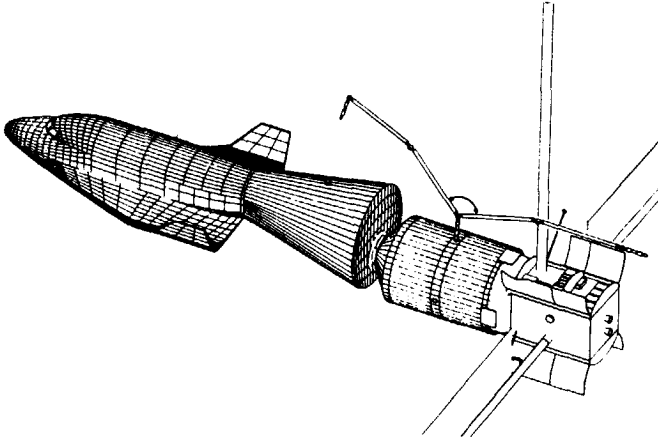
Figure 1.1: *Hermes, HERA and the Man-Tended-Free-Flyer (by courtesy of Fokker Space and Systems).*
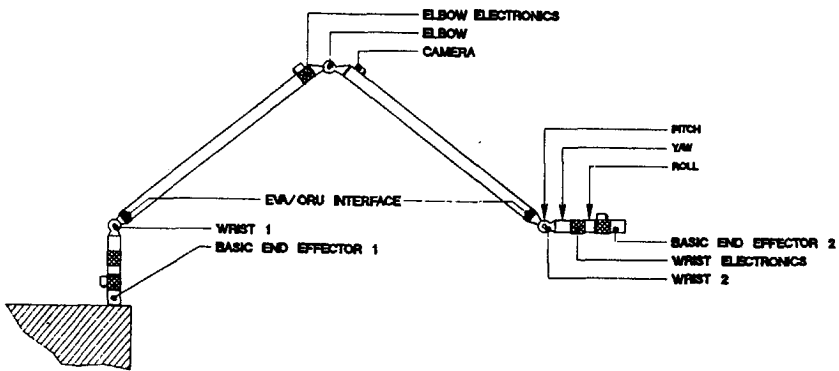
Figure 1.2: *HERA (by courtesy of Fokker Space and Systems).*

attached to the basic End–Effector. HERA will be used for the following tasks : Inspection, for instance of Hermes and the space station; the transfer of Orbital Replaceble Units (ORU's) with supplies or products; support of the astronaut in Extra Vehicular Activities (EVA's). For a more detailed description of HERA the reader is referred to [Hamann, Bentall, 1989; Andre, Schoonejans, 1989; Schoonejans et.al., 1990].

Two scenarios are foreseen to control the manipulator in space. Firstly one in which the operator is located in space, near the worksite. For Hermes this means that the human operator will be located in the cockpit. Secondly, one in which the human operator is located on Earth. A motivation for the second scenario is reduction of costs. Placing a human being in a space vehicle demands extra facilities for life support, such as a pressurized cockpit and the necessary safety devices. Moreover, placing the human operator on Earth eliminates the risk of life. However, it yields additional control problems.

Normally, the manipulator will be controlled under supervisory control. The task of the human operator is then planning, monitoring and fault management. However, a requirement is that under all circumstances the human operator must be able to control HERA manually. The human operator then acts as an on-line controller. Disturbances may occur in the controlled system, or more generally, the operator must be able to execute the task also in unforeseen situations. For instance, these situations may occur when the task has to be executed in an unknown or unmodelled environment. In addition, particular tasks can be such that manual control is preferred. For instance, the inspection of a spacecraft is a typical task for which the control of the manipulator cannot be foreseen in advance.

The manual control situation is shown in Fig. 1.3. In this control loop the task, the human operator, the system to be controlled, and the disturbances are given features. The only existing tool to optimize the closed loop performance is the design of the MMI. For both the manual and the supervisory control situation one must have certain knowledge of the items mentioned in order to design an effective MMI. Therefore, the tasks, the system, the human operator, and the disturbances will be briefly discussed from a human operator
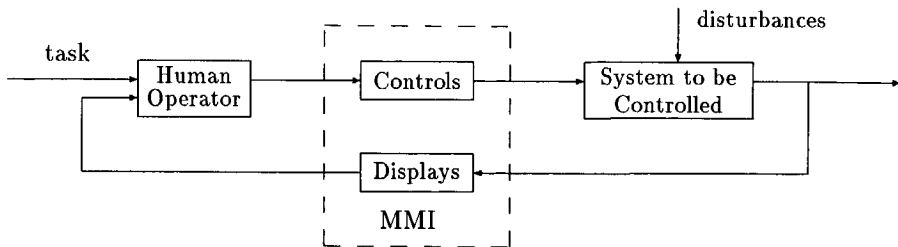
Figure 1.3: *Manual control situation.*

3

point of view.

Tasks

The tasks to be executed with a space manipulator demand a very high reliability. One wrong movement can cause the loss of a large amount of money. For HERA the tasks are broken down into a number of *elementary functions* [Andre, Schoonejans, 1989; de Waard, 1987] such as move, approach, grapple, insert, and retract. For each of these elementary functions the MMI has to be designed in a right way.

System

Velocities are limited, because for collision avoidance it must be possible to stop the manipulator, using brakes, within a reasonably short distance (0.1 meter for HERA). The joint angles are controlled by means of brushless DC-motors. A current limiter is built in to prevent overheating, thus limiting joint angle torques. Another reason for limiting joint torques is that Hermes is not a fixed object, but a vehicle floating in space. When the manipulator is being used, the position control of Hermes must still be able to realize the desired position, orientation and velocity of Hermes. These limitations will cause that the manipulator may be a rather *slowly responding* system. The time to stop the manipulator, by setting rate setpoints to zero, depends among other things on the motor (control) characteristics and the configuration of the manipulator. For HERA this stopping time may lie between 1 and 20 seconds.

Masses have to be moved at considerable distances of the rotation axes. This causes moments of inertia which, when transformed to the motor shaft, are still considerable compared to the internal inertia of the motor. Because the distances vary with the configuration of the manipulator, we have state-dependent dynamics. Moreover, because of the limitations in the joint torques and the effects due to coriolis and centripetal forces, a space manipulator has *non-linear dynamics* [Paul, 1981].

Each kilogram mass to be brought into space costs considerably. So, the manipulator will be constructed as light as possible, compromising with the desirable stiffness of the manipulator. Because of the long and lightly constructed links and the gearboxes in the joints, the manipulator will be *flexible*.

When the operator is located on Earth, *time-delays* are introduced in the control loop, caused by the transmission of signals from Earth to Hermes and vice versa. Using one or more data-relay satellites, the minimum time-delay will be about 1 second [Sheppard, 1986]. The effect of queueing and transmission errors is the introduction of an unpredictable and undesirable variation in the time-delay. It was estimated that the time-delays can vary between 1 and 3 seconds.

When the human operator is located in the cockpit of Hermes or on Earth, he cannot see

4

the manipulator and its environment directly, i.e. in three dimensions. The operator has to cope with two-dimensional TV-pictures. Even, when the operator is located in the cockpit of Hermes *direct vision is impossible*, since the cockpit will be so small, that the human operator will be located at the co–pilot's place.

To execute a task, 6 joints of the manipulator have to be controlled. Depending on the task allocation between man and computer, the human operator has to control up to *6 degrees–of–freedom.*

Disturbances

A control scheme is designed for a given model of the system. Unmodelled dynamics can cause unexpected movements of the manipulator, which the human operator may experience as disturbances. For instance flexibility effects can cause oscillations of the End–Effector. When looking through the End- Effector camera, the operator can experience these oscillations as disturbances.

Human operator

The knowledge we have of the control behaviour of a human operator, can often be represented by a model. There exist verbal, psychological and control models. Some of them are qualitative, others quantitative. Which kind of model is used depends strongly on the point of view of the user.

1.2   Problem definition

Normally the manipulator will be controlled under supervisory control. However, the operator must be able to execute the task also in unforeseen situations which, for instance, may occur due to disturbances in the controlled system. In addition, particular tasks can be such that manual control is preferred. Therefore, a requirement is that under all circumstances the human operator must be able to control HERA manually. This research deals with the manual control situation. In the case that a human operator has to control a space manipulator like HERA manually, he is faced with several difficulties :

- No direct vision.

- Non–linear and slow dynamics.

- Up to 6 degrees–of–freedom to be controlled.

- The presence of flexibility effects.

- The possible presence of time–delays.

The limitations of a human operator to cope with these difficulties are emphasized by the demand for a high reliability of the task execution. One wrong movement can cause the loss of the manipulator, ORU, or satellite. These considerations led to the central question of this research project :

> In which circumstances and with what aids can the human operator accomplish
> a required task in a reliable way ?

The design of the MMI (Fig. 1.3) is the tool to let a human operator cope with the difficulties in such a way that he will be able to accomplish a required task in a reliable way. The first and most important design issue is the task allocation between man and computer. On the basis of this task allocation the way in which the operator has to fulfill *his* task has to be determined, i.e. the controls and the information to be displayed have to be specified. The choices which have to be made in the design of a MMI depend on the task to be executed, the dynamics of the system to be controlled and the disturbances acting on the system, and the characteristics of a human operator. These factors were described in Section 1.1. To answer the central question of this research project the man-machine literature is reviewed in order to describe the performed research to let the human operator cope with the stated problems. Then, the knowledge about human control behaviour, reflected in some system theoretical human operator models is reviewed. On the basis of this literature review and some practical reasons a number of research issues was defined. The choices which were made are given in Chapter 3.

1.3   Layout of the thesis

In Chapter 1 the background of the project is described. The problems for a human operator to execute a number of tasks with a space manipulator manually are identified, and the problem definition of the project is given.

In Chapter 2 the man-machine literature is reviewed with respect to teleoperation. Then, some background on human control behaviour, reflected in system theoretical human operator models is given.

In Chapter 3 the research issues which were investigated are selected. These research issues determined the design of the experimental facility. The choices which were made in the design are discussed. Also the choices in the design of the experimental procedure are motivated.

In Chapter 4 a description of the experimental facility is given.

Chapter 5 deals with some visibility aspects for a rough positioning task.

Chapter 6 describes the research on task allocations between man and computer for an insert task.

The research towards the use of a predictive display is treated in two Chapters. In Chapter 7 the experimental evaluation is described of the use of two kinds of display: A display of the stopping configuration and a display of a predicted trajectory.
Chapter 8 deals with a study towards the question of what the optimal length of the prediction (time) horizon is when a predicted trajectory is displayed.

In Chapter 9 the results obtained are discussed.

Finally, Chapter 10 summarizes the results by a number of conclusions.

Chapter 2

State of the art

2.1 State of the art in teleoperation

2.1.1 Introduction

Teleoperation is the extension of a person's sensing and manipulation capability to a remote location [Sheridan, 1989]. A teleoperator consists of artificial sensors, arms and hands, sometimes a vehicle for carrying these, and communication channels to and from the human operator. Teleoperation is, among others, applied in situations, where it is not wise to let the human operator act at the workspace himself. The workspace can be hazardous, like in the nuclear industry (radiation), undersea and in space (temperature and lack of oxygen). In undersea applications the teleoperators, or the Remotely Operated Vehicles (ROV's) are used by the offshore oil and gas industry for instance for the monitoring of pipelines [Vadus, 1976; Wernli, 1982; van de Vegte, et.al., 1989]. The workspace can also be too small, such as in micro–surgery. For instance one form of teleoperator is the endoscope. Such a device has proven to be very successful for inspection, biopsy and simple surgery [Sheridan, 1989]. Other applications of teleoperation can be found in terrestrial mining, construction and maintenance, military operation (deactivation of mines) and in aids for the handicapped [Leifer, 1983].

A very important question, when designing a man-machine interface, is what the optimal task allocation between man and computer is for a particular situation. The possible task allocations form a continuum from very direct manual control to high-level supervisory control. Given the present technology, the most important question is how the robot and the human operator can best cooperate.
There is also the important question on what information should be displayed to the human operator. A human being can see, hear, feel and smell, so the display modalities can be visual, audible and kinaesthetic. The ideal of sensing sufficient information about the teleoperator and task environment, and communicating this to the human operator in a sufficiently natural way, so that the operator feels physically present at the remote side, is defined by Sheridan [1989] as *telepresence*.

In the next section the control aspects in teleoperation will be treated and in section 2.1.3 the display aspects. In section 2.1.4 the use of simulators is discussed.

2.1.2 Control aspects

The most important issue in the design of a MMI is the task allocation between man and machine, i.e. computer.

To execute a task, 6 joints of the manipulator have to be controlled. The operator can control the separate joints directly, in the so called *single-joint mode*. The task, however, is mostly defined in cartesian coordinates. In order to realize a movement of the End–Effector in a given direction in the cartesian coordinate frame, the human operator has to translate this desired movement to setpoints for the separate joints. For this translation he has to calculate the so called inverse kinematics which is a set of non-linear functions. Moreover, these non–linear functions consist of a coupled set of trigonometric equations. Therefore, the single-joint mode will only be used as a backup control mode for HERA, and it will be used to unfold the manipulator. The last task is defined in joint coordinates.

In the *End–Effector control mode* the inverse kinematics are determined implicitly, as when using a master-slave configuration [Ferrell, 1966], or explicitly by a computer. When using a computer the master does not need to be a physical replica of the slave manipulator. The computer calculates the necessary kinematical transformations between the degrees–of–freedom of the master and the degrees–of–freedom of the slave.

End–Effector control has two aspects. The first aspect is the Point-Of-Resolution (POR). It is defined as the origin of a local coordinate frame of which the position and the orientation have to be controlled. The second aspect is the reference frame. This is a coordinate frame which forms the reference base for the control of the POR. In [Pennington, 1983; Stark et.al., 1987] it is illustrated that indeed the operator executes a task more efficiently in the End–Effector control mode than in the single-joint mode.
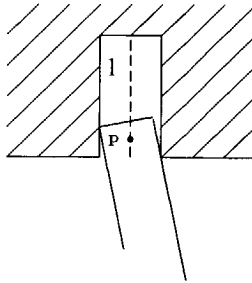
Figure 2.1: *Variable Point–Of–Resolution.*

An issue still to be investigated is the use of a variable POR, when inserting a peg into a hole. When jamming occurs and the tip of the peg functions as POR, both position and orientation commands must be issued to end the jamming situation. When as POR point p (Fig. 2.1) is used, which is located on the line l and in between the tip of the peg and the entrance of the hole, only orientation commands are needed to end the jamming situation.

Sensed force/torque information can be used in (local) control loops in order to make the insert-task easier for the operator. In [Hannaford, Kim, 1989] the sensed forces and torques are transformed into positioning commands which are superimposed on the operator's positioning commands. The stiff robot used gets some properties of a flexible manipulator: the peg "slides" into the hole.

Teleoperation under supervisory control, as in [Starr, 1981], has rarely been investigated until now. In supervisory control the human operator gives high-level commands to the manipulator system. The execution of these commands requires advanced control schemes, a model of the environment, collision avoidance algorithms, command languages, etc.. The task of the operator is the planning, monitoring and fault management. In what manner man and computer can interact best in a planning procedure is still a research issue. The development of command languages for teleoperation, environment modelling techniques and collision avoidance algorithms are in a preliminary phase.

In [Leifer, 1983] an interactive control system for the disabled is described. An interactive real-time control system and a command language have been developed to aid the disabled with a mobile robot in their Activities of Daily Life.

A special problem is the human control of redundant manipulators. Kinematically redundant manipulators have more (joint) DOF than DOF in task-space and, consequently, they have an infinite number of configurations for a given End–Effector position and orientation. Examples are a mobile robot and two cooperating robots. The inverse kinematics problem is equivalent to solving a set of non-linear trigonometric equations, which is underconstrained for a redundant manipulator. To solve the inverse kinematics for redundant manipulators a criterium function is defined to add more constraints. Such a criterium can be based, for instance, on distances of the teleoperator from obstacles in the environment as in [Das et.al., 1989]. There, a positioning task had to be executed with a 12 DOF manipulator/vehicle system. When the subjects had only to control the End–Effector (6 DOF) of the manipulator, a substantial improvement in completion time was achieved. In [Schneider, Cannon, 1989] a supervisory control system is described for two cooperating robots.

For manual control the control input of the system, provided by the human operator, must also be determined. The output of the control device can be transferred into position setpoints, velocity setpoints or acceleration setpoints for the manipulator. Acceleration control is mostly not very suitable, because it requires accurate timing by the operator to stop the

manipulator from moving. The best choice between position and velocity control depends, as the whole MMI design, on the task to be executed and the dynamics of the system to be controlled. For a positioning task in a large working space, as is the case for a space manipulator, position control suffers from poor resolution [Flatau, 1973; Kim et.al., 1987a]. For a fastly responding manipulator with large maximum velocities, position control is advised, whereas for a slowly responding manipulator (Fig. 2.2) or when the maximum velocities are small, velocity control is appropriate.

Numerous kinds of control devices exist. The control devices can be distinguished by the kind of output signals, discrete (on/off) or analogue, force or displacement operated, and the number of DOF. Generally a displacement operated device is favoured over a force operated control device [Lambooy, 1988; Sheppard, 1989]. An often stated advantage of a 6 DOF hand controller over two 3 DOF hand controllers is that the human operator has a free hand for other operations, but it is questionable whether he can do so. A disadvantage of a 6 DOF hand controller is the easy cross-coupling between the axes. Operators mostly prefer two 3 DOF handcontrollers [Sheppard, 1989].

Voice control will be applicable in supervisory control. Restrictions are momentarily the discrete utterance (a pause must be inserted between two words), limited vocabulary, the sensitivity to environmental noise, the impossibility to communicate with the environment, the reliability, and speaker dependent recognition. The last restriction can also be an advantage, because the manipulator will not react to other voices from the environment.
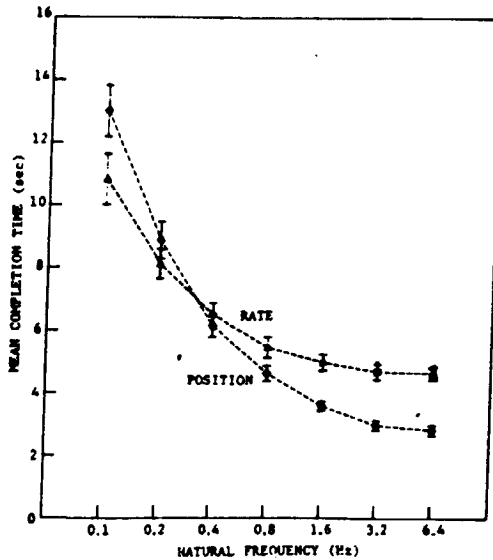
Figure 2.2: *Effects of natural frequency on task completion time for postion and rate control [Kim et.al., 1987a].*

2.1.3   Display aspects

One of the difficult problems for a human operator is the three–dimensional perception of the scene. Human depth perception is based upon a number of depth cues. These cues can be divided into two groups, the psychological cues and the physiological cues. Psychological cues cannot be explained by the physiological structure of the eyes. These cues are for instance linear perspective, texture gradient, intersectioning, and shades and shadows. The physiological cues are accomodation, convergence (Fig. 2.3), binoculair disparity and monoculair movement parallax. Several techniques for providing the operator with a three–dimensional perception are known and evaluated [Strattmann, 1988; Overbeeke, 1988; Klashorst, 1988]. These techniques are based on the depth cues. We will restrict ourselves to the techniques which can be used in space, i.e. we will assume that the camera's will only have pan/tilt capabilities.

One of the techniques is stereovision. With stereovision the operator's performance is mostly superior to the case when only monoscopic displays are used [Kim et.al., 1987b; Pepper et.al, 1983]. In [Drascic et.al., 1989] it is shown that the learning trend for monovision is much more pronounced than that for stereovision. However, there remains a number of problems when applying stereovision. The operator needs a means to separate the two (stereo) pictures, such as viewers or liquid crystal shuttering spectacles [Milgram, van de Horst, 1980] which may cause problems when also other displays have to be observed. A solution might be the integration of these displays in the stereo views. Another problem is that when operators are using stereovision for a longer period, they can get a headache or become sick [Lane, 1982].

Stereosystems are based upon three physiological depth cues: accomodation, convergence (Fig 2.3) and binocular disparity [Klashorst, 1988]. These depth cues do not work anymore when the distance to the observed objects becomes larger than 9 to 10 meter, because the angle of convergence becomes insensitive for offsets in position. One may think of placing the camera's further apart, thus enlarging the angle of convergence [Pepper et.al., 1983]. But to what extent this will influence the human depth perception is still not fully examined.

In teleoperation there exists a certain distance between the camera's and the operator, hence, the pictures have to be transmitted. Problems can occur due to bandwidth limitations. For instance the resolution and the frame rate [Massimino, Sheridan, 1989] of the pictures
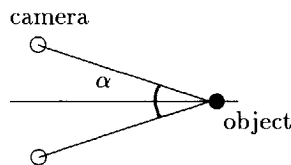
Figure 2.3: *Angle of convergence α.*

influence the operator's performance. So, preferably only essential parameters representing updating and correcting the picture must be communicated to the remote control center [Nguyen et.al., 1988]. Image compression techniques can also be used to reduce the number of data to be transmitted. How to achieve an efficient data reduction is still not fully examined.

Apart from TV-pictures also graphical display techniques can be used for providing the operator with a good 3D-perception. An advantage of graphical displays is that views can be provided from viewpoints where no camera is or can be present. A very useful technique is providing so called reference lines (Fig. 2.4) [Ellis, McGreevy, 1987]. In laboratory experiments the results obtained with monoscopic views with reference lines were as good as the results obtained with stereovision [Kim et.al., 1987b].

The viewpoint is also very important [Kim et.al., 1987b]. In [Das et.al., 1989] a number of criteria is stated on the basis of which a computer can calculate the *best* view. Then three options exist. The best view is determined by the operator himself, by the computer on-line or by the computer on request. Automatically changing the viewpoint is confusing to the viewer of the display because the operator looses the sense of location of the viewpoint. The research of Das [1989] showed that the performance of a well-trained operator is best when he himself has the freedom to select the viewpoint.
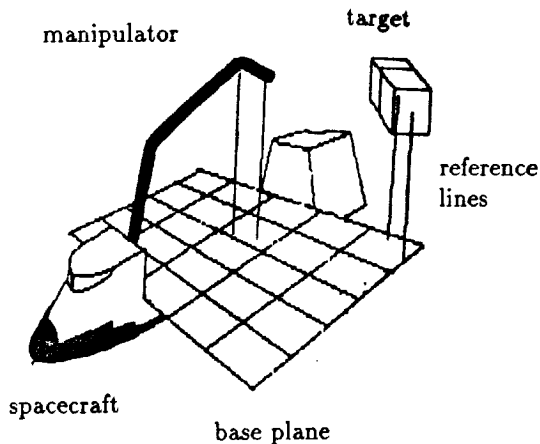
Figure 2.4: *Reference lines.*

For an insert-task, force feedback improves the operator's performance. Force feedback can be kinaesthetic [Bejczy, Handlykken, 1981] or visual [Bejczy, 1982] and it results in smaller task completion times, and in less and smaller exerted forces.

A predictive display shows to the operator a prediction of the future response of the system under control. Several kinds of predictive displays can be distinguished [Warner, 1969]. For instance, an important distinction exists between *in–line* and *off–line* predictive displays. In the case of an in–line display the operator is acting as an on–line controller. So, the display is used in a manual control situation. A certain assumption is made about the future commands of the operator. For instance, it is assumed that the operator's commands remain equal to his present command over the time–horizon the prediction is calculated. On the basis of this assumption the prediction is calculated and shown to the operator.

An off–line predictive display is used in a supervisory control situation. Some future control sequences, specified either by the operator or by a computer, are used to calculate predictions. When the operator is satisfied with the (predicted) future response of the system, the corresponding (stored) input sequence is used as control input for the actual system.

A prediction can be calculated by extrapolating the output of the system or by using a model of the system's response [van den Bosch, 1990]. The extrapolation methods are based on the Taylor series of the output function $y(t)$.

In what circumstances can a predictive display be of aid to the operator? Fig. 1.3 indicates that the characteristics of the task to be executed, the system dynamics and the disturbances will be of importance. In the following, some applications of predictive displays are described in order to identify the situations in which such a display can be useful. The overview is not restricted to the field of teleoperation. Also in other fields, like process control, interesting and relevant applications can be found.

When a system has difficult dynamics, for instance due to third order dynamics, a predictive display leads to smaller learning times [Kelley, Prosin, 1972] and the avoidance of potential collision situations [Kelley, 1971, pp. 141–148]. For systems with slow dynamics providing a predictive display proved to be helpful to the operator. In the case of ship handling [Veldhuyzen, 1976; Passenier, 1989] a predictive display led to a more accurate tracking of the route, but also to more energy consumption. The reason was that the operator began to issue more commands to achieve a more accurate tracking. For an industrial process [van de Veldt, 1986; Keyser, van Cauwenberghe, 1981] providing a predictive display led to a more economical use of the plant. Especially when the system is complex due to couplings or interactions between the inputs and outputs of the system to be controlled [van de Veldt, 1984] the predictive display turned out to be useful. The display resulted in smaller learning times and in a better performance with respect to time and average deviation from the setpoints.

Kelley [Warner, 1969, p. 21] found that when subjects in a submarine control task were allowed to adjust the prediction horizon, they elected to decrease it as the vehicle speed was increased. He also noted that in such a task, the prediction horizon should perhaps be in terms of distance rather than time.

Generally time-delays worsen the performance of the human operator [Ferrel, 1965; Hess, 1983; Hill, 1976; Starr, 1979; Ruitenbeek, 1984a] and force him to adapt a move and wait strategy. However, the seriousness of the time-delays must be regarded in relation to the dynamics of the system to be controlled [Ruitenbeek, 1984b; Bos, 1988]. Predictive displays form a solution to this problem [Milgram, Weverinke, 1985]. Only few predictive displays as in [Schenker, Bejczy, 1990] have been realized for a hardware system yet. Kineasthetic force feedback in the presence of time-delays can lead to instability [Ferrell, 1966]. In [Anderson, Spong, 1989] a new control law has been developed, based on network theory, which guaranties stability. In [Buzan, Sheridan, 1989] a predictor for force feedback has been developed. Both solutions have been tested on a hardware system with 1 DOF.

Still a research issue is how inaccuracies in a prediction influence the performance and behaviour of a human operator. Also the question must be answered how accurate a prediction has to be so that an operator can execute the task in a reliable way. This holds for manual control, but also for a supervisory control situation. In the latter case there is an extra complication. In order to improve the accuracy of the prediction a closed loop prediction scheme can be used, i.e. using the measurements to correct the prediction. But for failure detection, correcting the output of the prediction model with measurements can be undesirable. The operator just has to conclude from the difference between the trajectory of the prediction and the (delayed) display of reality that a failure occurred.

Summarizing, a predictive display can be of aid to the operator when the system to be controlled has complex or slow dynamics, when time–delays are present, to avoid collisions, or when the task to be executed requires optimization of a performance criterium like the control effort or the accuracy.

Flexibility effects can cause oscillations of the End–Effector, which can cause problems for the operator when he is looking through the End–Effector camera. To what extent the operator is capable to cope with the oscillating camera picture is still a research issue. Moreover, the provision of techniques which suppress the effects due to the flexibility of the manipulator is a point of study.

2.1.4   Simulators

Simulators as the HERA Simulation Facility Pilot [Prins et.al., 1989] can be used as a very flexible substitute for building expensive hardware to perform man-machine experiments. However, the real-time simulation of the complex dynamics of a space manipulator and the display of the arm plus the environment is still a problem. Since computer power is expected to improve drastically in the near future, attention must be paid to the development of such simulators. Simulators can also be used in providing a predictive display or as a planning tool: the operator gives commands to the simulation model and when he is statisfied with the response, the (stored) commands are issued to the real manipulator.

2.2 Some background on human operator modelling

2.2.1 Introduction

In order to design a good MMI, also knowledge about the control behaviour of a human operator is required. This knowledge is often represented by a model. Therefore, in this section human operator modelling is reviewed from a system theoretical point of view.
Human operator models can be a tool in the design and analysis of systems of which a human operator is an essential part [Pew, Baron, 1983; Stassen, van de Veldt, 1982]. In system theory, a well-proven approach to describe a system is to model its behaviour. With the model the following important goals can be achieved [Stassen et.al., 1990] :

- Reduction of the data measured to a set of relevant parameters.

- The possibility to recognize analogies.

- The prediction of the dynamic behaviour of a system under development.

- Quantitative knowledge required to optimize the system's performance.

Hence, models to describe the dynamic behaviour of the human and machine would be very desirable.

What demands should a model fulfill? The most important requirement is that the model should reflect the operator's capabilities and limitations. It must also be possible to validate the model. For instance the parameters in a system theoretical model must be identifyable. Or stated differently in [Pew, Baron, 1983] "As in any other application the models are only as good as the data on which they are based". Problems in the parameter identification may arise due to lack of available data or an inherently bad model structure.

"In linear system theory, it has been shown that the optimization of system performance can only be achieved if the dynamics of the system to be controlled are known and a performance function is defined [Francis, Wonham, 1975]. Similarly, for a design of an optimal filter, a cost criterion, the dynamics of the system to be controlled, and the statistics of the disturbances to be compensated have to be known [Kalman, Bucy, 1961]. Analogously, in order to control a system the human operator has to have knowledge of the system dynamics, the task, the disturbances and the available displays and controls (Fig. 1.3). This knowledge is called his *internal representation*. It is the subjective description of the way the human operator thinks the system behaves. In a human operator model this knowledge can be represented by an *internal model*. It is how the researcher describes the internal representation" [Stassen et.al., 1990].
In the past years several kinds of human operator models have been proposed: system theoretical, artificial intelligence based, verbal and psychological. It is remarkable that all concepts showed that the existence of an internal model is a necessary, but non-sufficient

condition in order to construct a human performance model [Stassen et.al. ,1990].

Rasmussen [1983] stated that in the control behaviour of a human being three levels can be distinguished (Fig. 2.5) :

- *Skill-Based* Behaviour (SBB)
  On this level the operator acts more or less automatically. Manual tracking tasks are for instance executed at the skill-based level.

- *Rule-Based* Behaviour (RBB)
  For instance the shut-down and start-up procedures of a power plant are executed on this level.

- *Knowledge-Based* Behaviour (KBB)
  When the circumstances are new, for instance when facing a never occurred and not foreseen alarm, the full range of problem solving behaviour is called forth. Then, the operator has to think of new procedures based on the fundamental knowledge he has about the system and the task.

This characterization of the control behaviour of a human operator is clearly related to the manual and supervisory control tasks as is illustrated in [Stassen, 1989]. However the boundaries are often vague.

In the following some major human operator models will be described. We will restrict ourselves to system theoretical models.
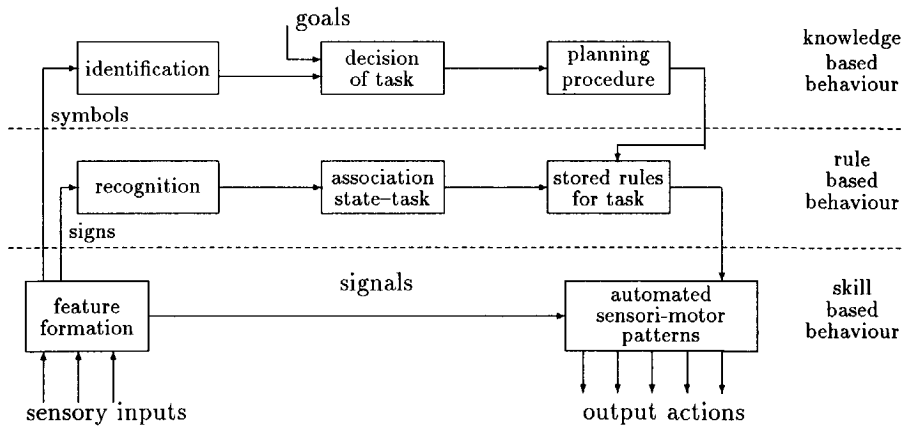
Figure 2.5: *Schematic model of three different levels of human information processing [Rasmussen, 1983].*

2.2.2   Human operator models

Describing Function Model

The Describing Function Model [McRuer, Jex, 1967] models the behaviour of the operator at the skill-based level. The human operator has a compensatory tracking task and the input is noisy like. The operator has to control a linear, time-invariant and Single–Input–Single–Output (SISO) system, represented by the transfer function H_c. H_p is the Describing Function describing the linear part of the control behaviour of the human operator and is given by :

$$H_p(j\omega) = K \cdot \frac{1 + j\omega\tau_1}{1 + j\omega\tau_2} \cdot \frac{1}{1 + j\omega\tau_n} \cdot e^{-j\omega\tau_v} \tag{2.1}$$

The remnant [Levison et.al., 1969] is by definition equal to the difference between the response of the linear system described by H_p and the actual response of the operator. Generally the remnant will not have a zero variance [Stassen, 1989] due to :

- Higher harmonics due to non-linear behaviour.

- Possible non-stationary operator behaviour.

- Observation noise due to inaccurate observation.

- Motor noise due to inaccurate motor control.

- Generation of test signals by the human operator in order to obtain more and/or better information about the system under control.

The information processing time is reflected by $e^{-j\omega\tau_v}$. The effects of a bandwidth limitation introduced by the neuro-muscular system is modelled by $\frac{1}{1+j\omega\tau_n}$. The two parameters τ_v and τ_n are fysiologically determined. For frequences lower than 3 Hz the two terms can be melt together to one term $e^{-j\omega\tau_e}$
The term K $\frac{1+j\omega\tau_1}{1+j\omega\tau_2}$ reflects the human capabilities to adapt to H_c. The adaptation of the human operator to H_c is given by the Cross-Over Model.

Cross–Over Model

The Cross–Over Model is based on the assumption that a well–trained and motivated human operator will behave as a good servo controller, taking into account his inherent limitations. This means that the human operator tries to follow the low frequency inputs and to suppress the high frequency inputs as well as possible. The human operator tries to maximize the open–loop gain, but without making the closed–loop system unstable. So, in the neighbourhood of the frequency where stability margins are important (the so called cross–over frequency ω_c) it holds that:

$$H_p(j\omega) \cdot H_c(j\omega) = \frac{\omega_c}{j\omega} \cdot e^{-j\omega\tau_e} \tag{2.2}$$

18

Hence, the Cross–Over Model predicts to what extent the human operator adapts his parameters K, τ_1 and τ_2 (Eq. 2.1) to the system to be controlled, represented by H_c.
An excellent feature of the Cross–over Model is that it predicts to which linear systems the human operator is not able to adapt himself. For instance, in the case that $H_c = (\frac{1}{j\omega})^3$ the operator should generate a term $(j\omega)^2$ in the numerator of his transfer function. So, the human operator is not able to generate the second derivative of his input for a reasonably long time.

Optimal Control Model

A well–known model in time domain is the Optimal Control Model (OCM) by Levison, Baron and Kleinman [1970]. The model is based on the assumption that a well–trained and motivated human operator, given his inherent limitations, will behave in an almost optimal manner. The structure of the OCM is shown in Fig 2.6. The observed output y contains those system variables explicitly displayed, as well as the first derivatives of those variables, which are implicitly derived by the human operator [Levison et.al, 1970]. The operator cannot extract higher derivatives. For instance when the position is displayed, the operator is able to make an estimate of the velocity, the first derivative of the position. So, the velocity part of the state is also represented in the output matrix, but not the acceleration part of the state. Other assumptions are that :

- The system to be controlled is linear, controllable and observable.

- The noise is gaussian white and independent.

- The control task can be described by a quadratic cost functional.

- The human operator has a perfect understanding of the dynamics of the system to be controlled, the statistics of the disturbances, the task to be executed and his own inherent limitations.
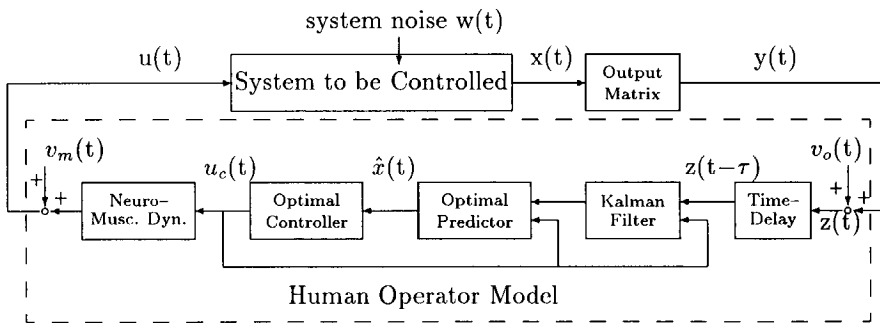
Figure 2.6: *The Optimal Control Model*

The assumptions are such that the separation principle holds [Kwakernaak, Sivan, 1972]. The OCM is only valid in stationary situations.

The limitations of the human operator are modelled by a pure time–delay, motor and observation noise and neuro–muscular dynamics.

The OCM can be simplified for slowly responding systems. Then it is plausible that the influence of the time-delay (ca. 200 msec.) and neuromuscular dynamics on the total man–machine performance may be neglected.

Now, consider a situation where the Cross–Over Model is valid. Suppose that the system to be controlled has the transfer function $\frac{1}{s^3}$ and only observation noise is present. Suppose, only position information x is displayed as the system's output. The Cross–Over Model predicts that an operator is not able to control this system with third order dynamics. A state–space realization of this system is :

$$\dot{z}(t) = Az(t) + Bu(t) \tag{2.3}$$
$$y(t) = Cz(t) + Ew(t) \tag{2.4}$$

where $z = \begin{bmatrix} x \\ \dot{x} \\ \ddot{x} \end{bmatrix}$, $A = \begin{bmatrix} 0 & 1 & 0 \\ 0 & 0 & 1 \\ 0 & 0 & 0 \end{bmatrix}$, $B = \begin{bmatrix} 0 \\ 0 \\ 1 \end{bmatrix}$, $C = \begin{bmatrix} 1 & 0 & 0 \end{bmatrix}$, and $Ew(t)$

represents the output noise.

Because the human operator is able to make an estimate of $\dot{x}$, but not an estimate of higher derivatives, thus $\ddot{x}$ in the example, C becomes:

$$C = \begin{bmatrix} 1 & 0 & 0 \\ 0 & 1 & 0 \end{bmatrix}.$$

The system (A, B, C) is controllable and observable. When the tracking task is described by a quadratic cost functional, this description of the control situation satisfies all conditions of the OCM. Contrary to the Cross–Over Model, the OCM does not predict that the operator will not be able to control the system, implying that the conditions for the validity of the OCM are too weak. This illustrates a strange contradiction present in the set–up of the OCM. On the one hand, it is assumed that when constructing the observability matrix C, the operator can extract first derivative information, $\dot{x}$, from a single display indicator, but he cannot extract higher derivatives, such as $\ddot{x}$ in our example. The result of the Kalman filter and the predictor part, however, is that the operator is able to reconstruct the whole state, i.e. he can extract all derivatives from a single display indicator. In the example this means that the operator is able to estimate $\ddot{x}$ when only x is displayed. For eliminating this contradiction one may think of replacing the demand of observability by the demand for the output matrix having full rank itself already. In the example above this means that also the velocity information $\dot{x}$ has to be displayed. Then C becomes the identity matrix, which has full rank 3.

Another problem is the identification of the parameters. The model is overparametrized. For instance, the observed output is τ seconds delayed in the operator himself, due to information processing time (Fig. 2.6). But, also internally, the operator compensates this

delay by calculating an optimal prediction over the same τ seconds, so that the parameter τ cannot be estimated. Also the determination of the noise intensity matrices for a certain, estimated Kalman gain, and of the weightings in the cost functional for a certain, estimated control law is a problem. These problems are called the *inverse optimal observer problem* and the *inverse optimal control problem* [Kok, Stassen, 1980; Kok, van Wijk, 1978], the first of which gives information about the operator's knowledge of his own motor and observation noises and the second on his notion of the task.

Fuzzy Set Models

A more recent approach is the use of fuzzy set theory [Zadeh, 1973, 1984]. In the fuzzy set theory, the notion of a membership function is added to the classical set theory. A membership function describes to what extent an element belongs to a set. Contrary to the classical set theory, the membership function can attain also values *between* zero and one. It is expected that fuzzy human operator models can model the qualitative (fuzzy) reasoning of man more accurately than the classical control theories. However, until now there are a few open problems. One cannot say in advance what rules the human operator will use. The rules may be derived from a mathematical model of the system, but which model should be used? From an identification point of view one would like to have a kind of canonical structure for a fuzzy model, preferably containing only a few parameters. For instance, only trapeziform membership functions would be allowed. However, the shape of the membership function may strongly depend on the opinion of an individual operator. It is still not clear what the sensitivity of the model is for different kinds of shape of the membership function.

Moreover, the human capabilities and limitations are not (yet) incorporated in a (canonical) structure of a fuzzy set model.

With respect to human operator modelling, the fuzzy set theory has been succesfully applied for describing the behaviour of a navigator on a ship [Salski, Noback, 1986; Salski, et.al, 1987]. Another example can be found in [Moray et. al., 1987].

Supervisory tasks are more or less vaguely defined and the operator has a lot of freedom in making decisions. Therefore, modelling human supervisory behaviour is very difficult. Two models which describe the behaviour of an operator during stationary process conditions are the OCDM [Kok, Stassen, 1980] and PROCRU [Baron et.al., 1980]. In the former the OCM is extended with a decision part. PROCRU models the behaviour of an aircraft crew. The state variables describing the aircraft dynamics are handled by the OCM, whereas verbal messages between persons are handled by a rule–based pattern recognition system. Recent developments concern the application of petri-nets [Blaauboer, Brinkman, 1990] and neural networks to human operator modelling.

2.2.3 Applicability of human operator models in space teleoperation

In this section an analysis will be made to what extent existing human operator models are applicable to a situation where an operator has to control a space manipulator. It will be analyzed whether these models may a priori be used to provide us with reliable quantitative information when designing a MMI.

The main application of human operator models has been to the manual control of linear, SISO, relatively rapidly responding systems [McRuer, Jex, 1967; van de Vaart, Hosman, 1988; Hess, Modjtahedzadeh, 1990], although some studies include MIMO systems [van de Vegte et.al., 1989; Weverinke, 1987; Johannsen, Govindaraj, 1980; van Lunteren, 1979]. Mostly, the operator had to perform a continuous tracking task. An extension towards step-tracking tasks can be found in [Ruitenbeek, 1984c, 1985]. Moreover, the tasks were mostly well defined and simple. A space manipulator has non-linear and complex dynamics and it is rather slowly responding. One may think of linearizing a model around a trajectory, but the limited torques may inhibit this approach. Furthermore, the input which has to be tracked, a trajectory in a three–dimensional space, must also be generated by the operator. The models developed for non-linear systems have always been tuned to the specific systems for which they have been developed. One may not just extrapolate them to other systems. In most models implicitly a very accurate internal representation is assumed. There have been only a few papers addressing the problem of imperfect knowledge [Baron, Berliner, 1977; van de Vegte et.al., 1989; Jain et.al., 1989]. When the operator has to control a space manipulator, the assumption of perfect knowledge is very questionable.

So concluding, the existing human operator models may not a priori be applied to the situation, where the operator has to control a space manipulator. But research in this direction is still needed.

Chapter 3

Tackling the defined problems

3.1 Selection of the research issues

In Chapter 1, the main difficulties for a human operator to control a space manipulator were identified :

- The possible presence of time-delays.

- The presence of flexibility effects.

- No direct vision.

- Non-linear and slow dynamics.

- Up to 6 DOF to be controlled.

For the placing of the operator two options exist : in space, near the worksite or on Earth. In the case of HERA the operator will be located firstly in the cockpit of Hermes. Only in the long term planning the operator will be placed on Earth. Therefore, the problem of time–delays was not studied in this project.

The expectation was that the control system could be designed in such a way that the flexibility modes are not, or only to a small extent, excited. Also pilot–experiments [Bos, 1988] gave the impression that the main problems due to the remaining flexibility effects would manifest themselves in the execution of an insert–task, where the visual information is provided by the End–Effector camera. Although the investigation towards the problem of the flexibility effects is an interesting one, it was not investigated due to the limited time which was available for this research project.

The experimental tools were restricted to the use of a graphical workstation. This fact implies already that the subjects could not have direct vision on the control scene.
Pilot experiments [Bos, 1988] indicated that displaying two orthogonal projections, without

perspectivity, of the scene provides an operator with an insufficient three–dimensional perception. Therefore, it was investigated how graphical displays can be used to provide the operator with a good three–dimensional perception. This was investigated for a task where global views of the scene have to be used.

In the case of HERA these global views are provided by camera's. However, only a very limited number of camera's is foreseen. Moreover, the possibilities for the placement of the camera's are very restricted by the environment. For instance, a side view cannot be generated from a point somewhere in space. The camera's have to be attached to Hermes, HERA or the Man–Tended–Free–Flyer (MTFF). The advantage of graphical displays is that they can provide views from any point, provided a model of the environment is available. In addition, they can serve as a back–up for the camera's.

The problem of controlling 6 DOF is most restricting for a task where a large accuracy is required, such as an insert–task, or a peg–in–hole task. Generally an insert–task has to be excuted in the End–Effector control mode. The End–Effector frame functions as reference frame, and the tip of the End–Effector or payload as POR. When using the End–Effector frame as reference frame, the direction of a translation depends on the orientation of the End–Effector. This might cause inefficient and unsafe situations. A possible solution which was investigated, is the use of the target frame as the reference frame. This can be done when the orientation of the target is known. Within the HERA project a camera is foreseen, located on the End–Effector. The camera picture will be processed, using vision techniques, into information about the relative difference in position and orientation between the End–Effector frame and the target frame.

Using the proximity information, closed-loop control schemes can be designed, which reduce the number of DOF to be controlled by the human operator. Therefore, it was investigated to what extent a reduction of the number of DOF to be controlled by an operator from 6 to 2 led to a "better" performance.

The motor torques limitations of HERA are such that a space manipulator can be considered as a slowly responding system. For other very slowly responding systems, the use of a predictive display generally led to a smaller learning time [van de Veldt, van den Boomgaard, 1986] and a better performance [Kelley, 1972; Keyser, van Cauwenberghe, 1981; Passenier, 1989; Johannsen, Govindaraj, 1980]. The use of two kinds of predictive display was evaluated at our laboratory: a display of the stopping configuration and a display of a predicted trajectory. The displays were evaluated for a rough positioning task in the presence of obstacles.

An important issue when displaying a predicted trajectory is how to choose the most effective length of the time–horizon over which the prediction has to be calculated. The most effective length will depend on the system dynamics, the task to be executed and the disturbances acting on the system. Experiments with subjects can be performed to investigate this issue, but these experiments will be very time–consuming. Therefore, a first investigation was performed whether predictive control theory can be used to investigate the most effective length of the time–horizon. Herefore, two kinds of experiments were performed:

one in which a human acts as a controller, and another in which the control is performed by a predictive controller.

It should be noted that the results of this research project for the manual control situation can also be of importance for the supervisory control situation. For instance, the question of providing the operator with a good three–dimensional impression of the scene, is of importance for both the manual and the supervisory control situation. In a supervising task, the operator has to be able to monitor the task execution. When the information provided to him is of a bad quality, then he might intervene unnecessary or too late.

So finally, three problems were investigated :

1. No direct vision.

2. Up to 6 DOF to be controlled.

3. Non–linear and slow dynamics.

3.2 Design of the experimental facility

3.2.1 Tasks

A space manipulator can be used for tasks like inspection, transfer of ORU's, EVA support and even berthing, i.e. using the manipulator to dock the space craft to a space station. To perform such tasks, a sequence of so called *elementary functions* has to be excuted [Andre, Schooncjans, 1989; de Waard, 1987]. An elementary function defines a specific part of a task. *Transition criteria* determine whether an elementary function has been accomplished and whether the next elementary function may be executed. For instance when an ORU on the MTFF has to be replaced, the End–Effector has to *move* firstly to the ORU. The positioning requirements which are part of the transition criterium, are not very strict. Then, the End–Effector has to *approach* the ORU, before the ORU can be *grappled.*
This breakdown of the tasks results in a set of elementary functions. All tasks can be represented by a particular sequence of elementary functions.

In our research the tasks were at first broken down into two basic tasks or elementary functions: A rough positioning task and an insert task. In the rough positioning task the End–Effector has to be moved over a considerable distance and the requirements on the end positioning are not so strict. The operator himself has to determine the path to be followed. In this task only the global views can be used. The insert task represents the fine positioning and the insertion of for instance an ORU into a storage hole. The visual information is provided by a camera on the End–Effector.
For the study towards the optimal length of the prediction horizon, when providing a display of the predicted trajectory, a track following task was defined. Contrary to the rough

positioning task, the trajectory is known and shown to the operator.

3.2.2   System dynamics modelling

The subjects have to experience the movements of the manipulator as continuous motions. The simulation has to be real-time. So, on the one hand, the model of the manipulator system can not be too complex, because of limited computing and graphic display power. Moreover, there was only a limited amount of time available to realize the experimental facility. On the other hand, the facility should still reflect the main characteristics of the system to be controlled. This is a necessary condition when one wants to be able to extrapolate the results of the experiments to a real world situation.

So, the question is now to what extent reality may be simplified to obtain results which can be useful in the design of a MMI of a space manipulator. In chapter 1, the main characteristics of the dynamics of a space manipulator were identified :

1. The presence of flexibility effects.

2. Up to 6 DOF have to be controlled.

3. Non-linear and slow dynamics.

In this research the flexibility effects were neglected. The assumption was that the control system would be designed in such a way that the flexibility modes will not be excited. However, this is a serious simplification of reality, and the influence of flexibility on the performance and behaviour of a human operator in the human control of a space manipulator must be a topic for future research.

The simulated robot had also 6 DOF.

At the time of implementation insufficient information about the actuator dynamics and the local (actuator) control loop was available. Therefore, the actuators were modelled as systems which could provide instantaneous constant, but limited torques. Due to the limited torques the manipulator may be slowly responding. To what extent slow dynamics were created depended on the mass attached to the End–Effector and the maximum velocities.

The manipulator was rate controlled. From the literature [Flatau, 1973; Kim et.al., 1987a] it followed that because of the large size and the slow dynamics of the manipulator, rate control had to be preferred. In fact, for these reasons HERA will be rate controlled.

3.3   Design of the experimental procedure

Several factors in the experimental procedure can influence the outcomes of an experiment: the order in which the experimental conditions have to be faced, the training, and the

instruction given to the subjects. The choices which were made concerning these factors are described in the following sections.

3.3.1 Training

The main purpose of the training sessions was to train the subject under all experimental conditions. A second purpose was to get some insight in the learning curves for the experimental conditions.

To train a subject, he has to perform several runs for each experimental condition he has to face with. Now two extreme options exist :

1. The subject performs the training runs for each experimental condition separately. For instance, he performs firstly 10 runs under condition A and then 10 runs under condition B.

2. The subject performes the training runs for all experimental conditions in an at random order. For instance, he has to face the experimental conditions in the following way : A B A A B A B B B A ....

The disadvantage of option 1 is that the learning effects between the experimental conditions are hard to compare. A subject can learn something about the system's behaviour which can also be of use in the case of condition B. Then, under condition B the subject starts already with a better performance than when he was still a complete novice. Also in option 2 the chance exists that a subject has to perform for instance 5 runs under condition A, before performing a run under condition B. Then the learning effects would not have been evenly spread over the experimental conditions. Therefore, the runs were chosen to consist of a sequence of random permutations of the number of experimental conditions.

3.3.2 Experiments

Contrary to the training, in an experiment the influence of still possible learning effects has to be minimized. Therefore, the order in which the runs were performed was randomized.

In reality astronauts will be trained extensively on Earth in executing the tasks. The number of tasks may be very limited. For instance, only two ORU's have to be transfered. Therefore, the behaviour of the astronauts may shift from really acting as an on–line controller, to more automatically executing a predefined control sequence. However, a purpose of this project was to investigate an operator's *ability* to control a space manipulator under different conditions. Therefore, automatic control behaviour had to be avoided. To avoid that the subjects would automatically execute a predefined control sequence, instead of determining on–line the required commands, the starting configurations were varied. There were as much starting configurations as there were runs per experimental condition. This causes that the averages showed must be considered as indications and that the data will not be normally distributed. Therefore, to test the significance of the results for each subject separately the Wilcoxon test for matched pairs was used [Siegel, 1956; Sachs, 1982].

When using the Wilcoxon test, it is assumed that the two sets of data are originated in the same population, which is plausible for each separate subject. When the results are averaged over the subjects this assumption is questionable. Therefore, when averaging over the subjects the Sign test was used to test the significance of the results.

On some performance measures the starting configurations have no influence. For instance, forces resulting from the insertion itself, will not depend on the starting point outside the hole. Because mostly the data were not normally distributed, the Mann–Whitney test was used to test the significance of the results with respect to these performance measures [Siegel, 1956; Sachs, 1982].

3.3.3   Instruction

For our experiments two extreme control strategies could a priori be distinguished :

1. As fast as possible, which may result into a rather inaccurate positioning and many incidents.

2. With a minimum number, preferable zero, of incidents which may result into a rather slow movement towards the target.

In space operations the tasks have to be completed in the first place safely and in the second place as efficiently as possible. To achieve this required behaviour the subjects were instructed to perform the task carefully as the *first priority* and as the *second priority*, to perform the task as fast as possible. The exact instruction given to the subjects for each experiment is given in the description of the experimental procedure in each chapter.

Chapter 4

Experimental facility

4.1 General description

The realization of the experimental facility has known a number of stadia, and it took 1.5 to 2 years. The experimental studies, reported in this thesis, were performed with different versions of the facility. However, the main structure of the facility remained the same. The structure is described below. Both the physical and the functional description are given.
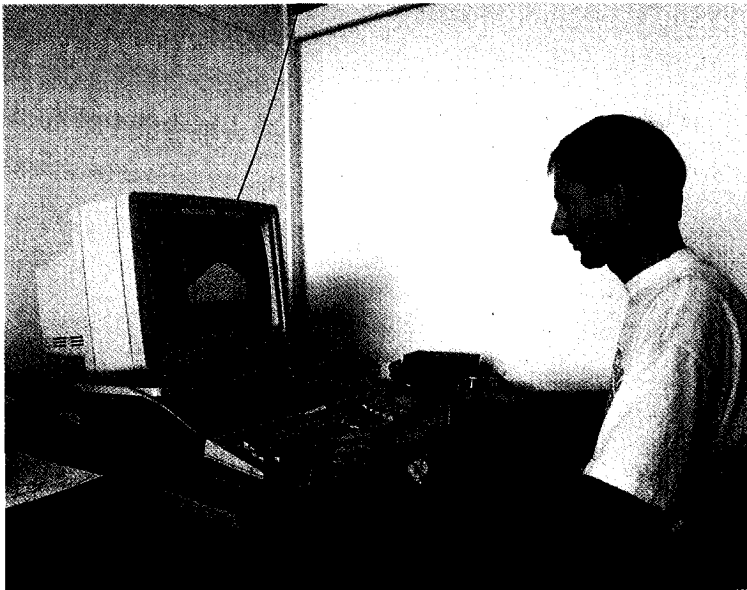

Figure 4.1: *Physical layout of the experimental facility.*

29

Physical description

The simulation program runs on a VAX–II–GPX workstation. The simulation program takes care of the input handling, the simulation of the manipulator dynamics, and the graphical display of the moving manipulator, and all other information to be displayed. The subjects experience the motions of the displayed items, such as the manipulator, as continuous motions.

The subject sits in front of a 19 inch diagonal monitor (Fig. 4.1), with a resolution of 30 pixels per cm. The picture they see consists of a representation of the manipulator, the control scene and some optional extra displays, such as a proximity display (Section 4.4.3). The subjects can generate control actions via a mouse and two joysticks. Each of the joysticks has three DOF, and the signals are fed into the workstation via an A/D-converter.

Functional description

The experimentator firstly has to construct an input file, in which the experimental conditions are defined. During an experiment, an unformatted data file is created, in which the subject's code, the date and time of the experiment, the experimental conditions, the issued commands of the human operator, and a number of performance criteria are recorded (Fig. 4.2). This file can be used for three purposes :

1. A table can be created in which the data of the file, except for the recorded issued commands, are listed. Optionally, this feature can be performed automatically.

2. The experimental run can be replayed on the monitor. There is a hold/continue feature available.

3. The experimental run can be replayed, fast time, in order to create a data-set for a time-plot of a selected variable. This data-set functions as an input file for the plot–package GRA. This plot–package was already used at the laboratory.

After each experimental run a number of performance criteria as well as a code for the run are written to a summary file. After the complete experiment, this summary file can be sorted. The sorted file can be split into separate files for each performance criterium, by u-sing the program *spline*. These files serve as data files for the statistical package SPSS/PC+.

A first step in the development of the experimental facility was the realization of a simula-tion of a planar manipulator. A planar manipulator is a manipulator with 3 parallel DOF, and it can only move in one plane. A purpose of this two–dimensional,2D, simulation was to serve as a training facility for the subjects. The subjects can firstly obtain experience in controlling a space manipulator and in understanding the experimental conditions in a more easy situation. They have only to control 3 DOF, and no problems with the three–dimensional, 3D, perception are present.

Of course, successively the subjects have to practice on the 3D simulation.
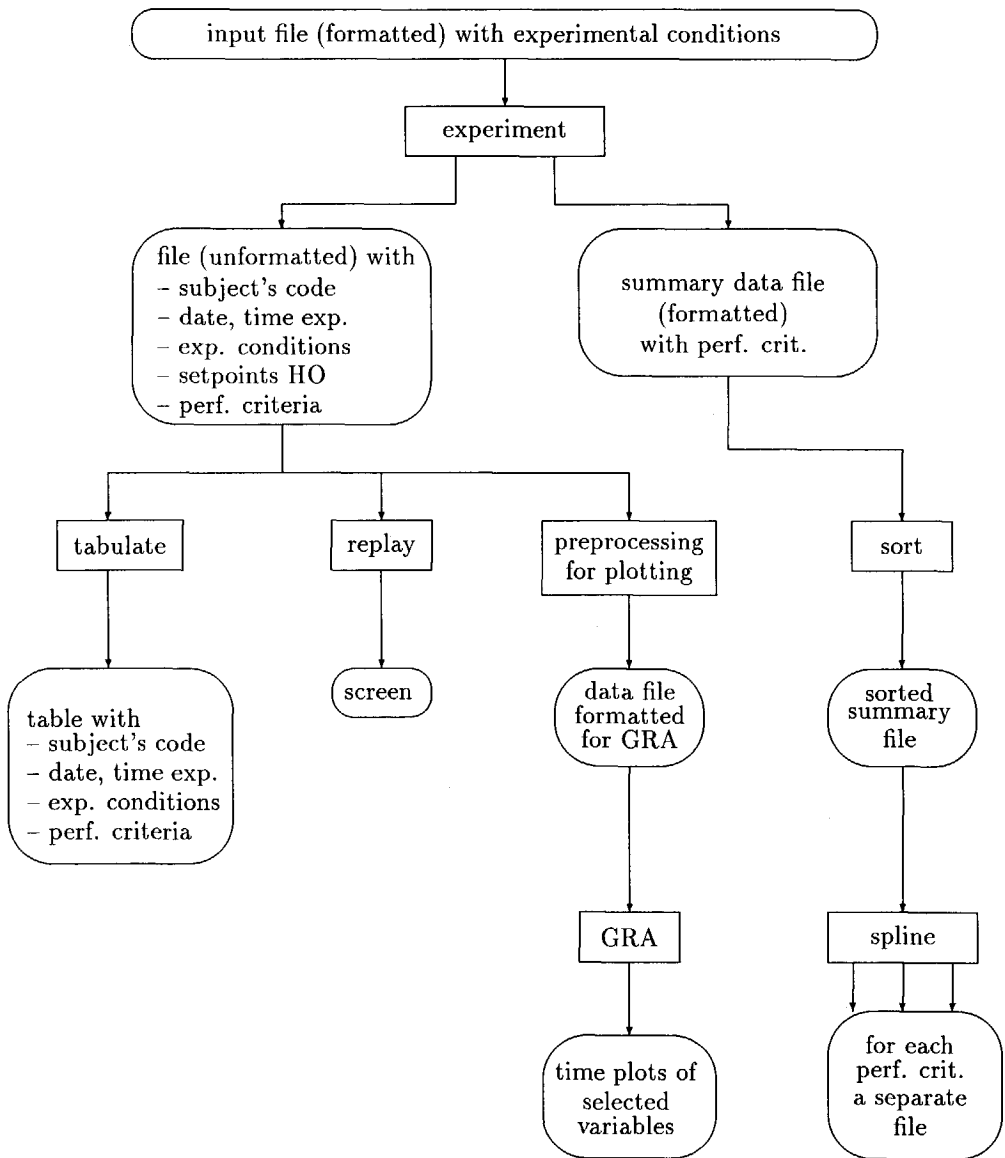
Figure 4.2: *Functional layout of the experimental facility.*

4.2 Tasks

4.2.1 Rough positioning task

Given a starting configuration, the subjects have to move the End–Effector into a specified position and orientation.

In the 2D simulation the tip of the End–Effector has to be positioned in the circle as shown in Fig. 4.3. The radius of the circle is 0.16 meter. The rest of the End–Effector has to be positioned within the rectangle which represents an orientation requirement.

The 3D version of the above described positioning requirements is shown in Fig. 4.4. The tip of the End–Effector has to be positioned in the dashed cube. The rest of the End–Effector has to be positioned in the whole cube.

It does not matter from which side the displayed imaginary areas, defining the positioning requirements, are entered. However, the manipulator is not allowed to intersect the solid vertical line in Fig. 4.3 nor the *safety plane* at the back side of the cube in Fig. 4.4. If it does, an *incident* has occurred. One may think of a situation where a satellite has to be grappled. When the manipulator should move too far, it would damage the satellite, which is of course not allowed at all.

To ensure a safe operation, the real borders of the environment are extended with software borders (Fig. 4.5). This software representation of the environment is used in our collision detection algorithm, in order to prevent real collisions. In the case of an incident the manipulator has a collision with the software environment.

When an incident is detected, an *emergency stop* is initiated by the control system. During the time it takes to stop the manipulator all commands of the operator are ignored by the control system. The manipulator is stopped by setting all joint setpoints to zero. The brakes are not used. The software borders are chosen in such a way, that the manipulator can be stopped in time to prevent a real collision with the environment.

When the manipulator has come to rest, the so called *recovery phase* is entered. The operators are instructed to bring the manipulator immediately back into the safe region. In the recovery phase the software checks whether the normal operational situation can be re–entered. When an operator nevertheless commands the manipulator in the wrong direction (away from the safe region) a collision with the real environment, i.e. a so called *accident* can occur. In our simulation an accident occurs when the manipulator intersects the dashed vertical line (Fig. 4.3) or a second safety plane located "behind" the first plane. The dashed vertical line and the second safety plane are not displayed on the screen.

The task is completed when the positioning requirements are fulfilled and the velocity of the manipulator is very small. Optional, the operator or the system checks whether these conditions are fulfilled.
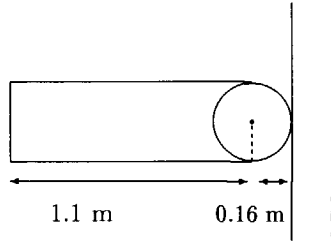
Figure 4.3: *Positioning requirements in the 2D simulation.*
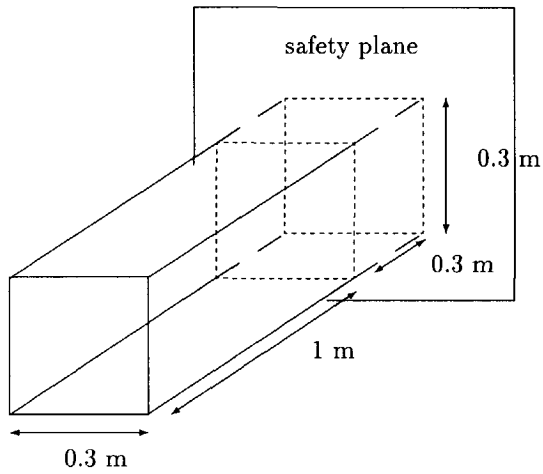
Figure 4.4: *Positioning requirements in the 3D simulation.*
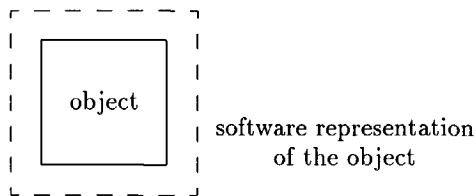
Figure 4.5: *Software borders.*

4.2.2　Insert task

Before an ORU can be inserted into the hole, the tip of the ORU has to be positioned within certain bounds. There are restrictions on both the position and the orientation misfits. The restrictions depend on the size of the object to be inserted and on the relative size of the hole. In Fig. 4.6 the tolerance of the hole is defined and the size of an ORU is given. A necessary condition to enter the hole is for instance that the misfits in position are less than the size of the tolerance [Doorenbos, 1989b].

When a subject tries to enter the ORU into the hole, whereas the boundary conditions are not fulfilled, the ORU hits the front plate and a so called *incident* occurs. The moment the software detects an incident, automatically an *emergency stop* is initiated (see also the previous section). During the period it takes to stop the manipulator the subject's commands are not executed. When the manipulator has come to rest, the so called *recovery phase* is entered. The subject is informed by a text on the camera view that an incident has occurred. The subject has to bring back the manipulator into the safe region, before the task can be continued.

When the ORU is in the hole two dangerous situations can occur. Firstly, the ORU can get stuck in the hole, i.e. a *jamming* situation (Fig. 4.7) can occur. Such a situation is detected by the software and the same strategy as after an incident ocurrance is followed. Secondly, the ORU might just touch one plane inside the hole. Then a *force* is excerted on the ORU, and because HERA is flexible, the manipulator would bend. However, in the software simulation the ORU intersects the plane inside the hole (Fig. 4.8). The exerted force is assumed to be a linear function of Δx, as defined in Fig. 4.8. When Δx exceeds a certain value an incident happens, and an emergency stop is initiated. If the subject controls the manipulator during the recovery phase in such a manner that Δx exceeds a second (larger) value, an accident happens.

　　The subject has to insert the ORU 50 cm into the hole. He is informed when he has accomplished the insertion.

4.3　System dynamics modelling

4.3.1　Manipulator kinematics

In the 3D simulation the manipulator has 6 DOF. It has two joints in the shoulder, one elbow joint and 3 joints in the wrist (Fig. 4.9). The two beam segments are each 5 meter long and the End–Effector is 1 meter long.

A serial link manipulator consists of a sequence of links connected together by actuated joints [Paul, 1981]. The only significance of links is that they maintain a fixed relation between the manipulator joints at each end of the link. Any link can be characterized by
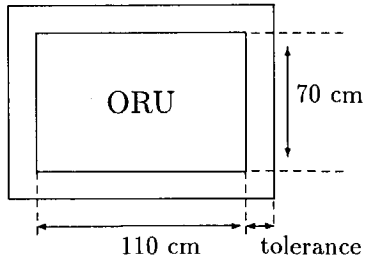
Figure 4.6: *Size ORU and tolerance.*
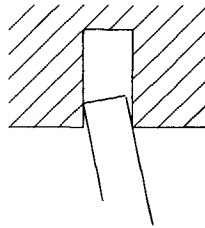
Figure 4.7: *Jamming.*
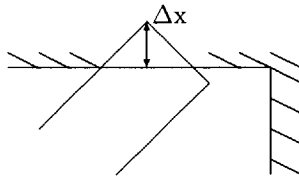
Figure 4.8: *Force definition.*

Table 4.1: Denavit–Hartenberg parameters

link	variable	α (degrees)	a (meter)
1	θ_1	90	0
2	θ_2	0	5
3	θ_3	0	5
4	θ_4	-90	0
5	θ_5	90	0
6	θ_6	0	0
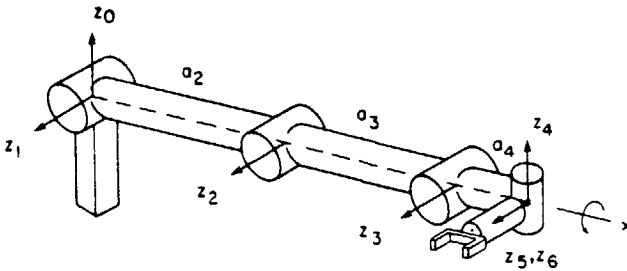
Figure 4.9: *Rotation axes of the manipulator [Paul, 1981].*
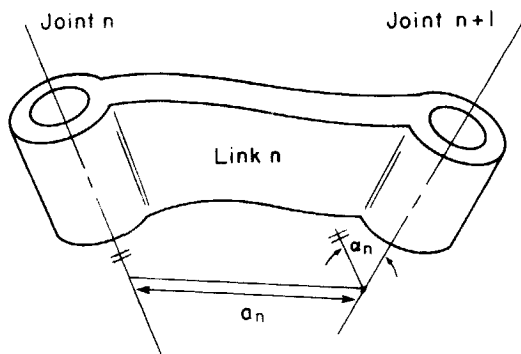
Figure 4.10: *Definition of the link parameters a_n and α_n [Paul, 1981].*

two dimensions: the normal distance a_n, and the (twist) angle α_n between the axes in a plane perpendicular to a_n (Fig. 4.10). The axes of the simulated manipulator are all parallel or perpendicular, so, α_n can be 0, 90 or −90 degrees. The manipulator has only two beam segments, or limbs, so, only two links have a non–zero length. The parameters a_n and α_n are the so called Denavit–Hartenberg parameters, and they are listed in Table 4.1.

The position and orientation of link n can be described with respect to the position and orientation of link n–1. This relation is given by the 4x4 A_n matrix [Paul, 1981, p. 53]. The A matrices can be derived from the Denavit–Hartenberg parameters. In our case it holds :

$$A_n = \begin{bmatrix} cos\theta_n & -sin\theta_n cos\alpha_n & sin\theta_n sin\alpha_n & a_n cos\theta_n \\ sin\theta_n & cos\theta_n cos\alpha_n & -cos\theta_n sin\alpha_n & a_n sin\theta_n \\ 0 & sin\alpha_n & cos\alpha_n & 0 \\ 0 & 0 & 0 & 1 \end{bmatrix}, \tag{4.1}$$

where θ_n is the controlled angle of joint n. The position and orientation of the End–Effector can be described by the so called T_6 matrix, which is a coordinate frame located in the wrist of the manipulator. The T_6 matrix is the product of the 6 A matrices :

$$T_6 = A_1 \cdot A_2 \cdots A_6. \tag{4.2}$$

The A matrices and the position and orientation of both the wrist and the tip of the End–Effector with respect to the base frame of the manipulator are given in Appendix A. Given the position and orientation of the wrist, the angle values of the joints can be calculated. These inverse kinematics are also given in Appendix A.

4.3.2 Manipulator and actuator dynamics: Model 1

At first the actuators are modelled as systems which could provide instantaneous constant, but limited accelerations. Model 1 was only used in situations where a mass of 3500 kg was attached to the End–Effector. Therefore, the maximum values of the accelerations are calculated from the maximum joint torques and the mass of 3500 kg attached to the End-Effector. The mass of 3500 kg is very large compared to the manipulator's own mass of about 230 kg. Moreover, the mass of 3500 kg can be considered as a point mass, whereas the mass of the manipulator is more distributed. Therefore, in this model only the mass of 3500 kg is taken into account.

The maximum joint acceleration is equal to the ratio of the maximum joint torque and the inertia. A decoupling control loop is assumed, so that the maximum accelerations can be calculated from Eq. 4.3.

$$\ddot{\theta}_{i_{max}} = T_{i_{max}}/(M \cdot l_i^2) \tag{4.3}$$

Here $\ddot{\theta}_{i_{max}}$ denotes the maximum acceleration of joint i, l_i denotes the distance of mass M to joint i, and $T_{i_{max}}$ denotes the maximum torque.

The inertia the actuators "feel" depends on the configuration of the manipulator. However, a control strategy is assumed which compensates the changes in inertia due to the manipulator movements. Therefore, the maximum accelerations are taken constant. Which

configuration is used for the calculation of the inertia depends on the experiment.

4.3.3 Manipulator and actuator dynamics: Model 2

Using the Lagrangian method [Brady, 1982] a rigid body model of the manipulator dynamics can be derived of the form

$$D(\theta)\ddot{\theta} + B(\theta, \dot{\theta}) = T, \tag{4.4}$$

where D is the inertia matrix and T is the input vector of torques to be applied by the actuators. In the term $B(\theta, \dot{\theta})$ the centrifugal and coriolis forces are represented. Due to the small velocities of a space manipulator this term can be neglected. Note that there is also no gravity present in space. So, the model used for the manipulator dynamics is

$$D(\theta)\ddot{\theta} = T. \tag{4.5}$$

The inertia matrix is calculated from a manipulator with a mass distribution as shown in Fig. 4.11. The computation of the inertia matrix can be found in Appendix B. Mass m_1 is 75 kg and m_2 equals 100 kg. M_3 represents the mass of the End–Effector together with the mass of the payload.

The actuators are modelled as systems which can provide instantaneous, constant, but limited torques. The model is shown in Fig. 4.12. T_d denotes the demanded torque to be applied by the actuator and T denotes the delivered torque.

4.3.4 Control schemes

The local control system for the actuators is shown in Fig. 4.13. The joint velocities are proportionally controlled. The proportional controller is a multivariable one, in order to compensate for the cross–coupling terms in the inertia matrix D. Let the proportional controller equal $K \cdot D$. For the part Σ of the system (Fig. 4.13) it holds:

$$\ddot{\theta}(t) = D^{-1}(\theta) \cdot D(\theta) \cdot K \cdot (\dot{\theta}_s(t) - \dot{\theta}(t)). \tag{4.6}$$

So,

$$\ddot{\theta}(t) = -K \cdot \dot{\theta}(t) + K \cdot \dot{\theta}_s(t), \tag{4.7}$$

Note that an input/output decoupled system is achieved.
When one of the calculated required joint torques to be applied by the actuators exceeds his limit, the local control system scales the required torques in such a way that they are all within their bounds, without changing the direction of the torque vector. The result is a vector of required joint torques T_d which the actuators are able to supply. The scaling makes that the End–Effector will accelerate only slower in the commanded direction.
When the torques have to be scaled, the scaling factor F is added to the closed loop expression of Σ:

$$\ddot{\theta}(t) = -F \cdot K \cdot \dot{\theta}(t) + F \cdot K \cdot \dot{\theta}_s(t). \tag{4.8}$$
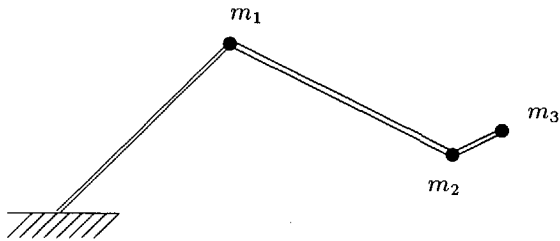
Figure 4.11: *Mass distribution of the manipulator.*
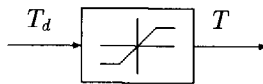
Figure 4.12: *Model 2 of the actuator dynamics.*
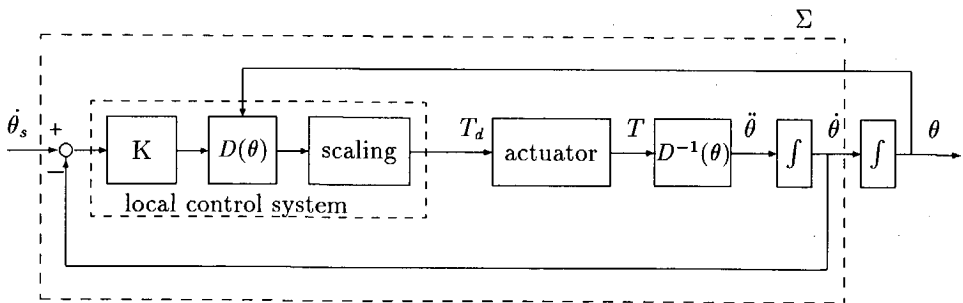
Figure 4.13: *Local control system for the manipulator whose dynamics are governed by Model 2.*

However, due to the torque limitations, the control system cannot decouple the system completely. The off–diagonal terms in the inertia matrix influence the torque vector to be scaled. The scaling, which is a non-linear operation, influences all entries in the joint velocity vector. So, changing one joint velocity setpoint can influence the response of the other joints, which means that the system is not a decoupled one.

In the experiments the operator gives rate commands to the End–Effector($\dot{X}_s$, Fig. 4.14). These velocity setpoints are proportional to the displacement of the joysticks. The velocity commands are transformed into a vector of incremental positioning commands dX, according to

$$dX = \dot{X}_s \cdot \Delta t = \begin{bmatrix} d_x \\ d_y \\ d_z \\ \delta_x \\ \delta_y \\ \delta_z \end{bmatrix}, \tag{4.9}$$

where Δt is the simulation time step, and where $d_x, d_y, d_z and \delta_x, \delta_y, \delta_z$ denote the differential translations and rotations about the x, y and z axes of a reference frame, respectively [Paul, 1981]. This vector dX defines the differential rotation and translation transformation Δ [Craig, 1986; Paul, 1981] :

$$\Delta = \begin{bmatrix} 0 & -\delta_z & \delta_y & d_x \\ \delta_z & 0 & -\delta_x & d_y \\ -\delta_y & \delta_x & 0 & d_z \\ 0 & 0 & 0 & 0 \end{bmatrix} \tag{4.10}$$

When a frame T is differentially transformed by Δ, the new T frame is given by $T := T(I + \Delta)$ or by $T := (I + \Delta)T$, where Δ is referenced to the T frame and the base frame, respectively. I denotes the 4 x 4 identity matrix.

In the control interpretation part the new required T_6 matrix, T_6^s, is calculated. The control interpretation of the differential transformation Δ depends on the reference frame used. Therefore, the transformations are described for each experiment separately. Via the inverse kinematics the required new angles, θ_s, are calculated from T_6^s. The required velocity
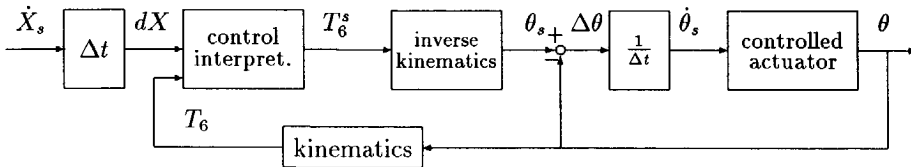
Figure 4.14: *Control scheme.*

40

setpoints of the joints are approximated by $\dot{\theta}_s = (\theta_s - \theta)/\Delta t$.

Another approach to calculate the desired joint velocities from the cartesian velocity setpoints is to calculate the inverse jacobian. This approach was not followed, because the software was not available, whereas the software of the inverse kinematics was available and the rest of the computation scheme described above was easy to implement. The performance of the control loop was sufficient for our purposes.

The joint velocities are also limited. Therefore, the calculated joint velocities also have to be scaled in order to preserve the right direction in which the End–Effector is moving or has to move. The result of this scaling is that the End–Effector moves slower in the commanded direction. However, the joint velocity limitations are such that in almost every configuration of the manipulator the maximum End–Effector velocities can be achieved.

The local control system described above is designed for Model 2 of the manipulator and actuator dynamics. When the dynamics are governed by Model 1 the control system is simplified. Then the local controller only consists of a pure gain in combination with the scaling part. But now, the required accelerations are scaled.

4.4 Displays

4.4.1 Global views

A picture which may occur in a 2D simulation is shown in Fig. 4.15. The manipulator is represented by three line segments. Also a representation of the task to be executed can be seen.

A global view which may occur in a 3D simulation is shown in Fig. 4.16. In the global view a representation of the manipulator arm, the space craft and a base plane can be seen.
 In the simulation the manipulator arm consists of 3 parts with the same width. The manipulator arm has a texture which consists of three line segments in the length direction (see also Fig. 4.17). In this way the operator can use the depth cue which is based on the relative sizes of the objects in the picture.
The reason for this relatively simple representation of the manipulator arm is the demand that the subjects experience the movements of the manipulator as continuous motions. This limits the available computation time between two succeeding pictures. Because the manipulator moves, it has to be drawn dynamically. The computer power available did, for instance, not allow solid modelling and shading techniques.

The positions of the objects are specified in the main coordinate frame which is attached to the space craft.

The base plane is divided into a number of squares. The number of squares can be specified by the user.

41
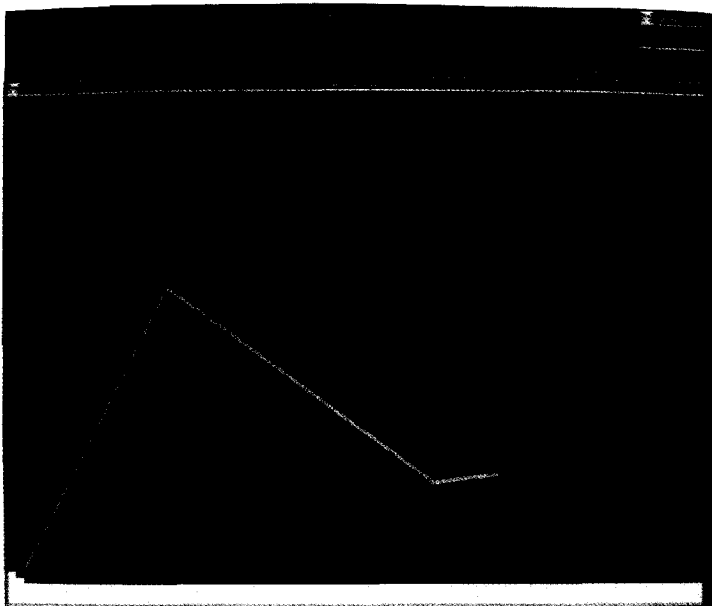
Figure 4.15: *Global view for the 2D simulation.*
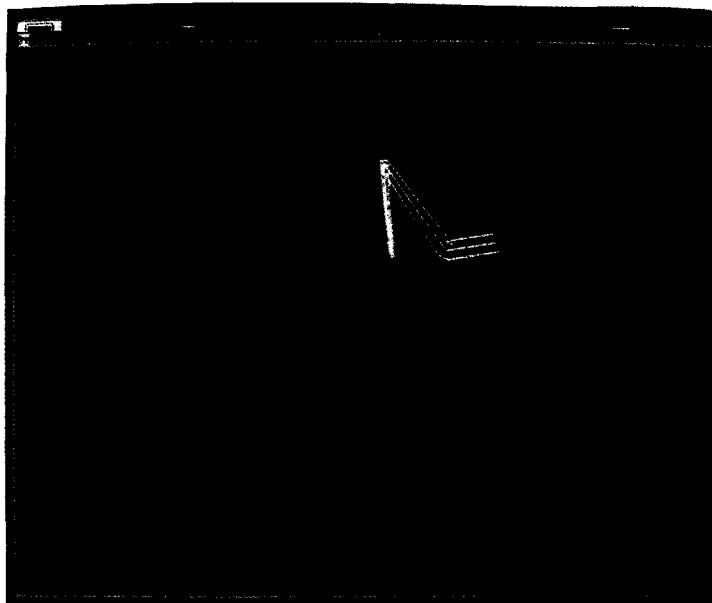
Figure 4.16: *Global view for the 3D simulation.*
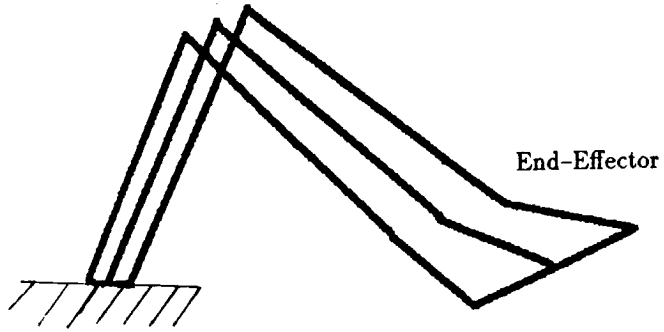
Figure 4.17: *3D representation of the manipulator arm.*
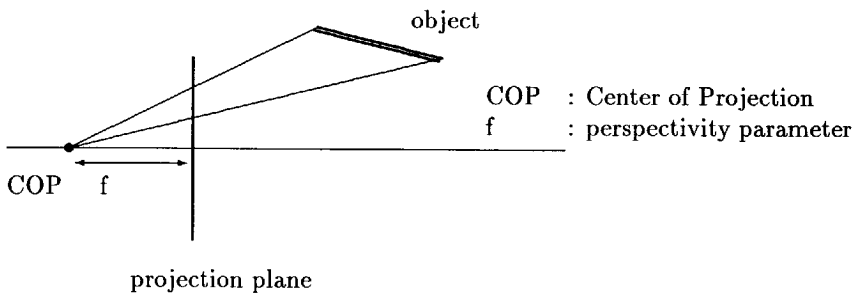
Figure 4.18: *Perspective mapping.*

Views of the scene are generated by the use of a perspective mapping [Hearn, 1986], of which the principle is shown in Fig. 4.18. The value of the perspectivity parameter can be specified by the user.

In the simulation a camera, located at the Center–of–Projection, COP, is always directed towards a *fixation point*. The location of this fixation point can be specified by the user. In the experiments the fixation point was located in the base plane.

The viewpoint of the camera, or the placement of the COP can be specified by the user. Firstly, he has to specify the distance of the COP to the fixation point (Fig. 4.19). Secondly, the user has to specify the values of two rotations around the fixation point : a rotation around the z–axis (specification of the azimuth angle) and a rotation around the (rotated) x–axis (specification of the elevation angle) of the main coordinate frame.

4.4.2   End–Effector camera view

An example of an image provided by the camera on the End–Effector is given in Fig. 4.20. The picture shows the part of the End–Effector or ORU that can be observed through the camera (white surface), the hole (black surface) and a so called vision target. In reality the shape and size of the vision target in the camera picture will result in information about the relative difference in position and orientation between the End–Effector frame and the target frame, i.e. in proximity information (see also the next section). In the most recent design the vision target consists of 3 circles, located on a straight line (Fig. 4.21). The middle circle is located in front of the two other circles. In the camera picture it can be seen when all position/orientation misfits are zero. Then the three circles are located on a straight line and their mutual distances are all equal to a predefined value. Misfits cause, for instance, that in the camera picture the three circles are not positioned on a straight line, or that their mutual distances have not the required value.

In our simulation the vision target was simplified to two squares (Fig. 4.22). The inner, twisted, square is in front of the other square. When the positioning misfits are zero, the inner square fits exactly in the outer square. Because the operator himself might also obtain three–dimensional information by observing the vision target, the vision target is also displayed in the camera picture (Fig. 4.20).

The camera is located 14.4 cm above the End–Effector surface and 64 cm from the tip of the End–Effector (Fig. 4.23).

The view provided by the End–Effector camera is generated by the use of a perspective mapping. The perspectivity parameter can be specified by the user.

4.4.3   Proximity display

Next to the End–Effector camera view, position misfit and orientation misfit indicators are displayed (see also Fig. 4.20). At the left side of the camera view the orientation misfits

44
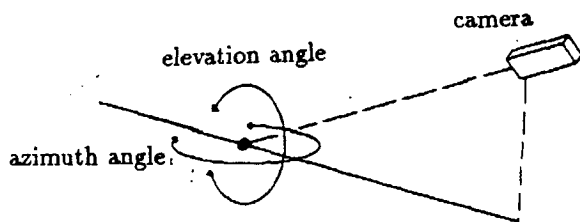
Figure 4.19: *Camera placement.*
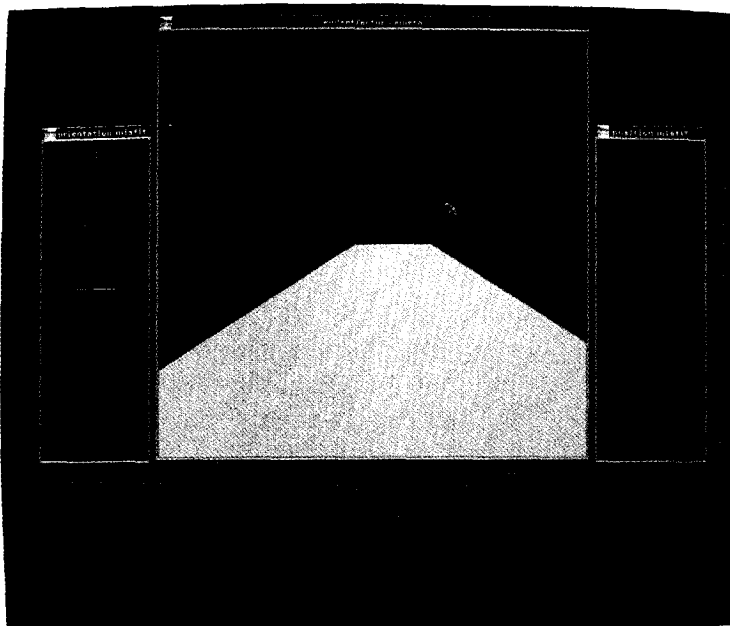
Figure 4.20: *End-Effector camera view.*

front view   top view

Figure 4.21: *The vision target.*

can be seen, and at the right side the position misfits are indicated.

When the End–Effector is, for instance, right of the middle of the hole, the left/right indicator shows a deflection to the right. The operator has to control the End–Effector to the left. in order to eliminate the position misfit. So, the operator has to control the End–Effector in the direction opposite to the displayed misfits.

The misfits are calculated relative to the target frame T_t. Firstly, the transformation matrix A_{EE} from the target frame to the frame located at the tip of the End–Effector, T_7, is calculated (Fig. 4.24):

$$A_{EE} = T_t^{-1} \cdot T_7. \tag{4.11}$$

Let

$$A_{EE} = (\vec{n}, \vec{o}, \vec{a}, \vec{p}) = \begin{bmatrix} n_1 & o_1 & a_1 & p_1 \\ n_2 & o_2 & a_2 & p_2 \\ n_3 & o_3 & a_3 & p_3 \\ 0 & 0 & 0 & 1 \end{bmatrix}. \tag{4.12}$$

The position vector $\vec{p}$ in A_{EE} is equal to the vector of position misfits. From the three orientation vectors $(\vec{n}, \vec{o}$ and $\vec{a})$ in A_{EE} the orientation misfits can be calculated [Craig, 1986, p. 41]:

$$yaw - misfit \quad = \quad atan2(a_2, a_3); \tag{4.13}$$

$$pitch - misfit \quad = \quad atan2(-a_1, \sqrt{n_1^2 + o_1^2}); \tag{4.14}$$

$$roll - misfit \quad = \quad atan2(o_1, n_1). \tag{4.15}$$

The sensitivity range of a display has to be such that the maximum allowed misfits for the insertion are within the resolution of the display. The operator has to see whether he can perform the insertion safely. Because of the small tolerances, and thus the small maximum misfits, the indicators show mostly a maximum deflection when starting the insert task. In the beginning the hole is relatively far away. Then the operator can use the proximity display only to determine the direction of the position and orientation misfits.

When a misfit comes in the sensitivity range of its indicator, overshoot easily occurs. Due to the limited accelerations of the manipulator and the large sensitivity of the indicators it appeared that the moment an indicator showed a visible change in its displayed misfit, the manipulator could not be stopped in time to prevent overshoot. Therefore, warning signs were built in, to indicate that a certain indicator will show a deflection change within a reasonably short time. The warning sign consists of a blue ball which appears and starts to flicker near the corresponding indicator. The blue ball disappears when the misfit becomes smaller than the maximum deflection.

When the End–Effector is not inserted yet, the display shows the proximity information. When the End–Effector is being inserted the proximity display can be interpreted as a force/torque display.

front view

top view
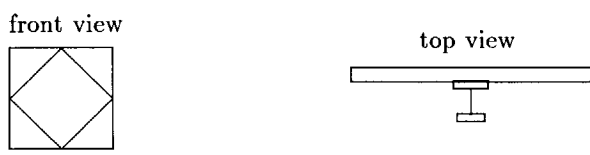
Figure 4.22: *The vision target in the simulation.*

camera

14.4 cm   64 cm
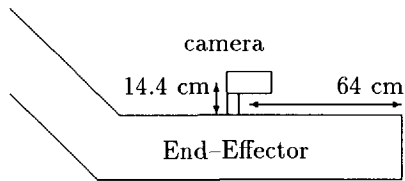
End–Effector

Figure 4.23: *End–Effector camera placement.*

B ⟶ T_7

T_t

A_{EE}
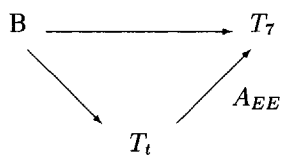
Figure 4.24: *Definition of the transformation matrix A_{EE} from the target frame to the frame located at the tip of the End–Effector.*

4.4.4 Predictive display

To let an operator cope with the slow and non-linear dynamics the use of a predictive display was investigated. A predictive display shows to the operator a future response of the system under control. A certain assumption is made about the future commands of the operator, on the basis of which the prediction is calculated.

Two kinds of predictive display were investigated. Firstly, the display of the stopping configuration, i.e. the configuration in which the manipulator will stop when setting all rate setpoints to zero. Secondly, showing a predicted trajectory of the manipulator over a certain time horizon. When calculating the prediction in the latter case, it is assumed that the rate commands remain constant over the prediction horizon.

display of the stopping configuration

The calculation of the stopping configuration is given in appendix C. The stopping configuration is displayed on the monitor as a *ghost manipulator*. In the 2D case the line segments of which the displayed ghost manipulator exists, are much smaller (Fig. 4.25). In this way the operator clearly knows which of the two displayed configurations is the stopping configuration.

In the 3D situation the distinction between the actual manipulator and the stopping configuration is achieved by displaying the stopping configuration in a different color, which is green (Fig. 4.26). Also the tip and the wrist of the stopping configuration can be projected on the base plane through the use of reference lines.
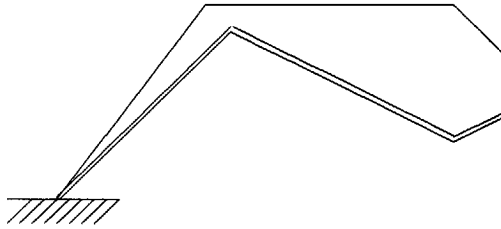
Figure 4.25: *Display of the stopping configuration for the 2D simulation.*
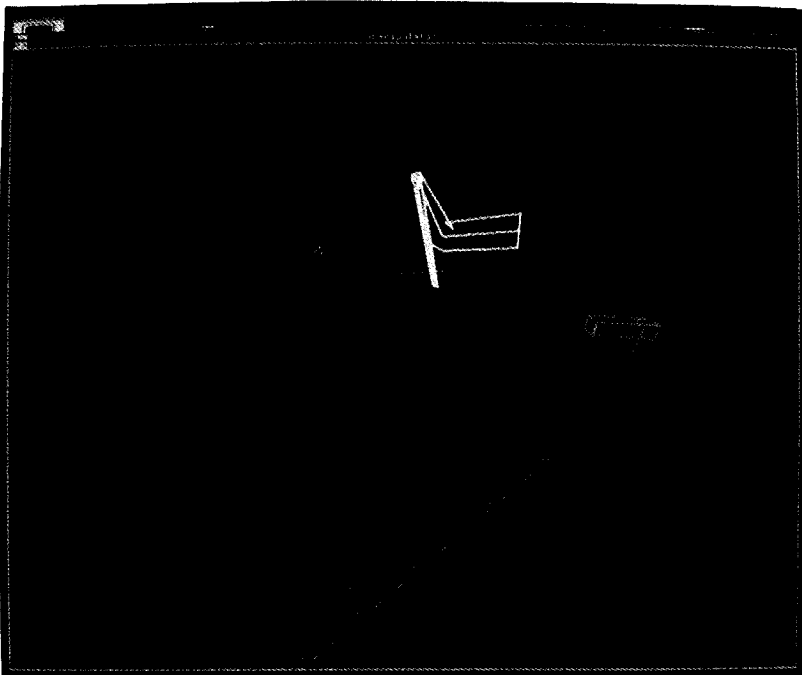
Figure 4.26: *Display of the stopping configuration for the 3D simulation.*

<u>display of the predicted trajectory</u>

In order to display the predicted trajectory over a certain time horizon, the time horizon is divided into three equal time intervals. For each end–point of such a time interval the predicted positions of the wrist and the tip of the End–Effector are calculated (see appendix D). The predicted trajectory of the wrist and the tip consists of the curve through their three predicted positions (Fig. 4.27). The end–points of the predicted trajectories of the wrist and the tip of the End-Effector are connected by a straight line. This line is the predicted orientation of the End–Effector. Pilot experiments [Bos, 1989] indicated that such a line would be desirable, because otherwise the subjects internally have to combine the two predicted trajectories in order to calculate an estimation of the predicted orientation.
In the 3D situation the three calculated positions of which a predicted trajectory consists, are projected on the base plane through the use of reference lines (Fig. 4.28). The predicted trajectory is displayed in green.

In pilot experiments [Bos, 1988] also the predicted trajectory of the elbow was displayed for safety reasons. Not only the End–Effector, but also the links can hit an obstacle. However, this extra information was rarely used. All subjects concentrated on the movements of the End-Effector. They mostly did not even notice the predicted trajectory of the elbow. Therefore, in the experiments reported in this thesis the predicted trajectory of the elbow was not shown.

In try–outs, displaying a predicted trajectory turned out to be favourable over the display of a predicted configuration, as it has been done for the stopping configuration. The predicted configuration showed only the connected, over the time–horizon predicted, positions of the elbow, wrist and tip. This fact was rated as a disadvantage when a curve has to be made around an obstacle. Another disadvantage was that the display of the predicted configuration is also too restless.

An important issue in the realization of a predictive display is the length of the time horizon over which the prediction is calculated. On the basis of the pilot experiments [Bos, 1989] it could be concluded that, for safety reasons, the prediction horizon must be longer than the time needed to stop the manipulator. Then the prediction covers also the stopping configuration. When the prediction horizon is smaller than the time needed to stop the manipulator, the prediction can move further on, although the rate setpoints are set to zero. The subjects experienced this fact as very confusing and dangerous.
The idea behind the applied concept was to let the prediction horizon equal the stopping time. However one wants also to see the predicted result of a command immediately. When the manipulator is at rest the stopping time is 0 seconds and no future results can be seen. Only when the manipulator begins to move gradually the predicted results become clear. Therefore, the length of the prediction horizon T_{pred} equals the maximum of a constant,
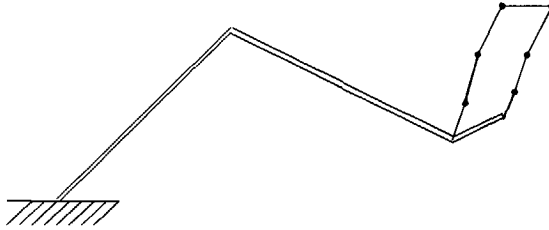
Figure 4.27: *Display of the predicted trajectory for the 2D simulation*
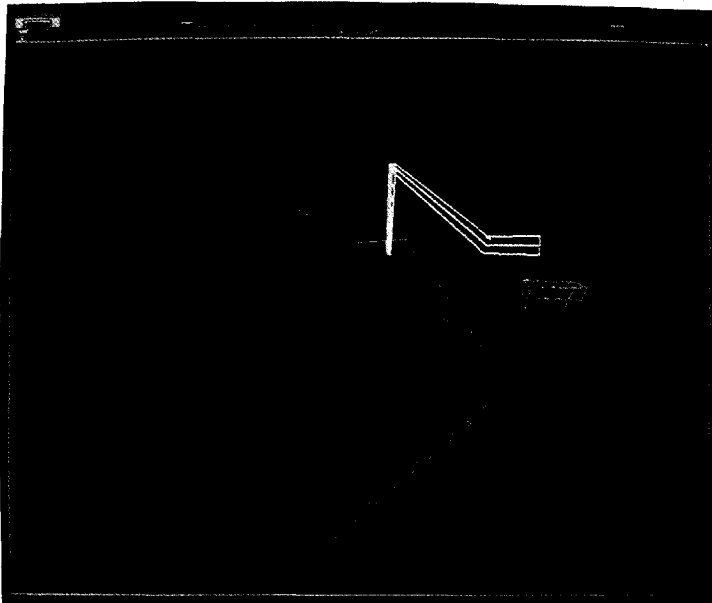
Figure 4.28: *Display of the predicted trajectory for the 3D simulation.*

minimal, time horizon T_{min} and the stopping time T_{stop} :

$$T_{pred} = maximum(T_{min}, T_{stop}).\qquad(4.16)$$

The time needed to stop the manipulator depends on the configuration of the manipulator and of course the actual velocity. Therefore, the actual prediction horizon is calculated on–line. The minimal horizon T_{min} is chosen such that it is mostly a bit larger than the stopping times.

Chapter 5

Visibility aspects for a rough positioning task

5.1 Introduction

When the human operator controls HERA, he can be placed in the cockpit of Hermes or on Earth. In both scenarios the operator cannot see the manipulator and its environment directly, i.e. in three dimensions, but he has to cope with two–dimensional TV pictures. Apart from TV pictures, the use of graphical displays is foreseen. An advantage of graphical displays is that they can be used for providing views from viewpoints where no camera is or can be present, provided that a model of the environment is available. The question is then how these displays can be used to provide the operator with a good, three–dimensional perception of the scene.

A first choice can be to use a *perspective mapping* [Hearn, 1986] of the scene (Fig. 5.1, see also Section 4.4.1). But there remain the questions of what viewpoint should be used, what field of view should be used, what a good value for the perspective parameter will be, and whether multiple views at the same time should be provided.

The viewpoint is determined by the azimuth angle, the elevation angle and the distance of the COP to the fixation point. The results in [Kim et.al., 1987], show that the elevation angle preferably has to lie somewhere between 30–70 degrees. The value of the azimuth angle is not so critical, but it has to be such that the compatibility between the direction of the operator's commands and the corresponding movements on the screen is preserved. The field of view (Fig. 5.1) is determined by the value of the perspectivity parameter and the size of the projection plane. The value of the perspectivity parameter f is the distance of the COP to the projection plane. The projection obtained with a wide field of view angle is similar to the picture taken by a wide–angle camera lens, and a narrow field of view angle to a telephoto lens. When the field of view is increased by decreasing the perspectivity parameter, a displayed object becomes smaller, because a "wider" environment has to be projected on the same projection plane. Therefore, task performance can degrade [Kim et.al., 1987]. A large value of the perspectivity parameter decreases the experienced perspectivity and the amount of three–dimensional information in the picture. When the

COP : Center of Projection

f : perspectivity parameter

FOV : Field of View

projection plane
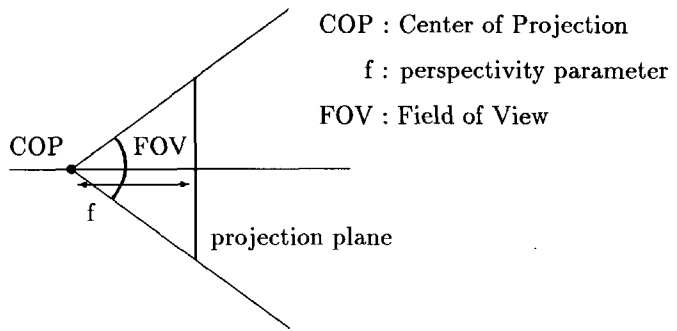
Figure 5.1: *Field of view.*

A, B, C, D : target locations
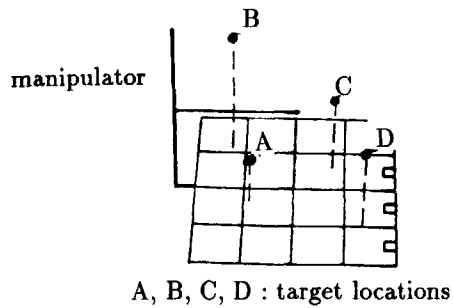
Figure 5.2: *Monoscopic perspective presentation using nominal perspective parameters used in [Kim et.al., 1987].*

value is infinity, a flat projection (without perspectivity) is obtained, which degrades the three–dimensional information.

In aircraft applications [Ellis, McGreevy, 1987] as well as in some teleoperation experiments [Kim et. al., 1987], the use of reference lines, i.e. projections of an object on a base plane or grid (Fig. 5.2, the dashed lines) gave good results. The use of reference lines can be motivated by the fact that a light source projects a shadow of an object on the ground. The presence of shadows is one of the depth cues for a human being [Strattmann, 1988; Overbeeke, 1988; Klashorst, 1988].

In [Kim et.al., 1987] the subjects had to execute a three–dimensional pick–and–place task. They had to control a cylindrical manipulator with 3 DOF. The manipulator was position controlled and it was fastly responding. The completion times varied from 2 to 10 seconds. In the monovision experiments only one picture was available. The results showed that the use of reference lines led to considerable smaller completion times. When the monoscopic display was defined with appropriate perspectivity parameters and provided with reference lines, the performance was equivalent to that of a stereoscopic display.

In the first experiment reported in this chapter, the results obtained by Kim were evaluated for a situation where the operator has to execute a rough positioning task with a space manipulator with 5 DOF. So, not only the position, but also the orientation of the End–Effector had to be estimated from the picture. In addition a space manipulator can be slowly responding and it is rate controlled. Contrary to [Kim et.al., 1987], where the subjects had to estimate the position of the End–Effector from only one viewpoint, in the experiments reported here the subjects could use two different viewpoints [Klashorst, 1989].

In the MMI of the American Remote Manipulator System a split–screen facility was provided [Covault, 1981a, 1981b]. In the second experiment the usefulness of such a facility was evaluated when two different views of the scene are available.

5.2   Purpose of the experiments

The questions which have been investigated here are whether the three–dimensional perception of the human operator improved in the case that:

1. the position and orientation of the End–Effector are visualized when projecting the End–Effector on a ground plane,

2. two views, instead of one, out of two available views are simultaneously displayed (split–screen).

The assumption was that a better three–dimensional perception would lead to a better control performance with respect to the performance criteria given in Section 5.4.4.

5.3 Experimental facility

The subjects had to execute a rough positioning task (Section 4.2.1). The subjects themselves had to determine whether the positioning requirements were fulfilled. The dynamics of the manipulator were governed by Model 1 (Section 4.3.2). The mass attached to the End–Effector was 3500 kg. The maximum translational velocities were 0.05 m/s. For a study towards visibility aspects for a rough positioning task the roll motion of the End–Effector, i.e. the sixth DOF, is of no importance. Therefore, only 5 DOF of the manipulator could be controlled in the experiments.

The experiments were performed in the End–Effector rate mode. The wrist of the End–Effector served as POR. The base frame served as reference frame. The directions of the base frame did coincide with the direction of the grid of the base plane. The use of the base frame as reference frame meant that the commands were issued in a frame B_1 of which the orientation is equal to the orientation of the real base frame B, but which is positioned at the POR, the wrist of the End–Effector. Let $[x_6, y_6, z_6]^T$ denote the position of the POR in the base frame. Then

$$B_1 = \begin{bmatrix} 1 & 0 & 0 & x_6 \\ 0 & 1 & 0 & y_6 \\ 0 & 0 & 1 & z_6 \\ 0 & 0 & 0 & 1 \end{bmatrix}. \tag{5.1}$$

The control scheme as given in Section 4.3.4 was used. In the control interpretation part the new T_6 matrix was calculated according to:

$$T_6^s = T_6 + B_1 \cdot \Delta \cdot B_1^{-1} \cdot T_6, \tag{5.2}$$

where Δ is referenced to the B_1 frame.

The translational rate commands were issued by the use of a 3 DOF joystick. The displacements of the joystick were proportional to the rate setpoints. A dead–band was used which was equal to one tenth of the maximum deflection. Because a second joystick was not yet available at the time of the experiments, a mouse was used as input device for the orientation commands.

pitch
0.010

yaw   – 0.025
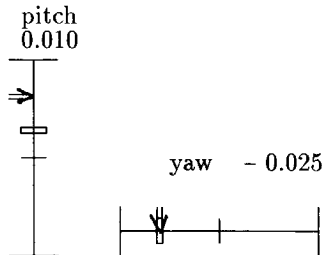
Figure 5.3: *The orientation command interface.*

Table 5.1: *Experimental conditions experiment 1.*

reference lines End–Effector	reference lines target	
	no	yes
no	A	C
yes	B	D

The layout of the graphical control interface for the orientation commands is shown in Fig. 5.3. By positioning the pointer of the mouse, the subjects could issue pitch or yaw commands. By pressing the left button on the mouse input device a command was issued. Then at the position of the pointer a bar was displayed in the scale of the pitch or yaw meter. Also a numerical display of the command was present. An arrow served as a display of the actual angular speed. During try–outs it turned out that the subjects had a strong need for a clear zero–rate command, so that they did not have to worry about the fine positioning of the pointer to realize a zero–rate command. This command could be realized by pressing the middle button on the mouse input device.

The subjects could switch between two camera views. An example of a camera view is given in Fig. 4.16 in Section 4.4.1. The views were different for different combinations of start configurations of the manipulator and target locations. By clicking a button on the mouse input device the subjects could switch between the two available views. The used value of the perspectivity parameter corresponded to a camera lens of 65 mm.

5.4 Experimental procedure

5.4.1 Experimental conditions

experiment 1

Investigated was whether the use of reference lines from the End–Effector did improve the performance of the operator.
However, the effectivity of the use of reference lines can depend on the target position. The target position can have a fixed and known position with respect to Hermes, which is for instance the case for an ORU storage location. Also, the target may float in space, which is the case when a satellite has to be grappled. The first situation is modelled in the simulation by projecting the target on the base plane too. So, four experimental conditions A, B, C and D were defined (Table 5.1).
The subjects were able to switch between the two available views.

experiment 2

Two views from different viewpoints were available. It was investigated whether the perfor-

mance of the operator improved when the two available views were displayed simultaneously on one monitor (split-screen). So two conditions were defined :

1. the display of only one view at the time, with the operator able to switch from viewpoint,

2. the display of two views simultaneously.

No reference lines were present.

5.4.2   Training

A first part of the training was a so called *system training*, where a subject became acquainted with the system to be controlled and with the experimental facility. This training lasted until a subject had achieved a constant level of performance. The system training lasted about 2 hours.
In the second part, the *task training*, a subject trained the different experimental conditions prior to the experiments. The same starting configurations were used as in the experiments. This training lasted about half an hour for each experiment.

5.4.3   Instruction

The most important goal in the task execution was to fulfill the requirements on the positioning accuracy. Then, the task was succesfully executed. In order to avoid that the subjects would lengthen their task execution to obtain a positioning as accurate as possible, also the instruction to execute the task as fast as possible was given. However, the emphasis was focussed primarily at a succesful task execution.

5.4.4   Data collection

The performance of the subjects was measured in terms of:

- Number of *incidents.*

- Number of *accidents.*

- *Completion time.*

- *Dead–time fraction*, i.e. the percentage of the completion time in which the manipulator did not move.

- Number of *viewpoint switches.*

- *Subject opinions.*

Table 5.2: *Number of incidents and accidents for 60 runs per experimental condition for experiment 1.*

experimental condition	incidents	accidents
no ref. lines	22	2
ref. lines from only EE	17	1
ref. lines from only target	18	1
ref. lines both EE and target	13	0

5.4.5   Subjects

Six male subjects performed the experiments. The subjects were Control Engineering students at the Delft University of Technology and were about 22 years old. The subjects were paid Dfl. 10,00 per hour.

5.5   Results

5.5.1   Results experiment 1: the use of reference lines

Incidents/accidents

In Table 5.2 the number of occurred incidents and accidents is given. It indicates that projecting the End–Effector (EE) on a base plane led to a safer task execution, both for a known and an unknown target position. The safest situation was the situation where the End–Effector as well as the target was projected.

Completion time

To give a general idea of the effects of the experimental conditions on the task completion time, the average completion times per subject are given in Fig. 5.4. When the target was projected on the base plane, 5 out of 6 subjects performed the task faster when also the End–Effector was projected. However, the differences for each subject were not significant at a 5% level. Generally 7 out of 10 runs were performed faster, which is illustrated for subject 4 in Fig. 5.5. Averaged over the subjects the significance was 5% (Sign).
When the target was not projected, projecting the End–Effector did not lead to a faster task execution.

Viewpoint switches

In Fig. 5.6 the number of viewpoint switches, averaged over the subjects, is shown. Projecting the End–Effector causes that the subjects switched less from viewpoint.
In Table 5.3 it can be seen that the number of viewpoint switches was (strongly) correlated with the completion time. Generally, the correlation decreased when the End–Effector was projected on the base plane.
When looking at the frequency of viewpoint switches (Fig. 5.7), it can be seen that it decre-
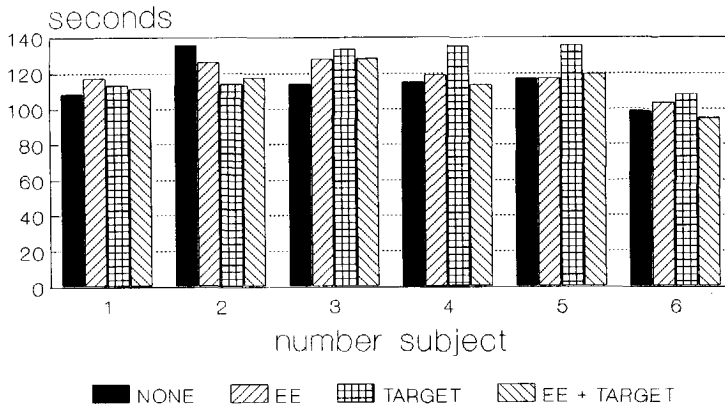
Figure 5.4: *Average completion times experiment 1.*
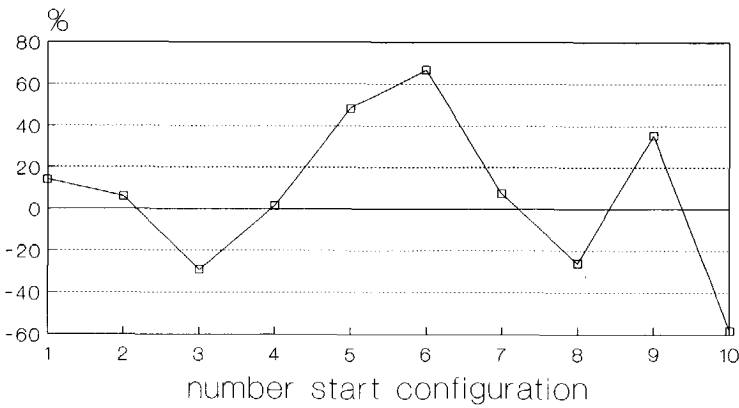
Figure 5.5: *Percentual improvement in completion times for subject 4 when adding reference lines from the End-Effector for a known target position; experiment 1.*

Table 5.3: *Correlations between the number of viewpoint switches and the completion times for experiment 1.*

A : no ref. lines
B : ref. lines from only End–Effector
C : ref. lines from only target
D : ref. lines from both End–Effector and target

difference	subject					
	1	2	3	4	5	6
A	0.74	0.97	0.92	0.91	0.82	0.66
B	0.88	0.84	0.75	0.68	0.60	0.93
C	0.93	0.91	0.76	0.87	0.65	0.39
D	0.55	0.27	0.67	0.23	0.79	0.59
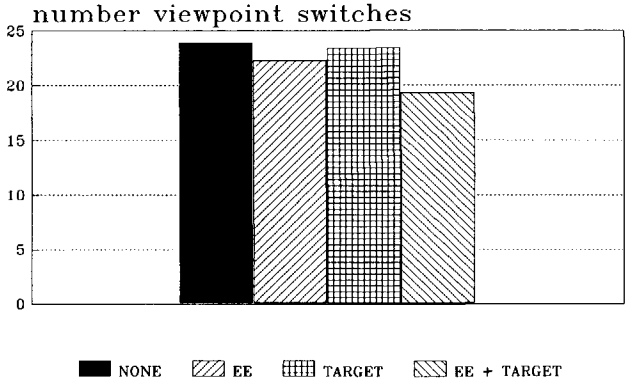
Figure 5.6: *Average number of viewpoint switches for experiment 1.*

Table 5.4: *Significance of differences in frequency of viewpoint switches for experiment 1.*

A : no ref. lines
B : ref. lines from only End–Effector
C : ref. lines from only target
D : ref. lines from both End–Effector and target

difference	subject						
	1	2	3	4	5	6	all
B < A	0.02	0.48	0.24	0.02	0.23	0.02	0.51
D < A	0.01	0.19	0.26	0.22	0.11	0.01	0.90
D < C	0.03	0.04	0.88	0.59	0.72	0.03	0.05

ases when projecting the End–Effector. From Table 5.4 it can be concluded that only for two subjects this result was significant at the 5% level, both for a known and an unknown target position. However, the lower frequencies indicate that the subjects could extract more information from one picture when reference lines were present.
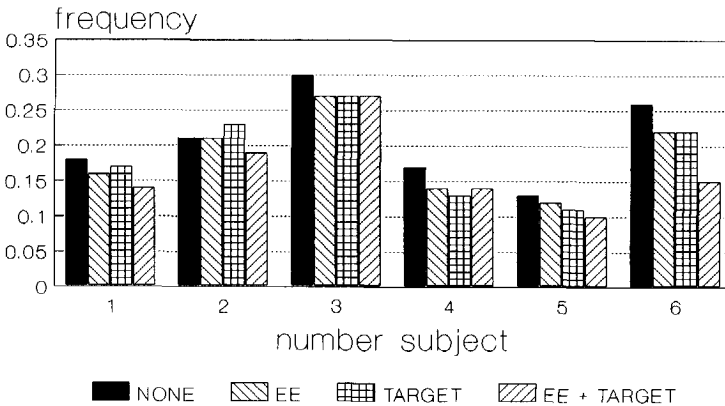
Figure 5.7: *Average frequencies of viewpoint switches; experiment 1.*

62

Table 5.5: *Number of incidents for 10 runs per experimental condition for experiment 2.*

experimental condition	subject					
	1	2	3	4	5	6
1 view	5	0	1	4	11	3
2 views	1	2	3	3	25	1

Table 5.6: *Significance of the difference in dead–time fraction for experiment 2 Wilcoxon test per subject and Sign test for all).*

difference	subject						
	1	2	3	4	5	6	all
2 views < 1 view	0.04	0.03	0.02	0.41	0.07	0.03	0.0002

5.5.2   Results experiment 2: the split–screen facility

Incidents/accidents

No accidents did occur. The number of incidents per subject is shown in Table 5.5. When the odd results of subject 5 are neglected, it can be seen that no clear difference with respect to the safety exists between the two experimental conditions.

Completion time

In Fig. 5.8 the average completion times per subject are shown. The differences were not significant at the 5% level. Generally 65% of the runs were performed faster when the two views were displayed simultaneously.

Dead–time fraction

In Fig. 5.9 the average dead–time fractions are shown per subject. The dead–time fraction is smaller when the two views are displayed simultaneously. The significance levels of the difference are shown in Table 5.6.

5.6   Subject opinions

Experiment 1 : the use of reference lines

The subjects clearly preferred the presence of reference lines from the End–Effector, both for a known and an unknown target position. The reference lines quickly provided the subjects with a good idea about the position and orientation of the End–Effector and target.
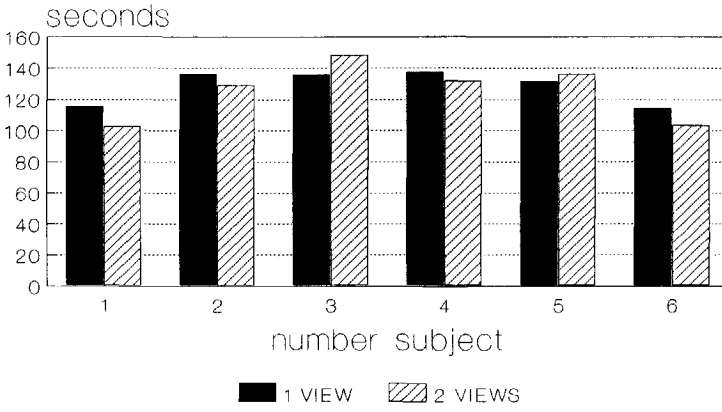
Figure 5.8: *Average completion times experiment 2.*
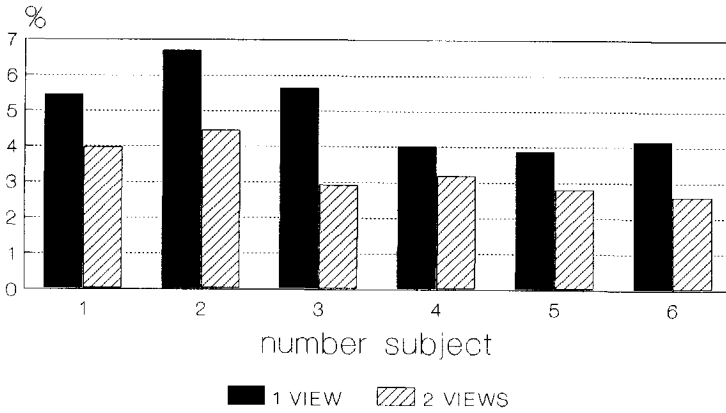
Figure 5.9: *Average dead–time fractions experiment 2.*

The subjects used the reference lines mainly in the beginning of a task execution and in the end positioning phase. In between these two phases the reference lines were of less use. This is not surprising because, except for the safety plane, there were no environmental restrictions to the movements of the manipulator. The subjects needed only an estimation of the start configuration of the manipulator and the end positioning requirements to plan a trajectory to be followed.

Experiment 2 : the split–screen facility

The subjects did not have a clear preference for one of the two situations. When two views were displayed simultaneously the subjects needed not to switch between the two views to obtain a good three–dimensional impression. Especially in the beginning of a task execution this was rated as an advantage.
The fact that the size of the pictures became twice as small when the two views were displayed simultaneously (split–screen) was rated as a disadvantage. Firstly, in the end positioning phase it was harder to decide whether the positioning requirements were fulfilled. Secondly, the smaller pictures gave the subjects a more remote feeling, i.e. the feeling of telepresence decreased compared to the situation with one larger picture. Some subjects experienced the switching between the two views as a natural action.

General remarks

The subjects found it hard to estimate the orientation of the End–Effector. The pitch and yaw movements seemed to be dependent. Consider for instance Fig. 5.10. Controlling the yaw movement makes that the tip of the End–Effector is moving "further away" from the camera. Therefore, the tip moves also "up" in the camera picture, and it seems that the pitch also has changed. However, the distance of both the wrist and the tip to the base plane remained the same, because the pitch was not commanded. This fact was experienced as very confusing.
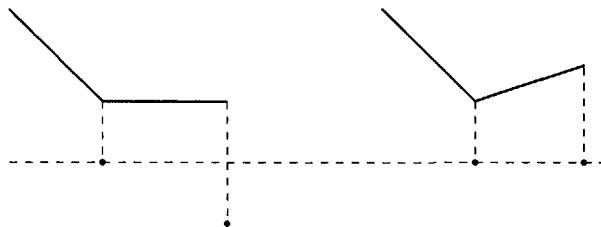
Figure 5.10: *Experienced interaction between pitch and yaw movements.*

Another problem for the subjects was to make a good estimation of the height. The use of reference lines improved the estimation considerably, according to the subjects.

The use of a mouse as input device for the orientation commands was not appreciated. A second joystick would have been far more pleasant.

5.7   Discussion

The large correlation between the number of viewpoint switches and the completion time can be explained by the fact that operators switch regularly from viewpoint to estimate the three–dimensional position of the End–Effector. In the situation with the most depth cues, i.e. the situation where reference lines were present from both the target and the End–Effector, there existed the least correlation between the number of viewpoint switches and the completion times. This implies that in that situation the subjects switched less regularly from viewpoint. The lower frequencies of viewpoint switches implies that the subjects had less need for a second view, which implies that they could extract better three–dimensional information from one view, when reference lines were present.

The research towards the use of reference lines did not lead to very clear results, contrary to the results in [Kim et.al., 1987]. This can have three reasons. Firstly, the task to be executed was not critical enough for misfits in position estimations by the subjects. The positioning requirements were not so strict. Secondly, the subjects could compensate the lack of a good three–dimensional perception from one view with no (or less) reference lines by intergrating the two different views more intensively. The higher frequency of viewpoint switches confirms this. In [Kim et.al., 1987] the subjects had only one view available. Thirdly, the lack of a clear difference in completion times can be explained by the small maximum velocities of the manipulator. Contrary to [Kim et.al., 1987] the manipulator responded quite slowly. So, the possibilities for a faster task execution were limited. One may compare this situation with two cars finding themselves in a traffic jam. Although the cars might have quite different maximum speeds, they are forced to drive equally fast.

To test the correctness of this explanation for not having obtained very clear results, a small experiment was performed. A subject had to execute the same rough positioning task, but now obstacles were present in the environment (Fig. 5.11), and the manipulator was unloaded, thus far more quickly responding. The maximum End-Effector velocity was 0.1 m/s. The target was projected on the base plane. It was investigated whether also projecting the End–Effector led to a better performance. The results are summarized in Table 5.7, and they support the stated explanation.

When looking at the viewpoint switches, the number of incidents and the subject opinions all together, it can be concluded that it is desirable to project the End–Effector on a base plane, especially for a known target position.

Also the comparison between the situation with no reference lines and the situation where both the target and the End–Effector are projected on a base plane is an interesting one. It gives insight into the desirability of a position measuring system for a satellite to be grappled. The results indicate that such a system would be useful to an operator. Of

Table 5.7: *Results for 14 runs with a faster responding manipulator, and with obstacles present in the environment.*

ref. lines from EE	number of incidents	completion time [s]	average number of viewpoint switches	average frequency of viewpoint switches
no	8	109	6.8	0.06
yes	0	73	1.6	0.02
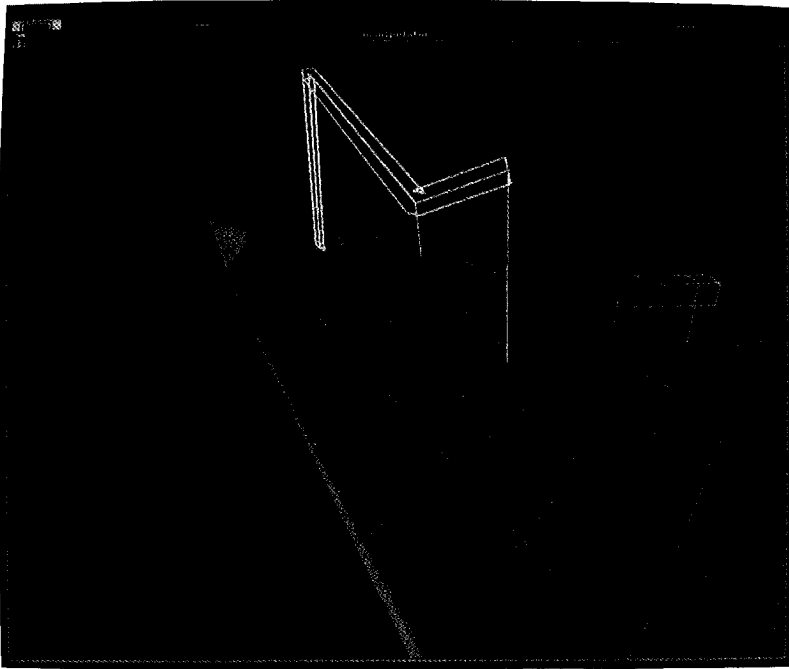
Figure 5.11: *Global view for a rough positioning task with obstacles present in the environment.*

course the profits have to be balanced against the extra costs of such a system.

When only one view was displayed at the same time, the dead–time fraction was larger. In this situation the subjects had to switch between the two different views. They mainly switched when the manipulator was at rest, to avoid dangerous situations. Despite of the larger dead–time fraction, the subjects performed the task at least as fast as when two views were displayed. Due to larger pictures the decision whether the end positioning requirements were fulfilled took less time.

When displaying two views simultaneously the subjects tended to control more DOF at the same time. This led to more failures and thus to more corrective actions. Mostly, the subjects forgot to give a zero–rate command for the pitch and/or yaw DOF. Contrary to the joystick, which was self–centering, the subjects had to give an active zero–rate command with the mouse. Probably, the mental load became too large when they controlled a large number of DOF simultaneously. This may be the reason that there was no improvement in the performance of the subjects, in spite of the fact that the subjects found that they had more information.

The results of experiment 2 indicate that a split–screen facility is not very necessary for the rough positioning part of a task. Especially when the pictures would be enhanced with better three–dimensional information through the use of reference lines a split–screen facility seems to be not very necessary. However, this was not investigated, so it is merely the opinion of the author. Note that this conclusion is restricted to the situation with two different *global* views. When the operator has to switch from a global view to the End–Effector camera view, indeed it can be desirable to present both views.

There were 14 uncompleted runs, i.e. runs which were ended by an accident or where the positioning requirements were not fulfilled. This is 4% of the total number of 360 runs in both experiments. The small number of uncompleted runs indicates that the subjects have executed the task according to the instruction.

In 25% of the runs at least one incident occurred. It was not clear whether this relatively large number was caused by a bad three–dimensional perception or by the second part in the instruction to perform the task as fast as possible. The latter may also have caused a number of incidents, because subjects are willing to take some risk in the task execution.

5.8   Conclusions

The presence of reference lines enhanced the three–dimensional perception, which resulted in a tendency towards a safer task execution.

A split screen facility for displaying two available survey views does not seem to be very necessary.

The task to be executed was not critical enough for misfits in position estimations by the subjects; the results did not lead to statistically significant conclusions.

Chapter 6

On task allocations between man and computer for an insert task

6.1 Introduction

A sub-task to be executed is the insert, or peg–in–hole, task. For instance, this task has to be excuted when a container with supplies has to be stored into a storage location or hole. Such a container is called an Orbit Replaceble Unit (ORU). Generally this insert task has to be excuted in the End–Effector control mode [Ravindran, Doetsch, 1982]. End–Effector control has two aspects. The first aspect is the Point-Of-Resolution (POR) which is defined as the origin of a local coordinate frame, related to the End–Effector of which position and orientation are the quantities to be controlled. The second aspect is the reference frame. It is the coordinate frame to which the operator's commands to the POR are referenced. In the case of an insert task, the End–Effector frame functions as reference frame, and the tip of the End–Effector or payload as POR.

When using the End–Effector frame as reference frame, the direction of a translation depends on the orientation of the End–Effector. This might cause inefficient control and unsafe situations. For instance, consider the situation as given in Fig. 6.1. When con-
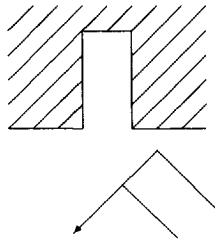
Figure 6.1: *Translation to the left in End-Effector frame.*

70

trolling the End–Effector to the left, also a translation away from the hole occurs. When controlling the ORU further forward into the hole, translations to a side of the hole may occur. Because the tolerance of the hole will only be a few milimeters, contact situations and even jamming (Fig. 4.7) may occur.

A possible solution is the use of the target frame as the reference frame (Fig. 6.2). This can be done when the orientation of the target is known. Within the HERA project a camera is foreseen, located on the End–Effector. The camera picture will be processed, using vision techniques, into information about the relative difference in position and orientation between the End–Effector frame and the target frame (Sections 4.4.2 and 4.4.3).

The possible benefits of using the target frame, instead of the End–Effector frame, have been studied in the first experiment.

However, the true limiting factor for the human operator is probably the fact that he has to control up to 6 DOF. When the relative difference in position and orientation between the End–Effector frame and the target frame can be measured, closed loop control schemes can be designed, which reduce the number of DOF to be controlled by the human operator. Consider for instance Fig. 6.3: when both the current postion (p_1) and the aimed position (p_2) are known, the aimed direction is known. Then, the operator needs only to provide a velocity setpoint, thus 1 DOF, in the specified direction. A similar scheme can be applied for the control of the orientation. In this way, the number of DOF to be controlled by the human operator is reduced to 2. The evaluation of such a control scheme has been performed in the second experiment.

6.2   Purposes of the experiments

For the execution of the insert task in the End–Effector control mode, it was expected that the use of the target frame (EE/target mode), instead of the End–Effector frame (EE/EE mode), would result in a safer and more efficient task execution. Also the reduction of the number of DOF to be controlled by the human operator from 6 to 2 was expected to result in a better task execution. Therefore the hypotheses to be tested in the experiments were :

1. The EE/target control mode leads to a safer and more efficient task execution compared to the EE/EE control mode,
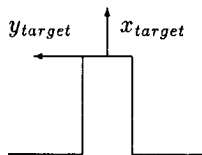
Figure 6.2: *Target frame.*

2. The 2 DOF control mode (2DOF mode) does lead to a safer and more efficient task execution, compared to both the EE/target control mode and the EE/EE control mode.

6.3 Experimental facility

The subjects had to execute an insert task (Section 4.2.2). They were informed by the computer whether the task was completed, through a green flickering ball in the proximity display. Visual information about the scene is provided by the camera on the End–Effector (Section 4.4.2) and the proximity display (Section 4.4.3). The angle of view of the camera was 90 degrees, and the perspectivity parameter equalled 120 mm.

The dynamics were governed by Model 1 (Section 4.3.2), where the state dependent dynamics, due to the changes in inertia, were not taken into account. For an insert task these changes are reasonably small, because the displacements of the masses are small. The maximum accelerations were:

$$\ddot{\theta}_{max} = \begin{bmatrix} 0.0026 \\ 0.0026 \\ 0.0026 \\ 0.006 \\ 0.0055 \\ 0.0270 \end{bmatrix} \; rad/s^2.$$

It was assumed that the control system was designed in such a way that the flexibility modes were not excited. This is an idealization of reality. The influence of the flexibility on an insert task must be subject of future research.
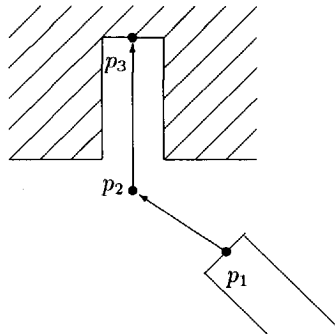
Figure 6.3: *2DOF mode.*

The subjects had to control all 6 DOF in the End–Effector modes and 2 DOF in the 2DOF mode. The subject controlled the manipulator by providing velocity commands $\dot{X}_s$ (Fig. 4.14, Section 4.3.4). Depending on the control mode 1 or 2 joysticks were used as input device.

The velocity setpoints were proportional to the displacement of the joysticks. A dead–band was used which was equal to one tenthed of the maximum deflection. The maximum velocities were determined after some preliminary experiments [Doorenbos, 1989b], and they were equal to:

up/down	: 0.0125 m/s;
left/right	: 0.0125 m/s;
forward/backward	: 0.025 m/s;
yaw	: 0.023 rad/s;
pitch	: 0.032 rad/s;
roll	: 0.023 rad/s.

The POR was the tip of the ORU, but in the inverse kinematics computation scheme the joint angles are calculated from the T_6 matrix which is located in the wrist. So the transformation graph as shown in Fig. 6.4 was used in order to calculate T_6^s, the required (new) position and orientation of the wrist. In this scheme B is defined as the base frame, A_7 as the translation from the T_6 frame (located in the wrist) to the tip of the ORU (T_7 frame), and A_t as the transformation matrix from T_7 to the target frame T_t.

When a frame T is differentially transformed by Δ, the new T frame is given by $T :=$ $T(I + \Delta)$, where Δ is defined with respect to the T frame and where I denotes the 4 x 4 identity matrix [Paul, 1981].

The control interpretation of the differential transformation Δ depends on the reference frame used. In the case of the EE/EE mode, T_6^s is calculated according to

$$T_6^s = T_6 \cdot A_7 \cdot (I + \Delta^{T_7}) \cdot A_7^{-1}. \tag{6.1}$$

In the case of the EE/target mode the new T_6 matrix was calculated according to

$$T_6^s = T_6 \cdot A_7 \cdot A_t \cdot (I + \Delta^{T_t}) \cdot A_t^{-1} \cdot A_7^{-1}. \tag{6.2}$$

$$B \longrightarrow T_6 \xrightarrow{A_7} T_7 \xrightarrow{A_t} T_t$$
$$\Delta^B \downarrow \qquad {}^{T_7}\Delta \downarrow \qquad \downarrow \Delta^{T_t}$$
$$B \longrightarrow T_6 \xrightarrow{A_7} T_7 \xrightarrow{A_t} T_t$$

Figure 6.4: *Transformation graph EE/target mode.*

Via the inverse kinematics the required new angles are calculated. The required velocity setpoints of the joints are approximated by $\dot{\theta}_s = (\theta_s - \theta)/\Delta t$.

In the 2DOF mode, the subject provides velocity gains along two known directions (Fig. 6.3): one direction for the position and one for the orientation. From these two vectors the vector dX is determined, with the target frame as reference frame. Then the same control scheme as in the EE/target mode is used.

The 2DOF mode is split up into two phases. In phase I, the approach phase, the ORU has to be positioned in a small neighbourhood of p_2 and the orientation of the ORU has to be very close to the orientation of the target frame. These bounds are such that the ORU can be brought into the hole safely. Phase II consists of bringing the ORU into the hole. The subject is informed when phase I is completed. The transition from phase I to phase II is automatically initiated by the system.

In phase II the target point p_3 was variable. It was located on line l through the middle of the hole (Fig. 6.5), and at a constant distance in front of the tip of the End–Effector. The reason for this choice of the location of p_3 will be explained by the following two–dimensional example.

Consider Fig. 6.5. P_3 is located at the back of the hole. An operator gives velocity commands V along the vector through p_1, the tip of the End–Effector and p_3. Let V_1 denote the projection of V on the x–axis (up/down direction). When p_3 is located nearer to p_1 on line l (Fig. 6.6), the projection V_1 becomes larger. So, the "response time" of the movement of the tip of the End–Effector towards line l becomes smaller. Since it is desirable to minimize the chance of contact with the interior of the hole, the "response time" of the tip towards line l has to be as small as possible, without causing much overshoot.

The distance of p_3 to the tip of the End–Effector must be larger than the product of the maximum End–Effector speed and the control time interval, which was about 0.34 cm during the experiments. Otherwise the system tends to become unstable. In the experiments the distance was set to 5 cm.

When the End–Effector nevertheless gets jammed in the hole, it has to be pulled back. In this situation one cannot just reverse the direction $(p_3 \overset{-}{-} p_1)$, because a translation away from line l would occur. This is impossible, just because the End–Effector is jammed. For

Figure 6.5: *First option for the location of point p_3.*
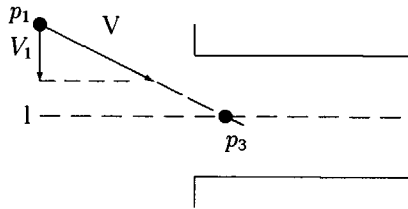
Figure 6.6: *Second option for the location of point p_3.*
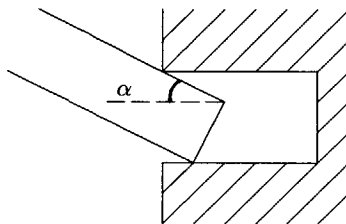
Figure 6.7: *Definition α for the jamming situation in the 2DOF mode.*

Table 6.1: *Experimental conditions.*

tolerance	taskallocation		
	EE/EE mode	EE/target mode	2DOF mode
1mm	A	B	C
3mm	D	E	F
5mm	G	H	I

pulling back, p_3 has to be located at a distance *behind* the tip of the End–Effector. This distance has to be chosen in such a way that a small movement towards line l is achieved. The movement towards line l may not be too large, just because the End–Effector is jammed. For instance, in the two–dimensional situation only movements are possible in the directions with smaller angles with line l than the angle α in which the End-EEfector is jammed (Fig. 6.7). In the experiments the distance equalled 10 cm.

6.4 Experimental procedure

6.4.1 Experimental conditions

A possible factor of influence on the desirability of a task allocation is the difficulty of the insertion, i.e. the relative size of the hole. The tolerance of the hole (Fig. 4.6, Section 4.2.2) must be seen in relation to the size of the object to be inserted. For a large object, a small change in orientation causes a large displacement of an edge of the object. In the case of HERA a tolerance of 1 to 5 mm is foreseen, when an ORU has to be inserted.

To test the hypothesis stated in Section 6.2, nine experimental conditions (A to I) were defined (Table 6.1).

To avoid that the subjects would automatically execute a predefined control sequence, instead of determining on-line the required commands, the starting configurations were varied. There were as many start configurations as there were runs per experimental condition. The order in which the runs were performed was randomized.

6.4.2 Training

Firstly, the subjects received a class introduction of about 1.5 hours, in which the experimental facility and the purpose of the experiment were explained. This was followed by a session of try-outs. Then in a session of about 2.5 hours each subject trained the insert task with the different task allocations. Pauses were built in to avoid fatigue. Only a tolerance of 1 mm was used, because the idea was that if the subjects were able to execute the insert task with a tolerance of 1 mm, for sure they would be able to perform the task with larger tolerances. Also in the training eight different starting configurations were defined, to avoid automatic control behaviour by the subjects, as mentioned in Section 6.4.1. The starting configurations differed from the ones used in the experiments. No remaining learning effects were found in the experimental data.

6.4.3 Instruction

The subjects were instructed to perform the task with the following priorities :

- *First priority* : perform the task carefully.

- *Second priority* : perform the task as fast as possible.

6.4.4 Data collection

The following performance data were recorded:

- *Approach time*, i.e. the time from the beginning of the task execution until the moment the End–Effector enters the hole.

- *Insert time*, i.e. the time from the moment the End–Effector enters the hole until the end of the task execution.

- Number of *incidents.*

- Number of *jamming* occurances.

- Total amount of *forces*, i.e. the absolute value of Δx, as defined in Section 4.2.2, and integrated during the insert time.

- *Deviation of the ideal track.* The ideal track is defined as the line through the middle of the hole. The absolute value of the position deviation of the tip of the End–Effector of the ideal track is integrated during the insert time. Then it is divided by the insert time.

- *Subject opinions.*

6.4.5 Subjects

The experiments were performed by three subjects. Subjects 1 and 2 had some experience with the system under control. They participated in previous visibility experiments [Bos, van de Klashorst, 1989]. All subjects were Aviation and Space Engineering students, right handed, male and they were about 22 years old. The subjects were paid Dfl. 10,00 per hour.

6.5 Results

Incidents / jamming

Subject 1 caused two incidents in the 2DOF mode. The incidents occurred in phase I. The edge of the ORU hit the front plane of the target environment, caused by the fact that the subject gave translation commands, but forgot to control the orientation. Subject 1 also

Table 6.2: *Means and standard deviations of the deviations of the ideal track (mm).*

subject	tolerance	EE/EE mode		EE/target mode		2DOF mode	
		mean	s.d.	mean	s.d	mean	s.d.
1	1mm	0.38	50%	0.43	20%	0.038	24%
	3mm	0.99	31%	0.97	34%	0.065	38%
	5mm	2.12	40%	1.82	26%	0.067	45%
2	1mm	0.40	55%	0.29	33%	0.031	24%
	3mm	0.95	40%	0.82	39%	0.075	33%
	5mm	1.63	63%	1.29	40%	0.074	54%
3	1mm	0.31	45%	0.30	33%	0.040	12%
	3mm	0.94	38%	0.88	42%	0.060	45%
	5mm	1.36	27%	1.07	38%	0.095	48%

caused an incident in the EE/target mode with a tolerance of 3 mm. This incident occurred inside the hole, because the forces became too large.

Subject 2 had in one run 2 jamming occurrances in the EE/EE mode with a tolerance of 1 mm. The jamming occurred at the end of the hole, where the orientation boundary conditions are most strict.

Forces

Only few contacts between the ORU and the interior of the hole occurred during the experiments. With a tolerance of 1 mm, contact situations occurred 5 times in the EE/EE mode, and 3 times in the EE/target mode. Once, forces were measured in the EE/target mode with a tolerance of 3 mm. No forces were measured in the 2DOF mode.

Deviation of the ideal track

The means and the standard deviations of the difference per second between the actual track and the ideal track, averaged over all subjects, are shown in Fig. 6.8. In Table 6.2 the results per subject are given. The standard deviation is given as a percentage of the mean. It can be seen that the mean deviation was on the average slightly larger in the EE/EE mode than in the EE/target mode. However, the differences for each separate subject were not significant at the 5% level. Here, the Mann–Whitney test was used, because the use of different starting configurations has no influence on the measurements which start only when the hole is entered. So, no paired comparisons need to be made.

The mean deviation was on the average much smaller in the 2DOF mode compared to the End–Effector modes.

It can also be seen that a larger tolerance of the hole leads to a larger mean deviation from the ideal track.
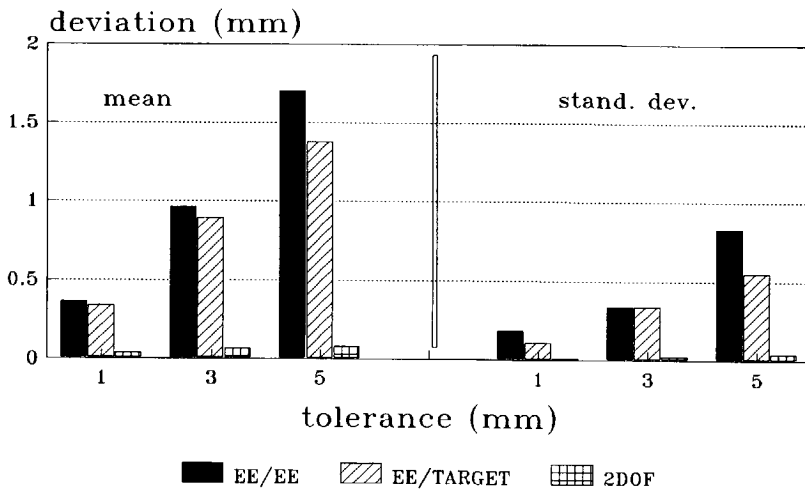
Figure 6.8: *Mean and standard deviation of the deviation of the ideal track.*
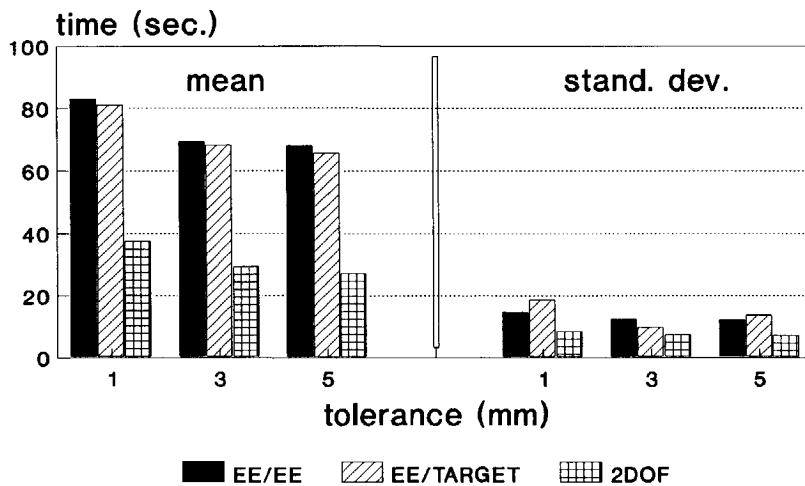
Figure 6.9: *Average approach time.*

Table 6.3: *Means and standard deviations approach times (sec).*

subject	tolerance	EE/EE mode		EE/target mode		2DOF mode	
		mean	s.d.	mean	s.d	mean	s.d.
1	1mm	85.7	16 %	80.5	19 %	39.5	22 %
	3mm	71.5	19 %	64.7	11 %	32.1	29 %
	5mm	67.2	13 %	64.2	18 %	30.5	24 %
2	1mm	90.6	16 %	92.5	23 %	38.9	27 %
	3mm	75.5	17 %	72.9	11 %	32.4	16 %
	5mm	75.4	12 %	77.4	16 %	28.2	30 %
3	1mm	72.7	14 %	70.0	18 %	34.1	16 %
	3mm	61.6	10 %	67.3	18 %	24.1	14 %
	5mm	61.4	23 %	55.3	13 %	23.1	11 %

Table 6.4: *Significance levels; Wilcoxon, two-sided; approach times for 3mm smaller than for 1mm.*

subject	control mode		
	EE/EE	EE/target	2DOF
subject 1	0.05	0.01	0.01
2	0.01	0.02	0.1
3	0.01	0.6	0.01

Approach time

In Fig. 6.9 the approach times, averaged over all subjects, are shown. In Table 6.3 the average approach times for each subject and the standard deviations are given. The standard deviations are given as the percentage of the mean.

Fig. 6.9 and Table 6.3 indicate that, for all tolerances, there were no structural differences in the approach times between the two End–Effector modes. This is also illustrated in Fig. 6.10 where the percentual differences were calculated as :

$$\%difference = \frac{(t_{EE/EE} - t_{EE/target})}{t_{EE/EE}} \cdot 100\% \qquad (6.3)$$

Compared to the End–Effector control modes (Fig. 6.9 and Table 6.3), the approach times in the 2DOF mode were about 50% shorter. For all tolerances, these differences were significant at the 1% level (Wilcoxon, two-sided).

Fig. 6.9 and Table 6.3 also indicate that the performance was worse for a tolerance of 1 mm compared to the other two tolerances. The differences between the means for the tolerances of 3 mm and 5 mm were small. These statements hold for all three control modes. The significance levels for the difference in approach times between the tolerances

80

of 1 mm and 3 mm are shown in Table 6.4. Averaged over all subjects, the significance level is 1% (Sign-test) for the EE/EE and the 2DOF mode, but 1.5% for the EE/target mode.

Insert time

In Fig. 6.11 the average insert times and the standard deviations are shown for each subject. The tolerance had generally no effect on the insert time. Therefore, in Fig. 6.11 the insert times are averaged over the tolerances. It can be seen that the differences in insert times between the control modes were small. The large standard deviation for subject 2 in the EE/EE mode is caused by the two jamming occurances.

The maximum velocity in forward direction was 0.025 m/s. So, the time needed to translate the required 0.5 m into the hole was 20 seconds. The acceleration and deceleration phases cause that the minimum insert time is a bit more than 20 seconds. Considering Fig. 6.11 again, it can be seen that generally the subjects were quite able to complete the insertion in a time optimal manner.

Subject opinions

The camera view was in general only used in the beginning of the task execution. The subjects stated that, after a first impression of the starting configuration, they hardly used the camera view as an information source. The proximity display provided them with more accurate and useful information.

Only subject 1 ascertained difference between the two End–Effector modes. He mentioned that during the training sessions, sometimes he was surprised by the outcomes of his control actions in the EE/EE mode, which led to a number of incidents. Therefore, subject 1 said that he performed the experiments more carefully in the EE/EE mode than in the EE/target mode.

Generally, the subjects applied the following strategy in the End–Effector modes. Firstly they controlled all three orientation DOF, and, if possible, up to two position DOF. This control configuration was maintained until the sensitivity range of one of the meters in the proximity display was attained, i.e. when one of the meters started to show less than the maximum deflection. Then all the DOF of the control devices were released. Subsequently, fine control commands were issued, one DOF at a time. First the orientation and then the position was controlled. When the misfits, displayed on the other five indicators, were satisfactory controlled, the distance was controlled and the hole was entered.

All subjects rated the 2DOF mode as superior to the two End–Effector control modes with respect to comfort of control, speed of task execution and safety. With respect to the accuracy subjects 1 and 3 rated all control modes as equivalent.

Figure 6.10: *Percentages improvement in approach time EE/target mode versus approach time EE/EE mode for subject 3.*
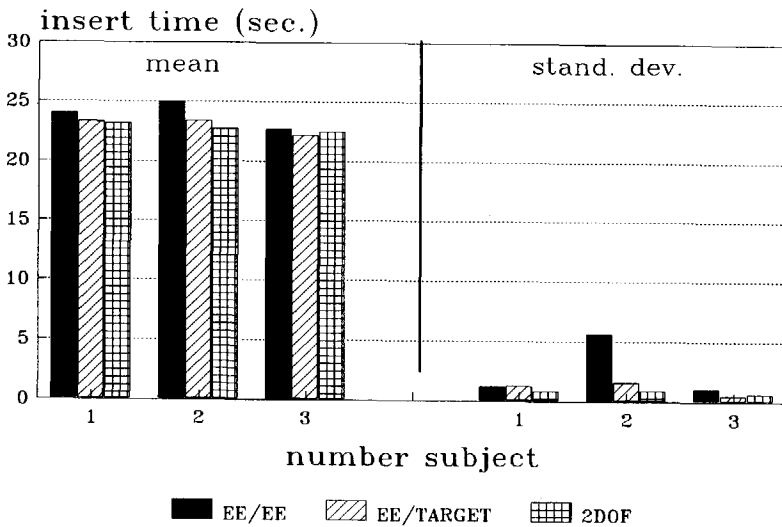
Figure 6.11: *Mean and standard deviations of insert time.*

6.6 Discussion

The applied control strategy in the End–Effector modes of controlling the orientation firstly is the result of the experiences the subjects had achieved in the training. In the training sessions they learned that incidents and jamming situations occured mostly due to orientation misfits. However, the consequence of controlling the orientation firstly is that the difference between the two End- Effector modes disappeared. The orientation of the two reference frames became the same. This explains that the performance with respect to both the safety and the economical measures was about equal for both the End–Effector modes.

Subject 1 said that he performed the experiments more carefully in the EE/EE mode than in the EE/target mode. Indeed, the only incident he caused in the End–Effector modes was in the EE/target mode. But, no further difference in performance was found in the data, as is illustrated in Fig. 6.12.
The small number of incidents and the small amount of the measured forces indicate that the subjects performed the task according to the instruction given to them.
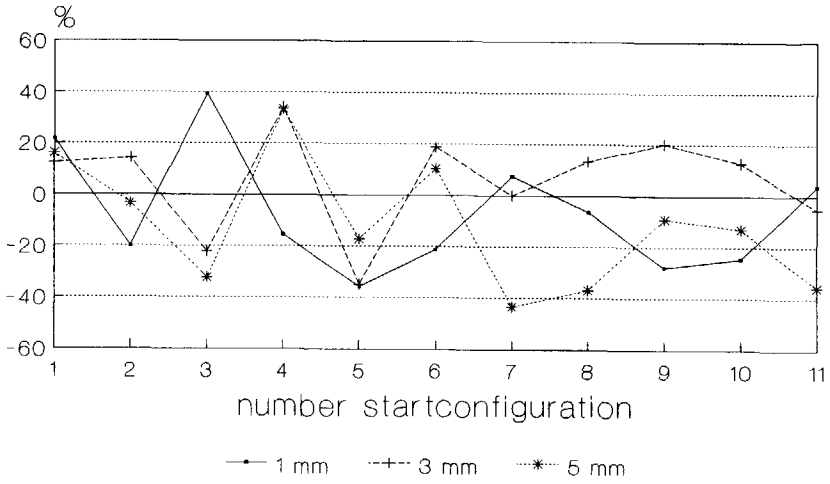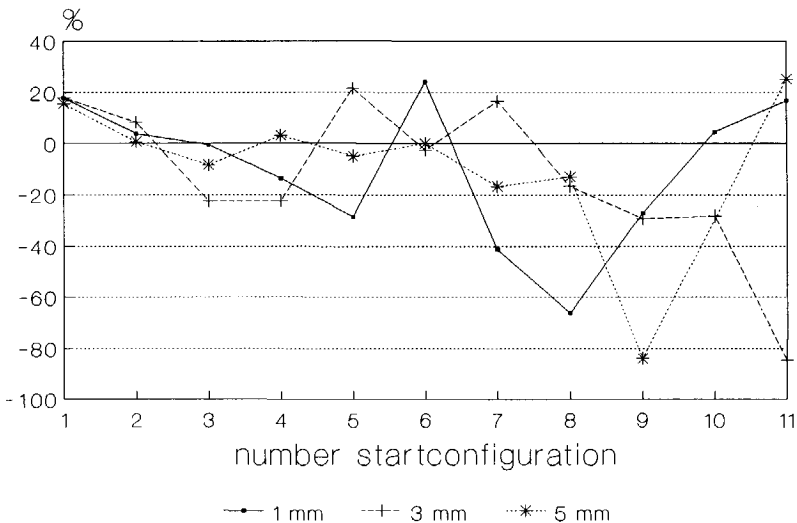

Figure 6.12: *Percentages improvement in approach time EE/target mode versus approach time EE/EE mode for subject 1.*

In the introduction it was stated that the true limiting factor for the human operator is probably the fact that he has to control up to 6 DOF. This is confirmed by Fig. 6.13 and 6.14. In these figures the percentages of the approach times where the subjects controlled a specific number of DOF simultaneously are shown. The two subjects controlled mostly none or one DOF at a time. The percentage of time they controlled two or three DOF is also substantial, but the subjects rarely did control more than 3 DOF simultaneously.

The large percentage of time the subjects issued no commands (Fig. 6.13 and 6.14) in the End–Effector modes, indicates that the task is critical. The subjects needed quite some time to plan their next control actions.

When the misfits were in the range of the proximity display, the subjects did only control one DOF at the time. In the 2DOF mode the computer takes care of the simultaneous control of the three position and/or the three orientation DOF. This explains the large difference in approach time between the End–Effector modes and the 2DOF mode (Fig. 6.9). When entering the hole the subjects needed to control only one DOF, assuming that there were no or only small orientation misfits left. This explains that there was no or only little difference in insert time between the three control modes (Fig. 6.11).

Finally, it can be concluded that for an insert task the large number of six DOF to be controlled by the operator is a very limiting factor for an efficient performance.

Subjects 1 and 3 rated all control modes as equivalent with respect to the accuracy. The mean deviation from the optimal track, however, was in the 2DOF mode much smaller than in the End–Effector modes. This contradiction can be explained by the limited resolution of the displayed proximity information. The subjects were not, or to only a small extent, able to notice the difference in accuracy. The large standard deviation in the mean deviation from the optimal track can also be explained by the limited resolution of the proximity display. Moreover, the resolution of the proximity display was less for a larger tolerance of the hole. This explains the increase in the mean deviation from the optimal track for increasing tolerances.

In the End–Effector modes the subjects controlled the manipulator on the basis of the information provided by the graphical proximity display. In the 2DOF mode the proximity information, consisting of accurate numbers, was used internally in the computer by the control system. So in the 2DOF mode the computer could control the manipulator on the basis of far more accurate information than the subjects could in the End–Effector modes. This fact can explain that the subjects could not achieve the same performance with respect to the deviation of the ideal track as the computer could.

The two incidents, which occurred in phase I of the 2DOF mode can be avoided by enlarging the distance of point p_2 (Section 6.1, Fig. 6.3) to the front of the hole. This distance must be chosen such that the maximum orientation misfit in the transition criterium from the rough positioning task to the insert task cannot lead to an incident when the tip of the End–Effector is translated to point p_2. Consider for instance Fig. 6.15. When p_2 is located at position x_1 then an incident is possible, which is not the case when p_2 is located at position x_2.

84
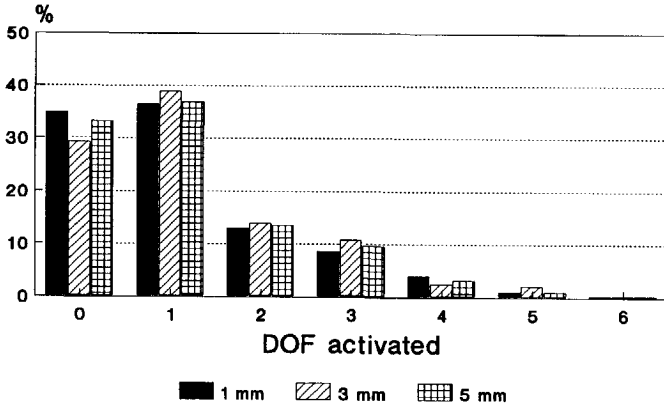
Figure 6.13: *Multivariable character of subject 2.*
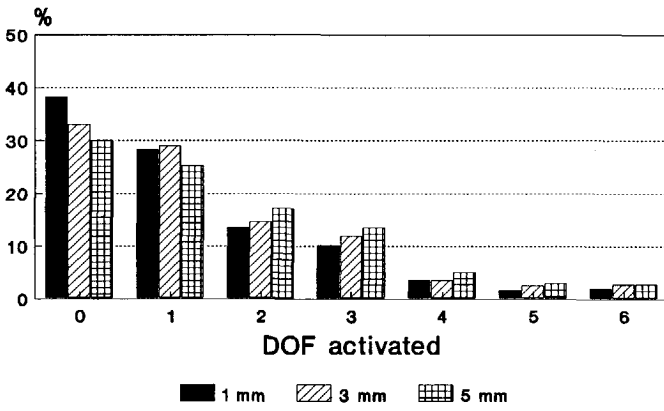
Figure 6.14: *Multivariable character of subject 3.*

The main information source for the subjects was the proximity display. This had two reasons. The first reason was that the proximity display provided the subjects with far more accurate information than the End–Effector camera picture itself. The subjects could not decide on the basis of the camera picture itself whether the hole could be safely entered. For instance, they could not see whether the End–Effector had to be moved 1 mm more to the left for a safe entry. The second reason was that there existed a clear one to one relation between the displayed proximity information and the DOF they had to control in the task execution. The subjects had to control the End–Effector in the direction opposite to the displayed misfits. The subjects had problems in estimating the orientation misfits from the camera picture itself. They had difficulties in deciding whether they had to give a roll, pitch or yaw command. The camera picture can be considered as an integrated misfit display, which means that the subjects firstly have to analyze the displayed information, before they know which DOF have to be controlled.

The author doubts whether the task can be completed succesfully when the proximity display is not present, for instance due to a failure. However, there may exist a certain redundancy because of the presence of a force/torque sensor. The human capabilities in failure situations are certainly a topic for further research.

The number of DOF to be controlled by the human operator was only reduced to 2 in the 2DOF mode. The two direction vectors were not joined into one six–dimensional misfit vector, in order to let the operator control only 1 DOF. The reason was that for the realization of this control mode, the vision target must remain present in the camera picture, in order to obtain the accurate proximity information. Now consider for instance Fig. 6.16. Suppose that the misfits in position are specified in meters and the orientation misfits in degrees. Then, numerically considered, the orientation misfits are relatively large compared to the position misfits. Because of the scaling of the accelerations the control system would firstly eliminate the relatively large orientation misfits, and the translations will be very small. Hence, the vision target could be no longer present in the camera picture. This scaling problem of the two different kinds of misfits illustrates that the construction of a 1DOF mode is not straightforward. For the 2DOF mode the subjects were instructed to keep track of the vision target.
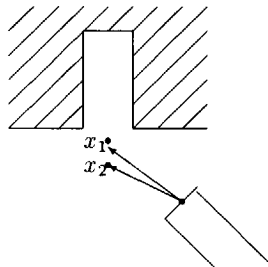
Figure 6.15: *Placement of point p_2 in the 2DOF mode.*
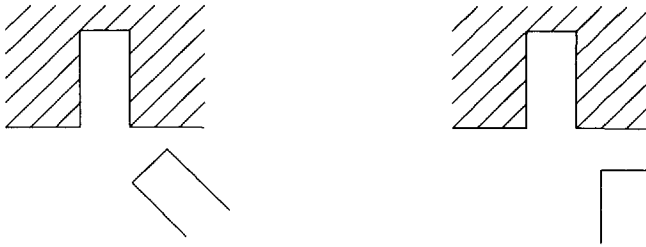
Figure 6.16: *Illustration of the scaling problem in the 1DOF mode.*

The question is always how man and computer can best cooperate, which implies that full automation needs not always to be the best solution. However, further automation still needs to be a research issue.

6.7 Conclusions

Referencing the operator's commands to the target frame, instead of to the End–Effector frame did not improve the human operator's control performance. The operator controlled the orientation first. In that way the difference between the two reference frames disappeared, before translation commands were issued.

The reduction of the number of DOF to be controlled by the human operator, led to a more efficient task execution. The 2DOF mode was judged by the subjects to be easier than both End–Effector modes.

Chapter 7

Non-linear and slow dynamics: aiding the operator with a predictive display

7.1 Introduction

As mentioned in Chapter 1, a space manipulator has non-linear dynamics. Moreover, due to the limited torques and considerable masses to be transferred the manipulator can be slowly responding. The time to stop the manipulator, by setting rate setpoints to zero, depends among other things on the motor dynamics and the configuration of the manipulator. For HERA this stopping time was estimated to lie somewhere between 1 and 20 seconds. Although for HERA a decoupling control loop is foreseen, the limitations of the torques and velocities make that there are interactions present in the dynamics.

The tasks to be executed demand a very high reliability. One wrong movement can be very costly. Moreover, the time and energy consumption should be as small as possible.

The slow and complex dynamics can cause problems with the timing of his commands for the human operator, which will worsen his performance. For instance suppose that the human operator, using velocity control, wants to stop the manipulator at a certain location. Then, given the actual position and velocity of the manipulator, he has to determine when to give the zero–rate command. Initial experiments performed in our laboratory showed that the subjects had problems with this aspect [Bos, 1988]. A possible aid for an operator to overcome the problems due to slow and complex dynamics is a predictive display. A predictive display shows the operator a future response of the system under control. A certain assumption is made about the future commands of the operator, on the basis of which the prediction is calculated. The provision of a predictive display to the operator might increase the safety and the economical use of the manipulator. Therefore, a pilot experiment was performed on the 2D simulation facility [Bos, 1989], in order to investigate the influence of a predictive display on the performance and behaviour of a human operator when he is controlling a space manipulator.

Two kinds of predictive display were investigated. Firstly, the display of the stopping con-

figuration, i.e. the configuration in which the manipulator will stop when setting all rate setpoints to zero. Secondly, showing a predicted trajectory of the manipulator over a certain time horizon. When calculating the prediction in the latter case, it was assumed that the rate commands remained constant over the prediction horizon. The subjects had to execute a rough positioning task in the presence of obstacles. The results showed that a predictive display can be a useful aid for the operator. The two kinds of predictive display did lead to a safer task execution. The display of the stopping configuration did lead to a faster task execution. The display of the predicted trajectory did lead to less energy consumption and a more calm control behaviour.

In this chapter the evaluation on the 3D simulation of these results is described.
Before the subjects performed the experiment on the 3D simulation, they had to execute the same experiment on the 2D simulation. Apart from training purposes this was done to get an impression of the relative difficulty the non-linear and slow dynamics cause for the operator in relation to the combined problem of the three–dimensional perception and the control of 5 DOF. Therefore, the results of the experiments on the 2D simulation are first briefly presented in Section 7.5.2.

7.2   Purpose of the experiments

The slow and complex dynamics of a space manipulator can cause a detoriation of the control performance of the human operator. In these experiments it has been investigated under which circumstances a predictive display can be helpful for the human operator in order to overcome problems due to these dynamics.
Two kinds of predictive display were considered:

1. *Display of the stopping configuration*, i.e. the configuration in which the manipulator will stop when all rate setpoints are set to zero.

2. *Display of the predicted trajectory* of the End–Effector over a certain time horizon. Here it is assumed that the rate commands of the operator remain the same over the prediction time horizon.

The usefulness of adding these displays to the MMI will depend on the system dynamics. At the time these experiments were conducted it was not clear what the dynamical characteristics of HERA would be, because the control system was not yet designed. Therefore, a number of conditions was defined which covered the whole possible range of response times. The usefulness of the two kinds of predictive display was investigated in relation to these conditions.

Another purpose of the experiments was to get an impression of the relative difficulty the non-linear and slow dynamics cause for the operator in relation to the combined problem of the three–dimensional perception and controlling 5 DOF.

7.3 Experimental facility

The subjects had to execute a rough positioning task (Section 4.2.1) in the presence of obstacles. The system determined whether the positioning requirements were fulfilled.
The dynamics of the manipulator were governed by Model 2 (Section 4.3.3).
Both the 2D and the 3D simulation were used. The picture the subjects saw in the 2D case is shown in Fig. 7.1. In the 3D case the subjects could choose between two camera pictures : a *side view* (Fig. 7.2) and a *top view* (Fig. 7.3). By clicking a button on the mouse input device the operators could switch between the two views. The subjects were instructed to switch only when they had released the joysticks. The interpretation of the joystick commands changes when changing from viewpoint, because the camera frame was used as reference frame.
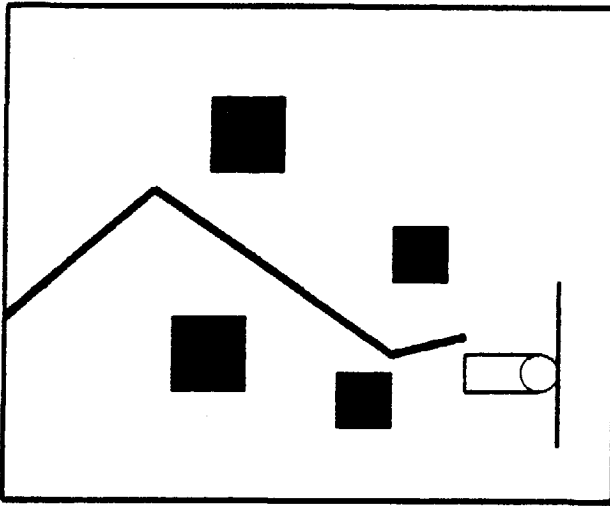
Figure 7.1: *Camera view in the 2D case.*
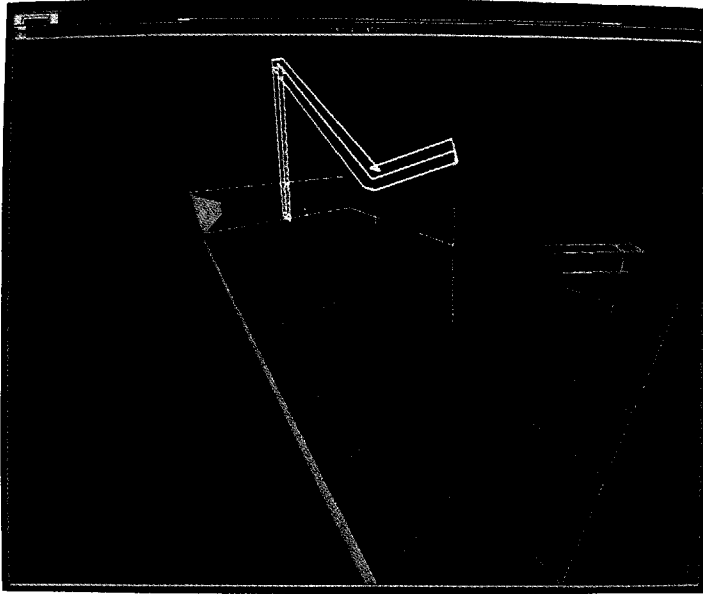
Figure 7.2: *Side view.*
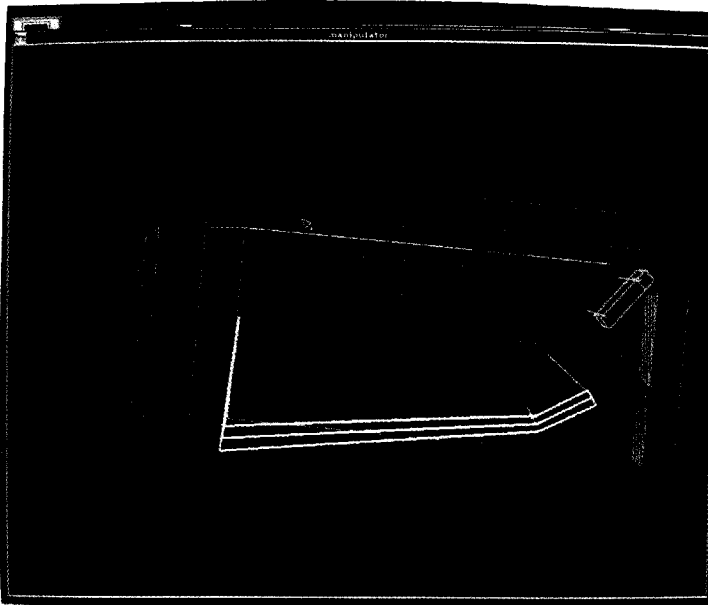
Figure 7.3: *Top view.*

91

For a rough positioning task the roll motion of the End–Effector, i.e. the sixth DOF, is not important. Therefore, only 5 DOF of the manipulator needed to be controlled in the experiments.

The experiments were performed in the End–Effector rate mode. The tip of the End–Effector served as POR. The camera frame served as reference frame, except in the case of the side view in the 3D simulation. There, a modified camera frame was used. Only the rotation of the camera around the z–axis (azimuth angle) was compensated. In this way the End–Effector moved parallel to the base plane and the obstacles when it was commanded to move "backwards". When the real camera frame would have been used, the distance between the End–Effector and the base plane would decline. The End–Effector would move towards the fixation point which is located in the base plane. This enlarges the risk of a collision with an obstacle, which is undesirable.

The camera frame was used as reference frame to obtain a compatibility between the direction of a command given by the operator and the direction in which the End–Effector moves on the screen. The use of a camera frame as reference frame meant that the commands were issued in a frame C, of which the orientation is equal to the three axes $(\vec{n}, \vec{o}, \vec{a})$ of the camera frame, but which is positioned at the POR, the tip of the manipulator. Let $[x_7, y_7, z_7]^T$ denote the position of the POR in the base frame. Then

$$
C = \begin{bmatrix} n_1 & o_1 & a_1 & x_7 \\ n_2 & o_2 & a_2 & y_7 \\ n_3 & o_3 & a_3 & z_7 \\ 0 & 0 & 0 & 1 \end{bmatrix}.
$$

In the 3D case the control structure was used as is described in Section 4.3.4 (Fig. 4.14). In the control interpretation part the new T_6 matrix was calculated according to:

$$
T_7^s = T_7 + C \cdot \Delta \cdot C^{-1} \cdot T_7 \Rightarrow \tag{7.1}
$$
$$
T_6^s = T_6 + C \cdot \Delta \cdot C^{-1} \cdot T_6 \tag{7.2}
$$

where Δ is referenced to a camera frame C. In the 2D case the End–Effector rate setpoints were transformed into joint rate setpoints via the analytical computation of the inverse Jacobian.

Two three DOF joysticks were used as input device. With the joystick at the left side orientation commands could be issued and with the joystick at the right side position commands. In the 2D case both position commands and orientation commands had to be issued with the joystick at the right.

The displacements of the joysticks were proportional to the rate setpoints. A dead–band was used which was equal to one tenth of the maximum deflection.

7.4 Experimental procedure

7.4.1 Experimental conditions

The dynamics of the manipulator are determined by the maximum End–Effector velocities, the mass attached to the End–Effector and the maximum joint torques. The joint velocity limitations are such that in (almost) every configuration of the manipulator the maximum End-Effector velocities can be achieved.

Which values for the maximum End–Effector velocities are used depend on the mass attached to the End–Effector and the maximum torques, because it must be possible to stop the manipulator, using brakes, within a reasonably short distance (0.1 meter for HERA). Two combinations of End–Effector velocities and the mass attached to the End–Effector which are foreseen for HERA, were used in the experiments:

1. A mass of 550 kg.
   Maximum translational velocities of 0.09 m/s.
   Maximum rotational velocities of 0.09 rad/s.
   This combination is defined as the *fast situation.*

2. A mass of 3500 kg.
   Maximum translational velocities of 0.05 m/s.
   Maximum rotational velocities of 0.05 rad/s.
   This combination is defined as the *slow situation.*

The fast and the slow situation were experienced to be quite different.
In order to cover the whole possible range of dynamics for a space manipulator, the maximum torques were varied. The vector of maximum torques is an element of R^3 (2D simulation) or R^6 (3D simulation), whereas for the experiment it was desirable to keep the values of each experimental condition on a one–dimensional scale. This was achieved by assuming a constant ratio between the maximum torques. One vector of maximum torques is chosen as the reference vector. An arbitrary vector of maximum joint torques is then a constant multiplied by the reference vector. These constants, the so called *torque constants*, are located on a one–dimensional scale.
As reference vector was chosen the vector $(100, 75, 100)^T$Nm in the 2D case and the vector $(100, 100, 75, 100, 100, 100)^T$Nm in the 3D case. In the experiments four different vectors of maximum torques have been used : 1, 2, 3 and 4 times the reference vector.
So, both in the case of the fast– and the slow situation, the subjects had to face 12 experimental conditions : A to L (see Table 7.1).

In order to be able to compare the results of these experiments with other ones, the times to stop the manipulator are calculated for a *standard* configuration, which is shown in Fig. 7.4. When only translation commands, $\dot{x}_p$, are issued, the maximum stopping times in this configuration, are achieved when $\dot{x}_p = [0.09, 0.0, 0.09]^T m/s$ in the case of the fast situation and $\dot{x}_p = [0.05, 0.0, 0.05]^T m/s$ in the case of the slow situation. The times T_{stop} to

Table 7.1: *Experimental conditions.*

kind of display	torque factor			
	1	2	3	4
plain	A	B	C	D
stopping configuration	E	F	G	H
predicted trajectory	I	J	K	L

Table 7.2: *Stopping times, T_{stop}, and stopping distances, D_{stop}, of the manipulator for the standard configuration, and the minimum lengths, T_{min}, of the prediction horizons.*

torque	fast situation			slow situation		
factor	T_{stop} [s]	D_{stop} [m]	T_{min} [s]	T_{stop} [s]	D_{stop} [m]	T_{min} [s]
1	6.2	0.39	6	19.3	0.68	10
2	3.1	0.20	5.5	9.7	0.34	9.5
3	2.1	0.13	5	6.4	0.23	9
4	1.5	0.10	4.5	4.8	0.17	8.5

stop the manipulator, and the corresponding distances D_{stop} are shown in Table 7.2. D_{stop} is the stopping distance of the tip of the End–Effector.

The mimimum lengths of the prediction horizon, T_{min} (Section 4.4.4), are also shown in Table 7.2.

To avoid during the experiment, that the subjects could recognize the control situation, the starting configuration of the manipulator was varied. Otherwise the subjects might automatically execute a predefined control sequence, instead of determining on–line the required commands. There were as many starting configurations as there were runs per experimental condition. The subjects performed 12 runs per experimental condition. So, in total the subjects had to execute 144 runs. To eliminate the influence of still possible

$\theta_1 = 0°$
$\theta_2 = 45°$
$\theta_3 = -90°$
$\theta_4 = 45°$
$\theta_5 = 90°$
$\theta_6 = 0°$
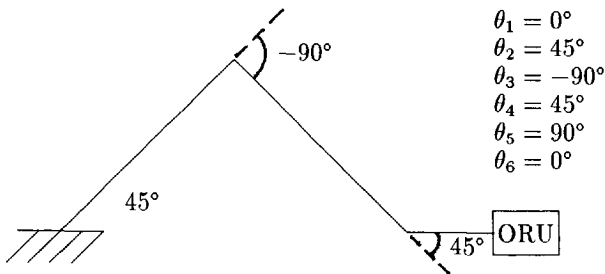
Figure 7.4: *Definition of the standard configuration.*

94

learning effects , the order in which the runs were performed was randomized. For each subject this randomization was different.

The experiments took about 3.5 (2D) and 4.5 (3D) hours in the fast situation and 5.5 (2D) and 7 (3D) hours in the slow situation.

7.4.2   Training

Firstly in the 2D situation the subjects performed 3 runs in which they got familiar with the different kinds of displays. They could ask questions. No measurements were taken. The training had the following purposes:

1. to train the subjects under all experimental conditions,

2. to compare the learning curves of the subjects for the experimental conditions.

The second purpose had two consequences. Firstly, the starting configuration of the manipulator had to be kept the same, otherwise no learning curves could be plotted. Secondly, the runs were not completely at random, but consisted of a sequence of random permutations of 12, the number of experimental conditions (Section 3.3.1). Apart from subject 1, the subjects performed a number of runs in which each starting configuration occured twice. The training took about 2.5 hours for the fast situation and 3.5 hours for the slow situation.

In the 3D situation the first session was used to familiarize the subjects with the 3D display, the DOF to be controlled and the use of the (modified) camera frames as reference frames. Then the subjects performed 4 runs per experimental condition, starting in a fixed starting configuration as in the 2D case. Furthermore, they performed a number of runs such that each starting configuration occurred 5 times (again except subject 1, see Section 7.5.1). The training took about 5 hours for the fast situation and 6.5 hours for the slow situation.

As a warming–up the subjects started with performing 4 runs, both for the training– and the experimental sessions. They performed a run with the display of the stopping configuration (condition E), a run with the display of the predicted trajectory (condition K), a run with no extra displays (condition D), and a run with the display of the stopping configuration (condition F).

7.4.3   Instruction

The subjects were instructed to perform the task carefully as the *first priority* and as the *second priority* to perform the task as fast as possible. To motivate the subjects in following the instruction they had to pay Dfl. 1,00 for each incident they caused. The subjects were paid Dfl. 10,00 per hour.

7.4.4 Data collection

The following performance data were recorded :

- The number of *incidents*.

- The task *completion time*.

- The *energy* consumption
  The square of the joint torques, integrated over the time, can be considered as a measure for the energy consumption.

- The number of *issued commands* (per second).
  In the manual control situation, the operator continuously gives commands. In our experimental facility the control signals from the joysticks were sampled. It was defined that an operator gives a different command when the absolute difference between two successive samples was larger than one fifth of the maximum command range. This was determined per input channel. For instance, two successive samples of the End–Effector rate setpoints are:
  $$\begin{bmatrix} 0.0 \\ 0.02 \\ 0.0 \\ 0.0 \\ 0.01 \end{bmatrix} \text{ and } \begin{bmatrix} 0.05 \\ 0.02 \\ 0.0 \\ 0.0 \\ 0.0 \end{bmatrix}.$$
  Then two setpoints have changed. So, two commands are added to the total number of issued commands.

- *Subject opinions*

7.4.5 Subjects

The experiments were performed by seven male subjects and one female. The subjects were students of the Delft University of Technology. Their age was about 22 years. Subjects 1, 2 and 4 had some experience in the control of a space manipulator. They participated in the pilot experiments reported in [Bos, 1989]. The subjects were paid Dfl. 10,00 per hour. Subjects 1, 2, 3, 5 and 7 performed the experiments in the slow situation. Subjects 2, 4, 6 and 8 performed the experiments in the fast situation.

7.5 Results

General remarks

On the one side, when the maximum torques are multiplied by a torque factor, the energy used increases with the square of this torque factor. However, on the other side the time needed to achieve a required joint velocity decreases linearly with the torque factor, thus causing a decrease in the energy used. So, taken both effects into account, the energy increases linearly with the torque factor. Therefore, in the following presentation of the results

Table 7.3: *Hypothesis: The order of the runs determines the result.*

c : corresponding hypothesis

nc : not corresponding hypothesis

result	order runs	
	plain, stop	stop, plain
stop faster	c	nc
plain faster	nc	c

Table 7.4: *Learning effects in the completion times of subject 1.*

Hypotheses: The order of the runs determines the results.

results experiment	corresponding hypotheses	not corresponding hypotheses
stop faster	16	8
plain faster	20	4
pred faster	15	11
plain faster	12	10

the energy used is divided by the corresponding torque factor. In addition, the presented values for the energy were divided by 1000 to avoid very large numbers.

When looking at the tables where significance levels are given, it can be seen that the results are more significant when applying the Sign test, than when applying the more powerful Wilcoxon test. The reason is that the Wilcoxon test is used for each separate subject, thus for a sample size of 12, whereas the Sign test is used over all subjects, thus for a sample size of 48. Generally, for increasing sample sizes, increasing significance levels will be obtained.

7.5.1 Results subject 1

Subject 1 served as a pilot–subject, to check the correctness of the experimental design. In the pilot–experiments [Bos, 1989] the subjects trained the task execution starting in a fixed configuration. In the experiments different starting configurations were used to avoid an automatic control behaviour of the subjects. This concept proved to be sound. Also in the evaluation experiments described in this chapter, this concept was used for subject 1. For the experiments in the 2D situation the concept proved also to be sound. However, in the 3D situation there were clearly learning effects present in the data. Subject 1 needed quite some time to understand the new situations, when faced with the different starting configurations. For instance, consider Tables 7.3 and 7.4.

For each starting configuration and each value of the torque constant the completion times were compared. The comparison was made between the plain situations, i.e. the situations with no extra display, and the situations where the stopping configuration or the predicted trajectory was displayed. When there are still learning effects present in the data,

97

Table 7.5: *Number of incidents for the 2D situation.*

kind of display	fast situation					slow situation				
	torque factor				total	torque factor				total
	1	2	3	4		1	2	3	4	
plain	4	0	1	1	6	4	0	1	0	5
stopping conf.	1	0	0	0	1	2	1	1	0	4
predicted traj.	1	0	0	1	2	2	0	0	1	3
total	6	0	1	2	9	8	1	2	1	12

one expects that the order in which the runs are performed determines the result of the comparison. For instance for starting configuration 5 a subject firstly performes the task without an extra display. Later on he performes the task with the help of the displayed stopping configuration. Then, it is expected that he performes the task faster in the latter case, so when the stopping configuration is displayed. Would he have performed the task firstly with the stopping configuration, then we expect that the task is executed faster in the plain situation (Table 7.3).

For each comparison of the completion times it was checked whether the outcome corresponds with our expectation. If the outcomes of the experiment would have been fully determined by the order in which the runs were performed, then the last column of Table 7.4 would consist of zero's. If the order of the runs played no role at all, i.e. when no learning effects would be present, the numbers in each column would be the same.

From Table 7.4 it can be seen that especially for the stopping configuration there were still learning effects present in the data. Therefore, the results of subject 1 are not taken into account in the further analysis.

The results showed that the order of the runs influenced the outcomes of the experiment to a larger extent than the experimental conditions. Therefore, the results indicate that in new situations or in an unknown environment the combined problems of the three–dimensional perception and the control of 5 DOF are more serious than the problems due to the slow and non-linear dynamics.

On the basis of these results the training for the other subjects was adjusted. Only few runs from the training starting configuration were performed, but more runs from the starting configurations which had to be faced in the actual experiment, were performed. Therefore, the training results are not presented.

7.5.2   Results two–dimensional situation

Incidents

In Table 7.5 the distribution of the number of incidents over the experimental conditions is given.
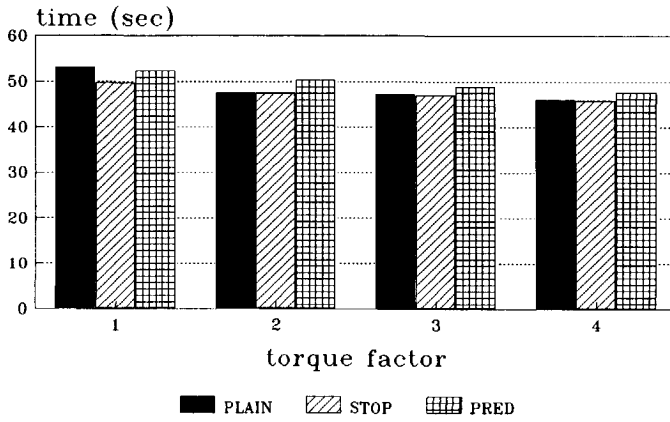
Figure 7.5: *Average completion times; 2D; fast situation.*
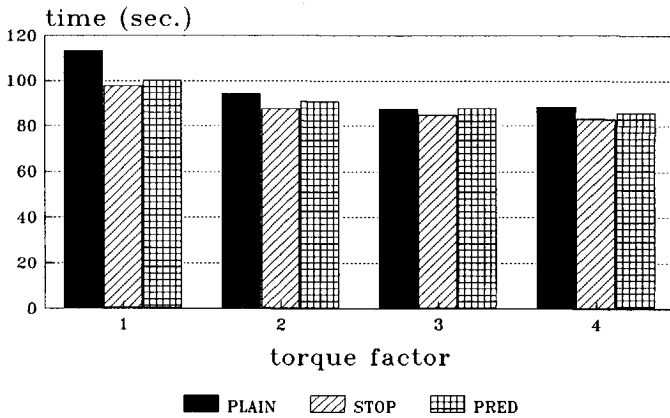
Figure 7.6: *Average completion times; 2D; slow situation.*

Completion time
_____

In Fig. 7.5 and 7.6 the completion times, averaged over the subjects, are shown. In the fast situation, it can be seen that the display of the stopping configuration did not lead to a faster task execution, except for maximum shoulder torques of 100 Nm (torque factor 1). For the latter the improvement was only significant (0.003%, Wilcoxon) for subjects 4 and 6. However, the magnitude of improvement was small. Totally 35 out of 48 runs were performed faster (1%, Sign). In the slow situation the display of the stopping configuration did lead to a significant (1%, Sign) faster task execution. Only for the torque factor 1 a substantial reduction of about 15% was achieved.
In the fast situation, the display of the predicted trajectory did even lead to larger completion times, again except for the torque factor 1. Averaged over the subjects the increase was significant at the 1% level (Sign), but the magnitude of the difference was small.
In the slow situation, for the torque factor 1, the display of the predicted trajectory did lead to a faster (about 12%) task execution.

Energy
_____

In Fig. 7.7 and 7.8 the energy used is shown. In the fast situation it can be seen that the display of the stopping configuration did not lead to a substantial decrease in the energy used. Only for the torque factor 1 the decrease is significant for subjects 2 and 4 at the 5% level (Wilcoxon). Totally 35 out of 48 runs were performed with less energy consumption (1%, Sign). In the slow situation the display of the stopping configuration did lead to a reduction of the energy used. A reduction of 20% was achieved.
When the predicted trajectory was displayed the decrease in energy consumption was substantial. A reduction of about 33% was achieved.
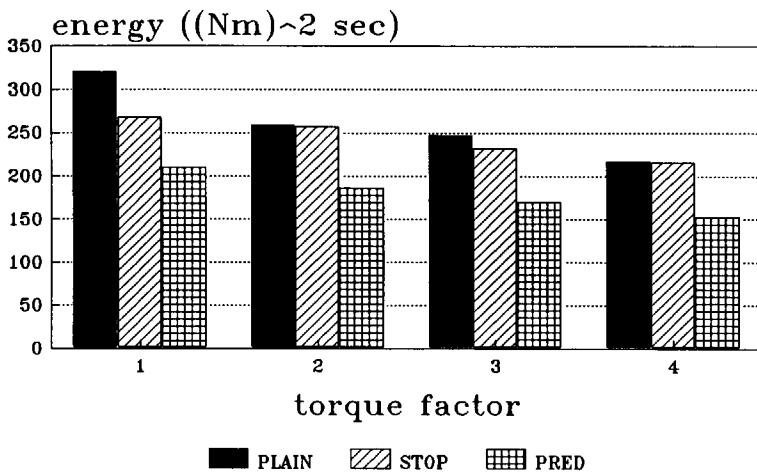
Figure 7.7: *Average energy used; 2D; fast situation.*
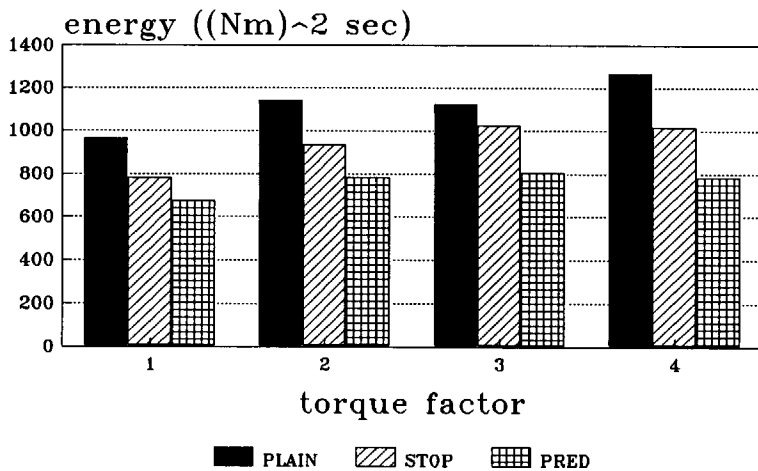
Figure 7.8: *Average energy used; 2D; slow situation.*

Table 7.6: *Number of incidents for the 3D situation.*

kind of display	fast situation					slow situation				
	torque factor				total	torque factor				total
	1	2	3	4		1	2	3	4	
plain	5	1	2	0	8	5	2	0	1	8
stopping conf.	1	2	0	0	3	0	0	0	1	1
predicted traj.	2	1	0	2	5	3	0	1	0	4
total	8	4	2	2	16	8	2	1	2	13

7.5.3   Results three–dimensional situation

Incidents

In Table 7.6 the distribution of the number of incidents over the experimental conditions is given. It can be seen that the plain situation with a torque factor 1 did lead to the most incidents.

Completion time

In Fig. 7.9 and 7.10 the completion times, averaged over the subjects are shown. In the fast situation it can be seen that the completion times were about the same. Only for a torque factor 1 the display of the stopping configuration did lead to a small reduction (7%). In the slow situation it can be seen that for the torque factor 1 both kinds of predictive display did lead to a substantial (ca. 20%) decrease. For the other torque factors a small (ca. 5%) decrease was achieved. The significance levels are shown in Table E.1. A "–" means that the significance level is larger than 10%. N is the sample size. The numbers between brackets stand for the number of runs with a smaller completion time. For instance, (34) means that in 34 out of 48 runs less time was used.
In Table E.2 the mean completion times per subject are shown. There existed clear differences in the performance between subjects.

Energy

In Fig. 7.11 and 7.12 the energy used, averaged over the subjects, is shown. In the fast situation it can be seen that with the display of the stopping configuration about the same amount of energy was used as in the plain situation. In the slow situation it can be seen that the display of the stopping configuration did lead to a small decrease in the energy consumption. This reduction was not very significant (Table E.3).
The display of the predicted trajectory did lead to a substantial reduction of about 25% in the slow situation and of about 18% in the fast situation. Even compared to the display of the stopping configuration a reduction was achieved. The significance levels are shown in Table E.3.

In Table E.4 the correlation coefficients between the completion time and the energy used
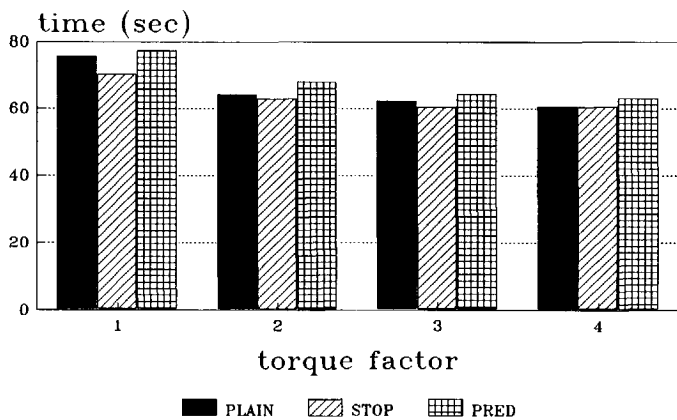
Figure 7.9: *Average completion times; 3D; fast situation.*
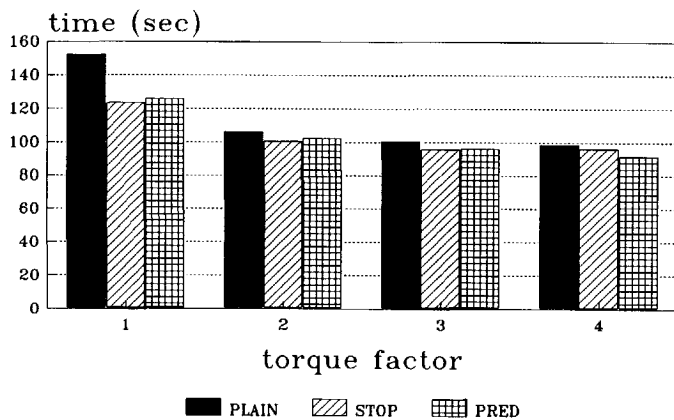
Figure 7.10: *Average completion times; 3D; slow situation.*
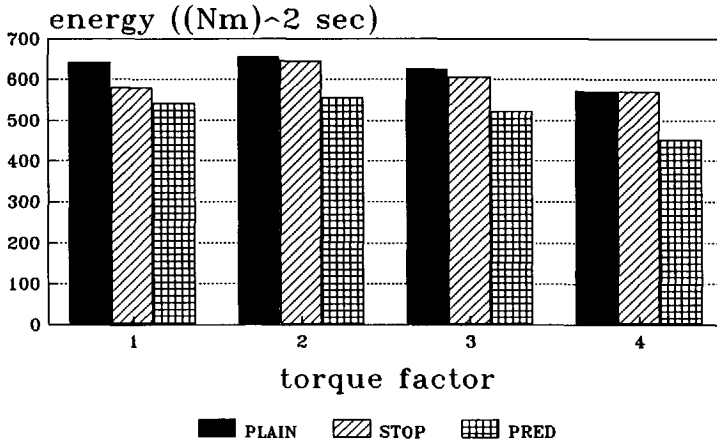
Figure 7.11: *Average energy used; 3D; fast situation.*
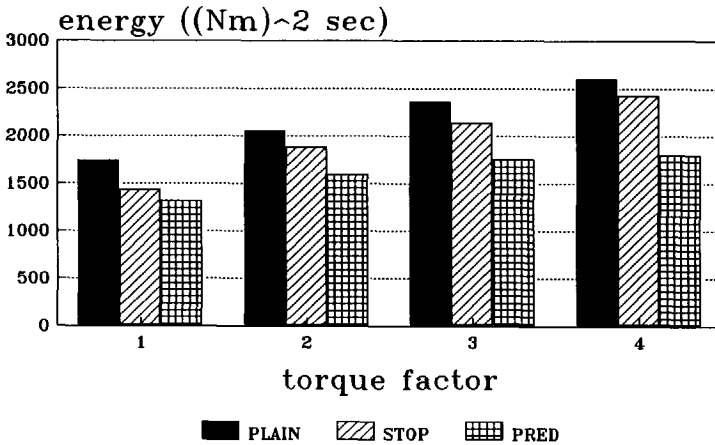
Figure 7.12: *Average energy used; 3D; slow situation.*

are shown. In the slow situation there existed a strong correlation (Fig. 7.13). In the fast situation it was less clear: For a torque factor 1 there existed a fairly strong correlation, contrary to the case with a torque factor 4. Generally, for increasing torque factors the correlation coefficients decreased.

In Fig. 7.14 and 7.15 the energy used per second, averaged over the subjects, is shown. It can be seen that the display of the stopping configuration did lead to about the same amount of energy consumption per second.
In the slow situation the display of the predicted trajectory did lead to a substantial reduction of about 6% for a torque factor 1 and 20% for the other torque factors. in the energy consumption per second, compared to both the plain situation and the situation where the stopping configuration was displayed. In the fast situation a reduction of about 14% was achieved.
The significance levels are shown in Table E.5. It can be seen that contrary to the other subjects, subject 6 did not use less energy per second.

Number of issued commands

In Fig. 7.16 and 7.17 the average number of issued commands is shown. It can be seen that with the display of the stopping configuration about the same number of commands were issued, whereas with the display of the predicted trajectory less commands were issued. In the fast situation only for subject 8 the decrease was significant at the 5% level. For the slow situation the significance levels are shown in Table E.6.
There existed not much correlation between the number of issued commands and the completion time. In about half of the cases the correlation coefficients were less than 0.6.

In Fig. 7.18 and 7.19 the average number of issued commands per second is shown. It can be seen that the display of the stopping configuration did lead to a more restless control behaviour, whereas the display of the predicted trajectory did lead to a calmer control behaviour. For the display of the stopping configuration these outcomes were not significant. For the display of the predicted trajectory the significance levels of the reduction in the number of issued commands per second are shown in Table E.7. In the fast situation only for subject 8 the result was significant at the 1% level.
In Table E.8 the correlation coefficients between the number of issued commands and the energy used are shown. The tendency is that for increasing torque factors the correlation coefficients also increase.
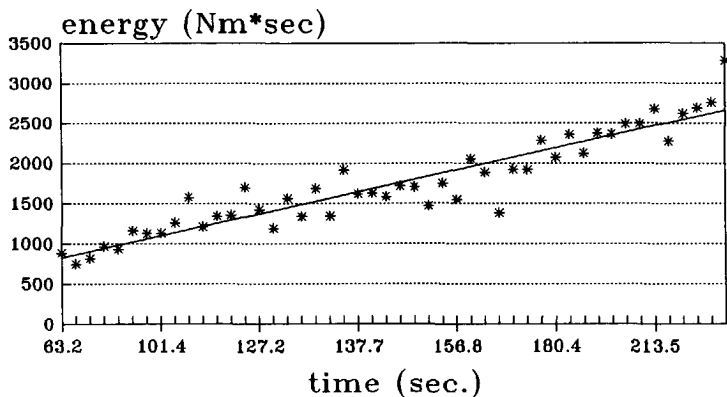
Figure 7.13: *Relation between the task completion time and the energy used; torque factor 1; correlation coefficient of 0.95; 3D; slow situation.*
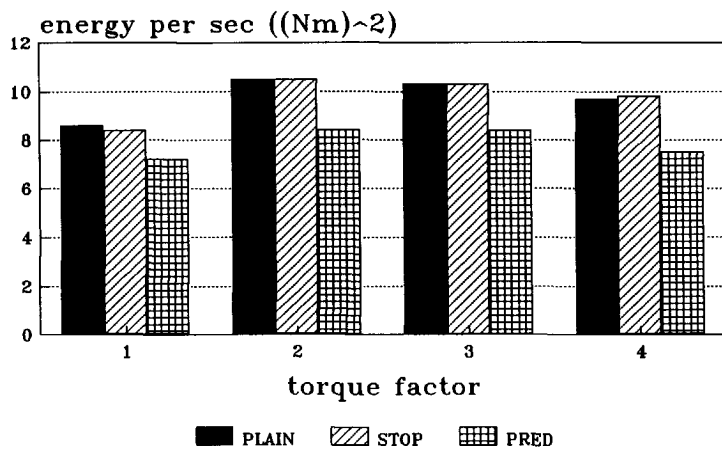
Figure 7.14: *Average energy used per second; 3D; fast situation.*

106
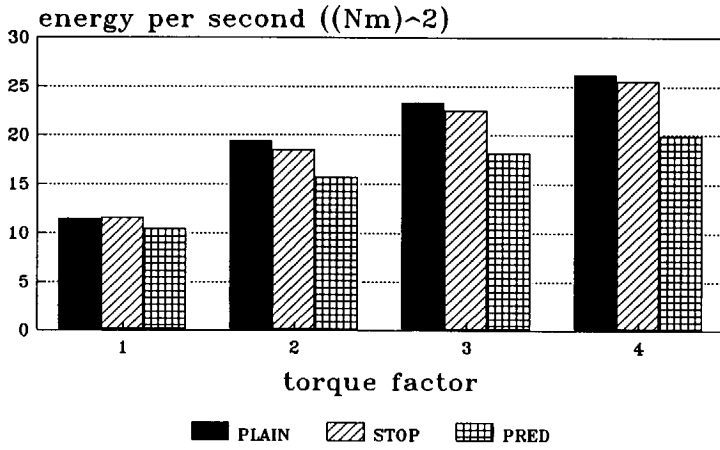
Figure 7.15: *Average energy used per second; 3D; slow situation.*
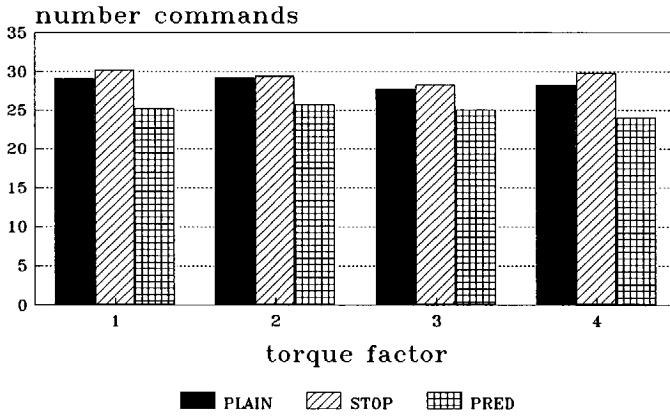
Figure 7.16: *Average number of issued commands; 3D; fast situation.*

107
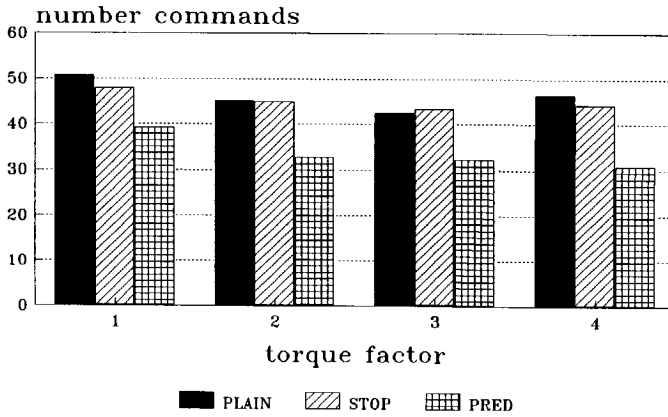
Figure 7.17: *Average number of issued commands; 3D; slow situation.*
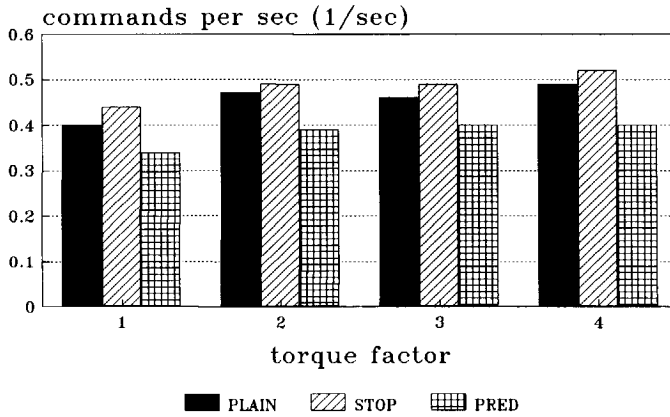
Figure 7.18: *Average number of issued commands per second; 3D; fast situation.*
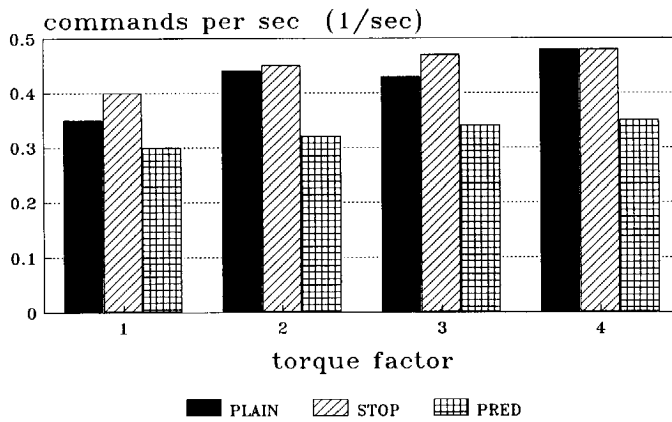
Figure 7.19: *Average number of issued commands per second; 3D; slow situation.*

7.6 Subject opinions

<u>Stopping configuration</u>

All subjects, except subject 6, rated the display of the stopping configuration as very useful, especially when the maximum shoulder torque was 100 Nm (torque factor 1). Subject 6 performed the experiments in the fast situation. The reason for his opinion was that the stopping distance was mostly too small to be of use. Only in the 3D simulation he thought that the display could be useful.

In the case of slow dynamics, the experienced advantages of the display of the stopping configuration were the increased safety, the easy end–positioning of the End–Effector in the target region, the ability for a faster task execution, and the increased controllability of the manipulator. There were doubts whether the display led to a better performance with respect to the energy used.

In the case of fast dynamics, there was also doubt whether displaying the stopping configuration led to a faster task execution, and there existed clearly less need for the display of the stopping configuration than in the slow situation.

Subjects 2 and 5 considered more or less the predicted stopping configuration as the one to be controlled. They compared the stopping configuration with the configuration of the real arm in order to estimate the trajectory the manipulator would follow. Subject 2 stated that in the 3D simulation he concentrated himself much more on the movements of the real arm than in the 2D simulation.

Most subjects controlled the orientation until the stopping configuration had attained the required orientation. Then only translation commands were issued. However, it was noticed that the real arm did not achieve this required orientation. This was considered as very confusing. The cause for this phenomenon lies in the definition of the stopping configuration. In the calculation it is assumed that *all* rate commands are set to zero, which is not the case when the subjects still give translation (rate) commands.

<u>Predicted trajectory</u>

All subjects rated the display of the predicted trajectory as very useful. The main experienced advantages were the increased safety, the increased controllability of the manipulator, and the use of less energy (except subject 5, slow situation).

In the slow situation the subjects thought that they could execute the task faster with help of the displayed predicted trajectory. In the fast situation the subjects tended to think that they used more time for the task execution.

Subjects 2, 5 and 8 said that the reason for the reduction in energy consumption was the ability to generate a more smooth trajectory for the manipulator when the trajectory was shown. Subjects 3 and 7 just thought that they controlled the manipulator in a more restless way.

Another advantage of the display of the predicted trajectory was that the End–Effector could be better controlled around obstacles. Especially in the 3D situation the predicted trajectory served as a tool to determine whether the End–Effector would safely move over an obstacle (Fig. 7.20).

The large amount of lines of which the displayed predicted trajectory consisted in the 3D simulation was rated as a disadvantage. The subjects suggested that the projection of only the end of the trajectory would be sufficient, although they noticed that it would be more difficult to see whether the manipulator can move safely over an obstacle (see also Fig. 7.20). Maybe projecting only the first and the last point of which the predicted trajectory consists will be a good compromise.

Sometimes some (unwanted) cross–coupling effects occurred between the axes the subjects controlled. For instance when a subject wanted to control the End–Effector to the right, also a (small) command downwards was issued. Without the displayed trajectory the subjects often looked at the joystick to avoid such situations. With the display there was no need to do so.

The subjects were also asked to give their opinion about the length of the used prediction (time) horizons. Subjects 5, 6 and 8 thought that the lengths were satisfactory, whereas subjects 2, 3, 4 and 7 thought that the time horizons were too large.

Stopping configuration versus predicted trajectory

Comparing the display of the stopping configuration with the display of the predicted trajectory the subjects had different opinions. The general trend was that for the end–positioning the stopping configuration was preferred, whereas for the navigation around the obstacles there existed a small preference for the predicted trajectory. A common suggestion was to
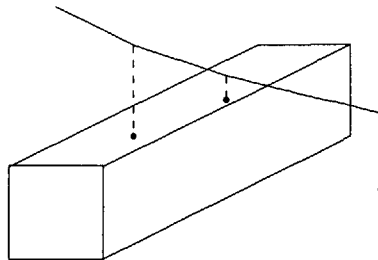
Figure 7.20: *Trajectory over an obstacle.*

provide a possibility to switch from the display of the predicted trajectory to the display of the stopping configuration.

Three subjects stated that a good use of the displayed predicted trajectory required more training than the use of the displayed stopping configuration.

<u>General remarks</u>

Before the beginning of a run, the subjects were informed which experimental condition they had to face. Subject 7 said that he only used the information about the dynamics he had to face, when no extra display was present. Otherwise he did not use the knowledge. He "just saw what happened".

Especially with the display of the stopping configuration the subjects were aware of the state–dependent dynamics. With this display also the increased stopping distance was noticed when they controlled the End–Effector in the right–down ($\searrow$) direction instead of in the right ($\rightarrow$) direction. This was considered to be a bit confusing.

Subject 3 experienced the slow situation as slow and therefore boring, which gave rise to loss of concentration. He stated that the loss of concentration led to dangerous situations and caused a number of incidents.

Subjects 3 and 7 stated that the dynamics with a torque factor 1 (slow situation) sometimes did give rise to a move–and–wait strategy when no predictive display was provided.

In the 3D simulation the subjects found it hard to estimate the orientation of the End–Effector. The pitch and yaw movements seemed to be dependent, as it is also reported in Chapter 5 (Fig. 5.10). Controlling the yaw movement makes that the wrist of the manipulator comes "closer" to the camera. Therefore, the wrist moves also "up" in the camera picture, although the distance of the wrist to the base plane remains the same. The pitch seems also to be changed. This fact was experienced as very confusing.

In the beginning the subjects experienced the combined problem of three–dimensional perception and the control of 5 DOF as difficult. It required a considerable amount of training, before a constant performance was achieved.

Subject 2 performed the experiments in both the fast and the slow situation. In the fast situation the manipulator moved faster which required more attention, but the manipulator also accelerated faster which required less attention. As a whole, the slow situation was considered to be the most difficult, demanding and fatiguing one.

With an extra display all subjects felt more secure.

Subject 4 suggested to take the directions of the grid lines in the base plane equal to the direction of the target. In this way it would be more clear in which direction the End–Effector has to be commanded.

7.7   Discussion

In the case that a predictive display was provided in the two–dimensional situation, most incidents were caused by the fact that the subjects took more risk during the task execution. With a predictive display the subjects felt more secure. So, while keeping the same safety level, they tried to optimize their performance with respect to the task completion time and the energy consumption.

In the three–dimensional situation this reason did account only for about half of the number of incidents. Another main cause for the incidents was the difficult three–dimensional perception. The reference lines provided the subjects with good information about how far the End–Effector is above an obstacle and about the horizontal distance to the obstacles located on the base plane. But the subjects had difficulties in estimating the distance of the links to an obstacle and the distance of the End–Effector to the obstacle which was floating, i.e. the obstacle which was not located on the base plane. A collision detection algorithm is very desirable, if not necessary for a guaranteed safe task execution. Such a collision detection system should not only intervene in the task execution, like our system in the case of an incident; it should also provide an operator with information about the cause of the warning/incident. For instance the collision detection system should display *link 2 hits top obstacle 3* in an alarm window, or should display the collision point directly in the (global) camera picture.

The subjects more or less considered the predicted stopping configuration as the one to be controlled. However, when the difference between the stopping configuration and the actual configuration becomes large, this strategy becomes dangerous. For instance, consider Fig. 7.21.   A subject controls the stopping configuration along the dashed line around the obstacle, but the real arm does "cut off" the curve. In this way a number of incidents occurred, when the stopping configuration was displayed.

When the predicted trajectory was displayed, two strategies were applied for the end–positioning of the End–Effector. The first strategy was to position the end–points of the trajectory on the required position. Then the speed of the End–Effector was slowly reduced (Fig. 7.22), such that the end–points remained on the same place. This strategy led to a safe, but slow end–positioning.

In the second strategy the predicted trajectory was allowed to intersect the safety line or plane (Fig. 7.23). The subjects estimated a ratio between the length of the predicted
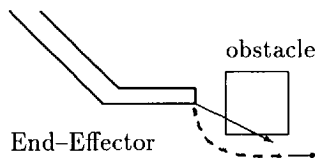
Figure 7.21: *Controlling the End–Effector around an obstacle.*
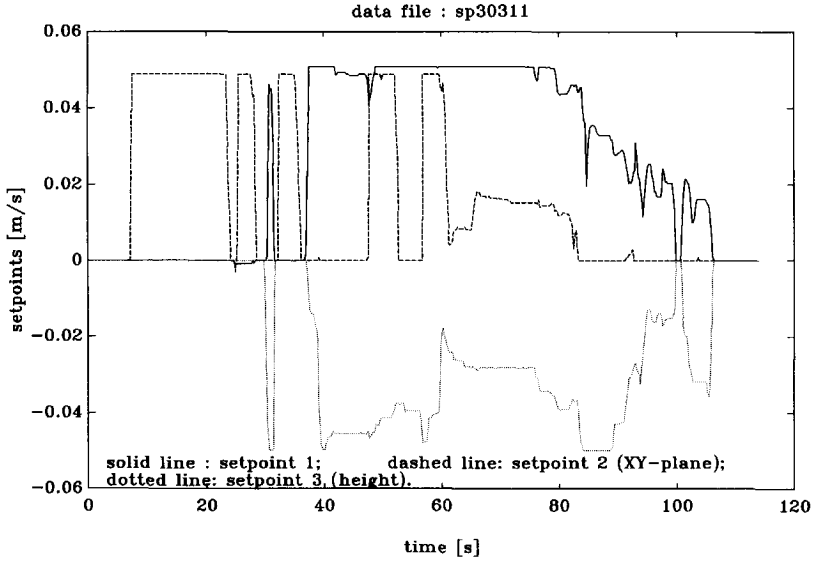
Figure 7.22: *Slowly reducing the End–Effector speed in the last phase with the display of the predicted trajectory; 3D; slow situation; torque factor 2; subject 3.*
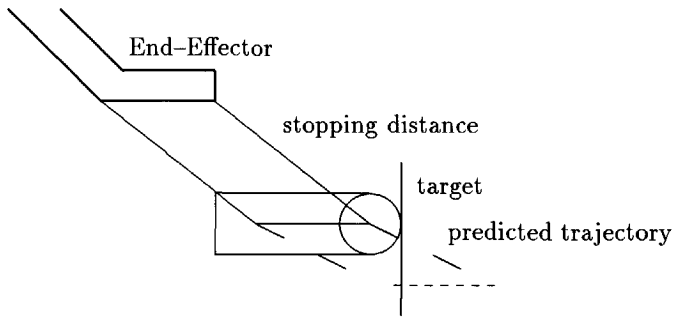
Figure 7.23: *Estimating ratio between the length of the predicted trajectory and the stopping distance.*

114

trajectory, the dashed line and the stopping distance, the solid line. On the basis of this ratio, the time instant was determined when to release the joystick in order to stop the End–Effector at the right place. This strategy led to an unsafe, but fast end–positioning. Often, for safety reasons, the subjects released the joystick a bit earlier than the time instant they had estimated for a time optimal end–positioning. However, sometimes the ratio was estimated wrong, so that a number of incidents occured.

Only 29 incidents occurred in a total of 1152 runs in the three–dimensional situation. This fraction of 2.5% is small and it indicates that the subjects executed the experiments according to the instruction given to them, which was to perform the task carefully as the first priority.

The subjects felt more secure with a predictive display when the time needed to stop the manipulator was larger than about 5 seconds or when the stopping distance was larger than about 0.2 meter. So, while keeping the same safety level, they thought they could perform the task more efficiently with respect to time or energy consumption. However, in both the two–dimensional and the three–dimensional situation the display of the stopping configuration led to a faster task execution if and only if the stopping time was larger than about 6 seconds or when the stopping distance was larger than about 0.3 meter.

The display of the predicted trajectory always led to less energy consumption (Figs. 7.11 and 7.12). The energy consumption was strongly correlated with the task completion time for each experimental condition. However, the display of the predicted trajectory led also to less energy consumption per second (Figs. 7.14 and 7.15). So, the length of the task execution was not the cause for the differences in energy consumption between the experimental conditions. The display of the predicted trajectory did also lead to a more calm control behaviour of the subjects. For instance, compare Fig. 7.24 and 7.25. The used energy and the number of issued commands were correlated, although the correlation coefficients were not so large. When the energy is divided by the number of issued commands, the difference between the experimental conditions disappears to a large extent (Fig. 7.26). This means that the reduction in the energy consumption is caused by the more calm control behaviour. Subjects 3 and 7 thought that they controlled the manipulator in a more restless way when the predicted trajectory was displayed. However, they issued less commands per second too. The reason for their opinion was that a small change in an issued command already made that the shape of the predicted trajectory became quite different. This reason may be the cause for the more calm control behaviour of the subjects.

The more calm control behaviour seems to be in contradiction with the results obtained in ship handling experiments [Veldhuyzen, 1976; Passenier, 1989]. However, in those experiments the subjects had to track a predefined trajectory, whereas in our experiments the subjects were free to choose the trajectory to arrive at the location of the target.

The subjects considered more or less the displayed stopping configuration as the one to be controlled. This may explain why, with the display of the stopping configuration, the differences in the energy consumption (per second) are not very clear, compared to the plain situation.
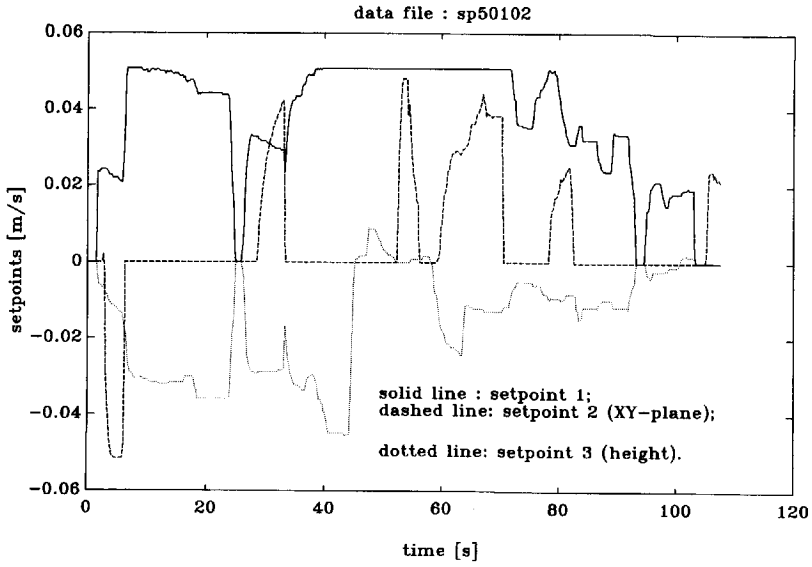
Figure 7.24: *Position velocity setpoints; plain situation; 3D; slow situation; torque factor 2; subject 5.*
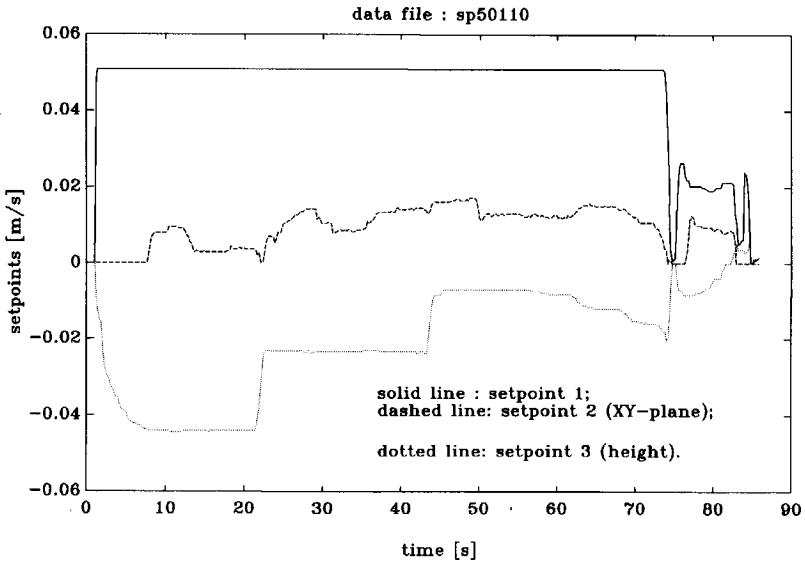
Figure 7.25: *Position velocity setpoints; display predicted tarjectory; 3D; slow situation; torque factor 2; subject 5.*

116

The smaller correlation coefficients, between the energy consumption and the completion time, for increasing torque factors, can be explained by the dynamics of the manipulator. For a small torque factor the manipulator is slowly responding. Therefore, the manipulator is still accelerating towards the desired velocity determined by the previous command, when a new command is given. In an extreme situation the manipulator is always accelerating, also when an operator issues very few commands. So, instead of the control behaviour, the task completion time is a main factor of influence on the energy consumption. When the manipulator is very fastly responding, the manipulator only accelerates shortly when a command is given. So, then the control behaviour of an operator is the main factor of influence. Summarizing, the faster the manipulator responds, the more the control behaviour is of influence on the energy consumption. This is confirmed by the fact that the correlation coefficients between the energy consumption and the number of issued commands increased when the torque factor increases. Moreover, in the fast situation the correlation coefficients were larger than in the slow situation (Table E.8).

The subjects differed from opinion about the lengths of the prediction (time) horizons. This can be caused by the fact that the lengths of the minimum horizons, T_{min} (Section 4.4.4) were not an experimental condition, i.e. they were not varied in the experiments. Therefore, the subjects could not compare an applied time horizon with other ones for given dynamics of the manipulator. In addition, on the basis of the results no statement can be made whether the length of a prediction horizon should be based on the stopping time or on the stopping distance. In Chapter 8 this issue will be discussed in more detail.

In the slow situation the subjects controlled more DOF simultaneously when a predictive display was provided, as is illustrated for subject 2 in Fig. 7.27. Especially with the display of the predicted trajectory the percentage of time the subjects controlled more DOF simultaneously was larger. The significance of this fact decreased for increasing torque factors. In the fast situation the differences disappeared to a large extent (Fig. 7.28).
One cause for the more simultaneous control of the DOF when the predicted trajectory was displayed can be found by considering Fig. 7.24 and 7.25 again. It can be seen that with the display of the predicted trajectory the subject issued a command with a smaller magnitude over a longer period, instead of using a more bang–bang control strategy for each DOF in the plain situation. No clear evidence was found that the subjects controlled position and orientation DOF in a more mixed way.
In the fast situation the differences between the experimental conditions disappeared to a large extent. This may have two reasons. Firstly, in the fast situation the manipulator is more quickly responding than in the slow situation. The times needed to stop the manipulator are smaller. Therefore, the subjects were able to control more DOF simultaneously, also when no predictive display was provided. However, there existed only a very small shift towards controlling more DOF simultaneously for increasing torque factors. So, this reason can only to a small extent account for the lack of difference in the fast situation. Secondly, in the fast situation the manipulator moves with a larger velocity than in the slow situation. The manipulator arrives much sooner in a critical safety region. Therefore,
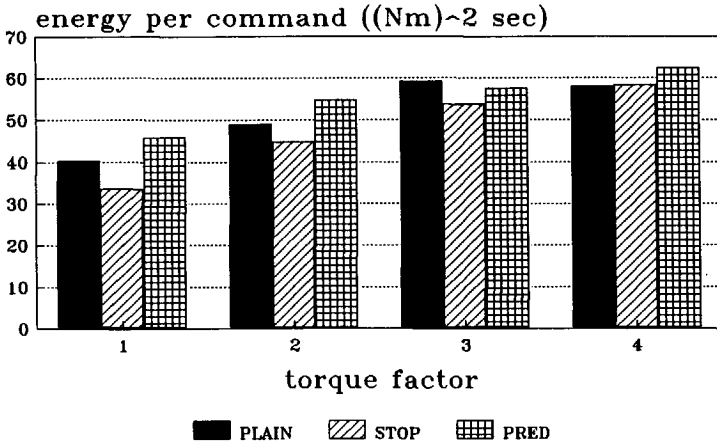
Figure 7.26: *Average energy used per issued command; 3D; slow situation.*
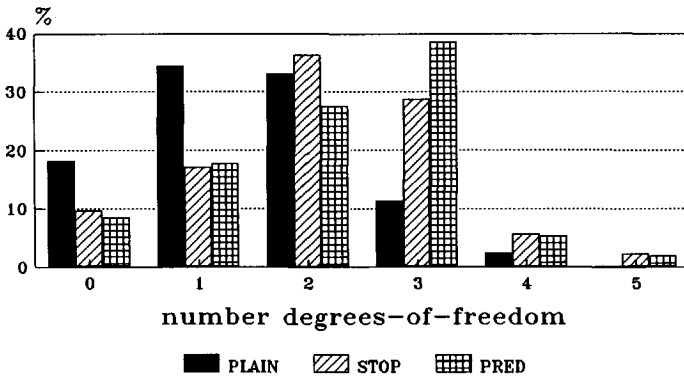
Figure 7.27: *Percentages of time that a specific number of DOF is controlled simultaneous; 3D; slow situation; torque factor 1; subject 2.*

118

although a predictive display is provided, the operator has not enough time or capacity to control more DOF. When starting a movement of the manipulator the number of DOF which are controlled increases sequentially in time. When starting the movement not all DOF are immediately controlled. When a subject had time and confidence to do so, he added more DOF.

Subjects 3 and 7 stated that the dynamics with a torque factor 1 in the slow situation sometimes gave rise to a move–and–wait strategy when no predictive display was provided. In Fig. 7.27 it can be seen that this strategy resulted in a substantially larger percentage of time in which no commands were issued. Only for subjects 2 and 3 proof for the applications of a move–and–wait strategy could be found in the data.

When the subjects controlled the End–Effector for instance in the right–down ($\searrow$) direction instead of in the right ($\rightarrow$) direction the stopping distance increased. This was considered to be a bit confusing. A cause of this phenomenon is that the maximum End–Effector velocities are specified along the axes of the reference frame. Let for instance v_{max_x} denote the maximum velocity in the right, x direction and v_{max_z} the maximum velocity in the down, z direction. The maximum velocity in the right–down direction is now $\sqrt{v_{max_x}^2 + v_{max_z}^2}$, which is larger than the maximum velocity along one of the axis. To let the subjects experience the dynamics of the manipulator less "direction–dependent", an overall velocity V_{max} could be specified. Then the commanded End–Effector velocities along the axis of the reference frame have to be scaled in such a way that the direction of the command remains the same :

1. Calculate the size V of the commands velocity vector.

2. IF $V > V_{max}$ THEN divide each commanded axis by $\frac{V}{V_{max}}$.

Now, the maximum velocity vectors no longer form a cube, but a ball.
Another cause for the fact that the stopping distance depends on the direction the End–Effector is going, originates in the presence of off–diagonal terms in the inertia matrix. These off–diagonal terms cause substantial interaction effects. The multivariable control system was designed to eliminate the interactions by choosing the controller equal to a gain times the inertia matrix (Section 4.3.4). However, the control system cannot decouple the system completely, because the motor torques are limited. The scaling part of the control system prevents that a motor has to provide a torque larger than the maximum torque it can exert. The off–diagonal elements in the inertia matrix influence the torque vector to be scaled. The scaling, which is a non-linear operation, influences all entries in the joint velocity vector. So, changing one joint velocity setpoint can influence the response of the other joints, which means that the system is not a decoupled one.

The subjects switched rarely from viewpoint. The side view was the main information source for the subjects. They used the top view mainly to estimate and control the yaw movement of the End-Effector correctly. Subject 2 issued most viewpoints switches. He

switched in about 45% of the runs. Subjects 3 and 6 switched in 28%, subject 8 in 18%, and subjects 4, 5 and 7 in only 3% of the runs. Mostly, the subjects switched only once to the top view and back again to the side view. The small amount of viewpoint switches indicates that the side view in combination with the reference lines provided the subjects with reasonably well three–dimensional information. However, for a good understanding of the task environment the subjects were allowed to feel around with the End–Effector in the first training session. They needed this feeling around mainly for determining when it was safe to move under the floating obstacle.

The fact that no remaining learning effects were found in the data indicates that the training was sufficient. In addition, despite of the fact that the subjects were made familiar with the different starting configurations, the task was such that a closed–loop behaviour of the subjects was guaranteed.

The results of the 2D and the 3D situation are in agreement with each other.
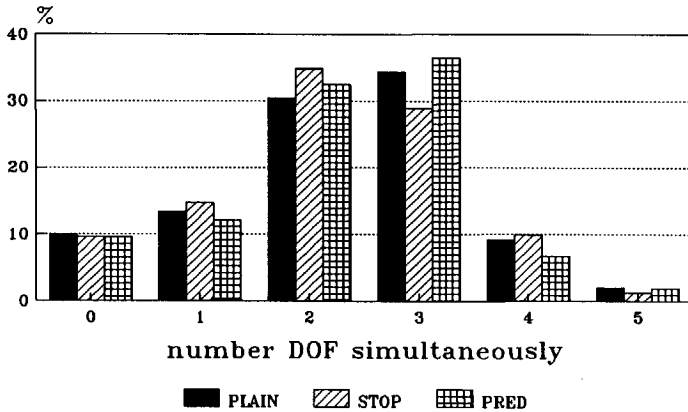
Figure 7.28: *Percentages of time that a specific number of DOF is controlled simultaneous; 3D; fast situation; torque factor 2; subject 2.*

7.8 Conclusions

The subjects felt more secure with a predictive display when the time needed to stop the manipulator was larger than about 5 seconds or when the stopping distance was larger than 0.2 meter.

The display of the stopping configuration led to a faster task execution when the time needed to stop the manipulator was larger than about 6 seconds or when the stopping distance was larger than 0.3 meter.

The display of a predicted trajectory always led to less energy consumption, due to a more calm control behaviour of the subjects.

The results indicate that a collision detection system is very desirable, if not necessary for a guaranteed safe task execution.

In new situations or in an unknown environment the combined problems of the three–dimensional perception and the control of 5 DOF are more serious than the problems due to the slow and non-linear dynamics (Section 7.5.1).

Chapter 8

Describing the operator as a predictive controller

8.1 Introduction

An important issue when displaying a predicted trajectory is how to choose the most effective length of the time horizon over which the prediction has to be calculated. In the experiments of which the results are given in Chapter 7, the length of the prediction horizon T_{pred} equalled the maximum of a constant, minimal, time horizon T_{min} and the stopping time T_{stop}:

$$T_{pred} = maximum(T_{min}, T_{stop}). \tag{8.1}$$

This choice was made to ensure that the prediction covers the stopping configuration (Section 4.4.4). The minimal horizons T_{min} were chosen such that it was mostly a bit larger than the stopping times. The subjects differed from opinion about the lengths of the used prediction horizons, probably because the subjects could not compare a used time horizon with other ones for given dynamics of the manipulator. The most effective length will depend on the system dynamics, the task to be executed, and the disturbances acting on the system (Fig. 1.3). Experiments with subjects can be performed to investigate this issue, but these experiments will be very time consuming. Moreover, when it is decided to investigate the use of a predictive display, it would be nice when, for that particular situation, in advance a good choice can be made for the prediction horizon.

Apart from (time consuming) experiments with subjects, control theory might be used to investigate the most effective length of the prediction horizon in relation to the system dynamics, the disturbances and the task to be executed. From the existing human operator models the OCM (Section 2.2.2) has been used to study the effects of a predictive display on the performance and behaviour of a human operator. Before further discussing the use of the OCM in studying predictive display applications, it should be noted that predictive displays can be divided into two categories:

1. The prediction is calculated for only one time instant in the future.

2. The prediction is calculated for a set of future time instants, i.e. a predicted trajectory is determined.

Mostly, a predictive display from the first category is used to cope with a system with time–delay. Only a prediction is calculated over a time horizon equal to the time–delay. In the OCM already an optimal predictor is incorporated, which compensates the human's inherent delay. When only a prediction is made to compensate time–delays, this human delay is often neglected, or assumed to be included in the total system time–delay [Milgram, Weverinke, 1985], and the optimal predictor of the OCM itself is used. In [van de Vegte et.al., 1990] a bit different approach was used. There, the human's inherent delay was neglected and, contrary to the OCM, the (output) prediction was calculated before the state estimation part. In this way the human operator's knowledge of the time–delay is removed from the state equations of the human's internal model, since delay compensation is deemed to be carried out for the operator by the predictor display.

In the case of the second category of predictive displays in which a predicted trajectory is determined, a way to calculate the prediction, so that the OCM can be used, is using the extrapolation method. The prediction is approximated by calculating a Taylor series of the predicted variable, where third and higher order terms are neglected [Johannsen, Govindaraj, 1980]. The extrapolated values are approximately correct estimations of the future outputs, assuming that the control inputs to the system will not change very much during the prediction horizon. The set of estimated future points of which a predicted trajectory consists, can be expressed in the state variables. The future points are added to the output vector, so that a different ouput matrix C is obtained. In [Johannsen, Govindaraj, 1980] the different C matrix gave rise to different fractions of attention, thus to different observation noise–to–signal ratios, and thus to different observation noise covariance matrices. The different C matrix and the different observation noise covariance matrices accounted for the differences in performance when a predictive display was provided.

In the above described methods the predictive display influences *the quality of the state estimation* $\hat{x}(t)$, thus influencing the performance of the total closed loop system. Another way of thinking can be that a predictive display influences *the determination of the control law*. In the derivation of an optimal control law a predicted trajectory is implicitly used in the determination of the control gains. To determine the control inputs the following, infinite time, cost functional is minimized:

$$J = \int_0^\infty (x^T(t)Qx(t) + u^T(t)Ru(t))dt \tag{8.2}$$

Q and R are the weighting matrices for the state and the input respectively. The optimal control law L is given by

$$L = -R^{-1}B^T K, \tag{8.3}$$

where K can be determined by solving the algebraic Ricatti equation

$$A^T K + KA - KBR^{-1}B^T K + Q = 0, \tag{8.4}$$

where A and B are the system matrix and the control matrix of the linear system to be controlled, respectively. So, to determine the control law, the response of the system due to future inputs is taken into account (Eq. 8.2). However, it is not necessary to calculate predictions of the output explicitly. To incorporate a prediction horizon one may think of using a finite time cost functional. Then the control law is given by solving $K(t)$ from the differential Ricatti equation

$$A^T K + KA - KBR^{-1}B^T K + Q = -\dot{K}; \tag{8.5}$$
$$K(t_e) = 0. \tag{8.6}$$

However, it is implicitly assumed that a human operator determines future inputs at all time instants in the prediction time horizon, i.e. the control horizon is equal to the prediction horizon. However, this is very questionable. The operator probably takes just one, maybe two future control actions in consideration. Moreover, providing a predictive display influences directly the control commands issued by an operator [Veldhuyzen, 1976; Passenier, 1989; this thesis, Chapter 7], whereas in the set–up of the OCM the determination of the control law is independent on the provision of a predictive display, since a predictive display only causes a different quality of the state estimation $\hat{x}(t)$. In a predictive controller a calculated prediction influences directly the values of the control commands. Therefore, predictive control theory seems to be a more natural control theory to perform an investigation towards an optimal length of a prediction horizon with. A first interesting study towards the use of predictive control theory to model human control behaviour is reported in [van de Veldt, Boomgaard, 1986], where the use of predictive displays in (chemical) process control was considered. However, the experimental conditions for the computer and the human subjects were not quite comparable. For instance, the computer used a predicted trajectory, whereas the subjects could observe only the end–point of the prediction.

8.2 Problem definition

The basic issue in which we were interested was the determination of the optimal prediction horizon in relation to the system dynamics, the task to be executed, and the disturbances
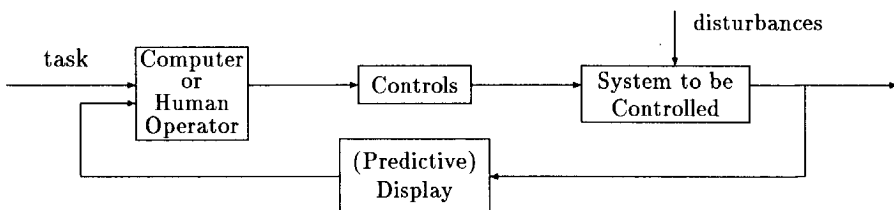
Figure 8.1: *Control situation.*

acting on the system, when a predictive display is provided. Because experiments with subjects will be very time consuming and might be very expensive, a first investigation was performed whether predictive control theory can be used to investigate the optimal length of the prediction horizon. Hereto, two kinds of experiments were performed: one in which the control is performed by a predictive controller, and another in which a human acts as a controller (Fig. 8.1).

8.3 Predictive control theory: general principle

A predictive controller uses an explicitly calculated prediction of the system's response. In the calculation of the prediction a mathematical model of the system is used. Several predictive controllers exist [van den Bosch, 1990]: the Smith controller [Smith, 1959], Model Algorithmic Control (MAC) [Rouhani, Mehra, 1982], Generalized Predictive Control (GPC) [Clarke, 1987], Unified Predictive Control (UPC) [Soeterboek, 1990], Dynamic Matrix Control (DMC) [Heintze, 1988] and state–based predictive control [van den Bosch, 1991].

Predictive controllers can be divided into the same two categories as predictive displays:

1. The prediction is calculated for only one time instant in the future.

2. The prediction is calculated for a set of future time instants, i.e. a predicted trajectory is determined.
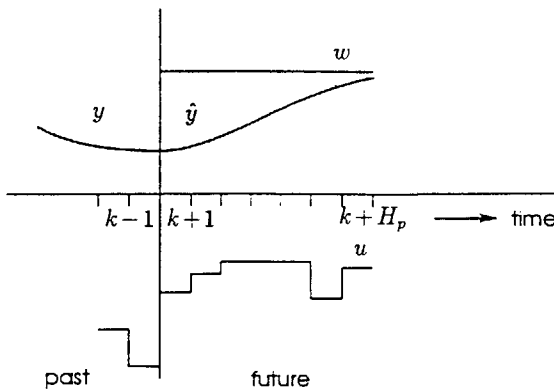
Figure 8.2: *General principle of a predictive controller.*

Mostly, a predictive controller from the first category is used to control a system with time-delay. Only a prediction is calculated over a time horizon equal to the time–delay.

We will restrict ourselves to the second category of predictive controllers. In these predictive control algorithms five steps can be distinguished (Fig. 8.2):

1. Generation of the reference trajectory w
   Originally, predictive controllers were applied in the process industry. There, step–wise setpoint changes have to be realized. Mostly, a certain desired response of the system towards this setpoint is required. This can be realized with the help of a reference trajectory. Mostly, a first order response is used. More generally, the reference trajectory describes the desired future response of the system.

2. Calculation of the predicted trajectory $\hat{y}$
   With a model of the system a prediction of the response is calculated. This prediction is calculated over a certain time horizon H_p, the *prediction horizon*. In the calculation of this prediction it is assumed that the future input signals to the system remain equal to the present input signal.

3. Correction of the predictions
   Because of modelling errors, and disturbances acting on the system the predictions will show a certain inaccuracy. The prediction can be corrected, or improved, in several ways. For instance, in DMC the same model, with which the predicted trajectory is calculated, is used to estimate the actual output value. The difference between the actual and the estimated output value is added to the predicted trajectory. In this way static, or low frequency disturbances, are compensated.

4. Determination of the future control actions u
   The computer calculates such future actions that the predicted output of the system is as close as possible to the desired reference trajectory. Herefore, a criterion function is minimized. This criterion function not only can contain a penalty for future tracking errors, but also a penalty for large control actions, or for large changes in the control actions.

5. Addition of the control actions
   Because mostly incremental control actions are determined, they have to be added to the present input.

8.4 Experimental set–up

8.4.1 Introduction

The main issue was the determination of the optimal prediction horizon. In this research it was investigated whether predictive control theory can be used to determine the best pre-diction horizon in the case that a human operator controls a space manipulator. It has to

be emphasized that the research must be considered just as a pilot study. Therefore, it was decided to start with a simplified control situation, in which only a planar manipulator had to be controlled. Because it is not straightforward to incorporate orientation requirements in the display, the orientation was fixed. So, both the computer and the human operator had to control 2 DOF.

The optimal length of the prediction horizon will depend on the task to be executed, the dynamics of the (controlled) manipulator, and the way in which the predicted trajectory is calculated. In this research only the dynamics were varied.
Normally in a rough positioning task a human operator has to plan a path himself. However, in predictive control theory a predetermined path is used. To create comparable control situations for both the computer and the human operator two options exist:

1. Extend the predictive control theory used to model human control behaviour, with a path planning module.

2. Fix the path to be followed for both the computer and the human.

A path planning module must be able to generate the same paths as a human operator does. The determination of such a planning module is not straightforward, and may require quite some time. Therefore, the second option was chosen.
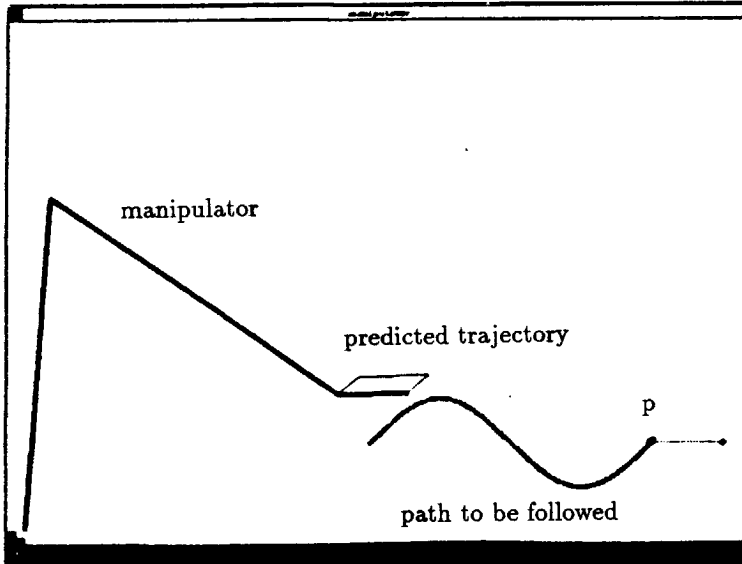
Figure 8.3: *The display of the manipulator, predicted trajectory, and the path to be followed.*

A rough positioning task can be divided into two phases: a track following phase and a stopping phase. In the track following phase, a curved path is tracked, whereas in the stopping phase mostly a straight line is followed. Therefore, the task to be executed was to follow a path, consisting of both a curved part and a straight line (Fig.8.3). Point p is a critical point in the sense that at that place an unforeseen, not smooth, curve has to be taken, for instance due to previous bad planning activities of a human operator.

An inherent problem is that the path to be tracked, as presented to the human operator on a display, has no time–scale attached to it, contrary to the reference trajectory as used in predictive control theory. Through a reference trajectory it is prescribed where the manipulator has to be at each future time instant. For a given path to be tracked, path constructing techniques can be used which take into account the limited accelerations caused by the limited torques. For instance, the manipulator has to be brought to rest at point p (Fig. 8.3), before the straight line can be followed. In this way perfect tracking of the trajectory can be achieved.

However, when subjects would be instructed to track the displayed trajectory only as accurate as possible, the danger for the application of a move–and–wait strategy exists. A predictive controller cannot apply such a move–and–wait strategy. Therefore, the following instruction was given to the subjects:

- *first priority*
  Keep the maximum velocity in the horizontal direction.

- *second priority*
  Track the displayed trajectory as well as possible.

Now, in the used path construction algorithm for generating the reference trajectory for the predictive controller, only in the beginning and at the end of the trajectory the limited accelerations were taken into account [van den Bosch, 1991]. For the rest of the points it was assumed that the manipulator moved with the maximum horizontal velocity.

When using a trajectory like a circle as the path to be followed, the horizontal velocity of the reference cannot be kept constantly at its maximum, because also the vertical velocity is limited. Therefore, a sine was used of which the combination of its amplitude and frequency was such that the absolute value of its derivative was never larger than 1. Then, the horizontal velocity always has to be larger than the vertical velocity, so that the limitation on the vertical velocity needed not to be taken into account. In addition, the sine part of the trajectory was such that the manipulator could track it perfectly, because the required torques were always less than their maximum values.

8.4.2 Experimental facility

The experiments with subjects were performed with the 2D simulation (Chapter 4), where the subjects had to control a planar manipulator. The predictive controller was implemented on a VAX 3100 M76 computer, using the simulation package $Matrix_X$.

Task

The path to be followed is shown in Fig. 8.3 and described in more detail in Section 8.4.1. The subjects were instructed to keep the maximum velocity in the horizontal direction as first priority, and as second priority to track the displayed path as well as possible. Therefore, no input weighting was present in the cost functional used by the predictive controller.

Controlled manipulator

The subjects controlled a planar manipulator. The dynamics of the manipulator were governed by Model 2 (Section 4.3.3). The experiments were performed in the End–Effector rate mode. The tip of the End–Effector served as POR. To track the desired trajectory only positioning rate commands, so 2 DOF, needed to be controlled.

The End–Effector rate setpoints were transformed into joint rate setpoints via the analytical computation of the inverse jacobian. A joystick was used as input device. The displacement of the joystick was proportional to the rate setpoints. A dead–band was used which was equal to one tenth of the maximum deflection.

Controller

Of course, in the case of the experiments with subjects a human functioned as the controller.

Although the manipulator is a non-linear system the idea was to use a state–based predictive controller. The model of the manipulator would be linearized. However, it appeared that an appropriate linearization algorithm was not available. The linearization algorithm available in $Matrix_X$ was not capable to linearize the model of the manipulator, probably because the torque limitation is a non–differentiable function. Predictive control schemes for systems with bounded inputs exist [Tsang, Clarke, 1988]. However, in our situation the torques are not the inputs for the system, but the End–Effector velocity setpoints are. The torques are bounded internal variables in the system, so that the predictive control schemes mentioned for bounded inputs form no solution. The End–Effector velocity command is two–dimensional and bounded. Now, when a certain control resolution is assumed a grid search method can be used to determine the optimal input. The predictions were made with the non-linear model of the manipulator. So, only the general principle of a predictive controller was used.

Calculation and display of the predicted trajectory

The calculation of the predicted trajectory for the human control situation is given in Appendix D. The display of the predicted trajecory is described in Section 4.4.4.

For the calculation of a predicition in the case of the predictive controller the non-linear model of the manipulator was used.

Table 8.1: *The three defined dynamical conditions.*

	Dynamical conditions		
	A	B	C
mass [kg]	3500	3500	1900
max. EE velocity [m/s]	0.09	0.05	0.09
stopping time [s]	10.1	5.9	5.9
stopping distance [m]	0.45	0.15	0.27

8.4.3 Experimental procedure

Experimental conditions

Now that the task has been defined (Section 8.4.1) the optimal prediction horizon has to be determined in relation to the system dynamics and the disturbances acting on the system. The dynamics are determined by several factors: The maximal joint torques, the maximum End–Effector velocities and the mass attached to the End–Effector. These factors determine more general characteristics like the stopping time and the stopping distance. Both the torques and the mass influence the maximum accelerations. Therefore, it was sufficient to vary only the mass and keep the maximum joint torques fixed. The applied vector of maximum torques was:

$$T_{max} = \begin{bmatrix} 300 \\ 225 \\ 300 \end{bmatrix} Nm.$$

To make sure that a predictive display will be of use to an operator, the independent variables V_{max}, the maximum End–Effector velocities, and m, the mass of the payload, were chosen such that the manipulator was slowly responding. In condition A (Table 8.1) the manipulator is very slowly responding, so that an operator will have to use a predictive display to execute the task properly. For condition B the combination $V_{max} = 0.05$ m/s and $m = 3500$ kg, which was foreseen for HERA, was used. To tackle the question whether the optimal prediction (time) horizon should be related to the stopping time or the stopping distance, a condition C was defined which was charaterized by the same stopping time as condition B, but with a different stopping distance (Table 8.1). The values for the stopping times and distances were evaluated for the critical point.

The optimal prediction horizon as a function of the dynamics had to be determined. So, for each defined dynamical condition the performance was measured for a number of prediction horizons. In Table 8.2 the experimental conditions are shown for the manual control situation. Contrary to the computer control situation, it was possible to add the conditions with no predictive display, to check whether a predictive display leads to an improvement in the performance.

130

Table 8.2: *Experimental conditions for the manual control situation.*

	dynamics	prediction horizon [s]						
		0	1	2	4	6	8	10
A	3500 kg / 0.09 m/s	A0	A1	A2	A4	A6	A8	A10
B	3500 kg / 0.05 m/s	B0		B2	B4	B6	B8	
C	1900 kg / 0.09 m/s	C0	C1	C2	C4	C6		

Training

The subjects trained until a more or less constant performance was achieved, which was after about 6 hours training. Subject 1 achieved a constant performance after performing 8 runs, and subject 2 after 9 runs per experimental condition.

Instruction

As was motivated in Section 8.4.1 the following instruction was given to the subjects:

- *first priority*
  Keep the maximum velocity in the horizontal direction.

- *second priority*
  Track the displayed trajectory as well as possible.

Data collection

The following performance criteria were recorded:

- The task *completion time.*

- The *energy* consumption. The square of the joint torques, integrated over the time, can be considered as a measure for the energy consumption.

- The *Root Mean Square Error* (RMS). The RMS is defined as

$$RMS = \sqrt{\frac{1}{N} \cdot \sum_{k=1}^{N} e(k)^2}, \tag{8.7}$$

where N is the number of samples and $e(k)$ is the error at the time instant k. The value of $e(k)$ for each k is the perpendicular distance of the End–Effector to the track to be followed.

- *Subject opinions.*

Subjects

The experiments were performed by the computer and two male subjects. Their age was about 23 years. Subject 1 was a novice. Subject 2 participated in the experiments reported in Chapter 7. The subjects were paid Dfl. 10,00 per hour.

8.5 Results

Completion time

Only after a very few runs, the subjects performed the task almost as fast as possible [van den Bosch, 1991]. This fact is illustrated in Fig. 8.4. The experiments consisted of at random permutations of the 17 conditions. The completion time for 1 "run" in Fig. 8.4 is the average over the completion times belonging to the 17 conditions. The minimum average completion time was about 70 seconds. So, it can be concluded that the subjects took good care of the first priority to maintain the maximum velocity.

RMS

The results for the computer and the manual control situation are illustrated in Figs. 8.5 and 8.6, resp. For both the control situations it can be seen that the shorter the prediction horizon was, the better the sine–part of the desired path was followed, but the larger the overshoot was at the critical point. The longer the prediction horizon was, the more the curves in the desired path were "cut off". When no predictive display was provided, the generated tracks by the subjects were always more swaying.

For conditions B and C in the computer control situation the optimal length of the prediction horizon to cope with the critical point seems to be the same (Fig. 8.7). Conditions B and C are characterized by the same stopping time. Therefore, the optimal length seems to be directly related to the stopping time, when unforeseen curves have to be taken.
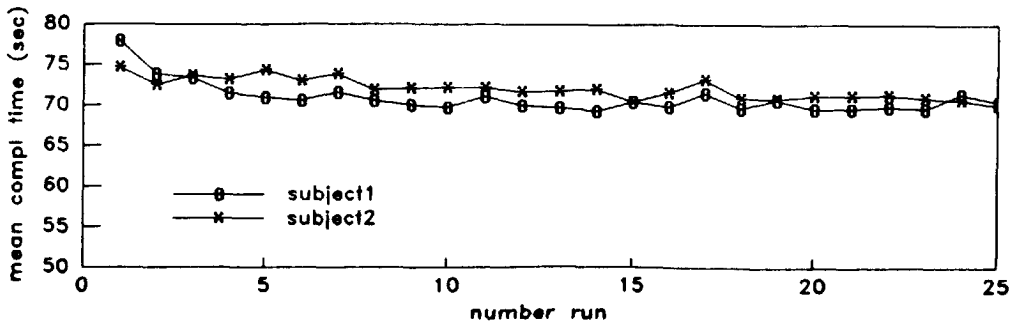
Figure 8.4: *Average completion times.*
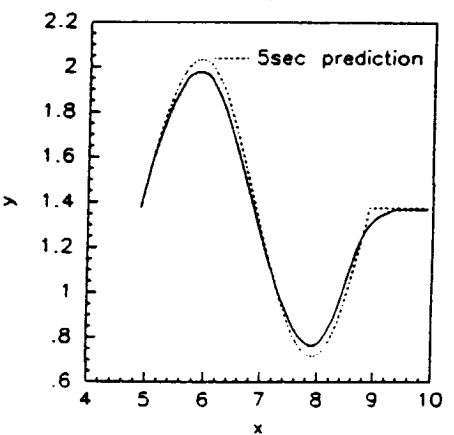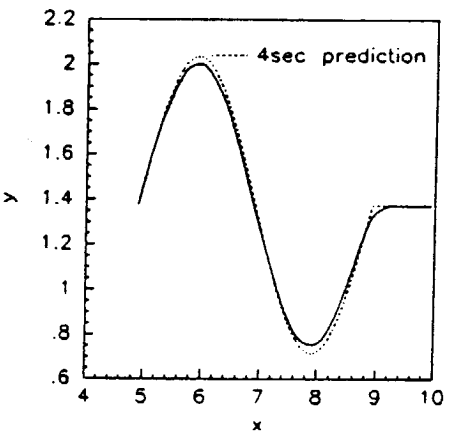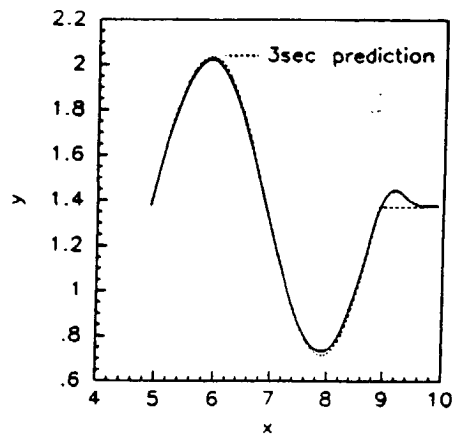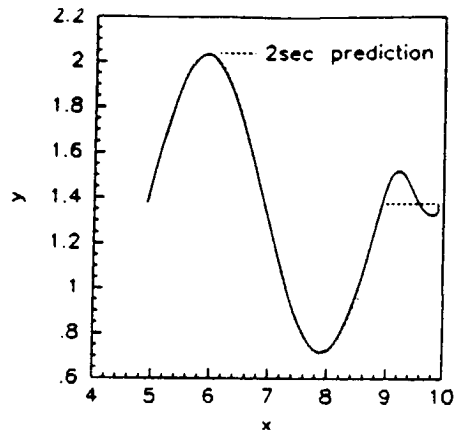
Figure 8.5: *Computer tracks.*
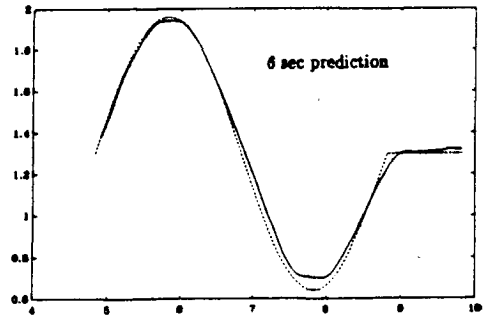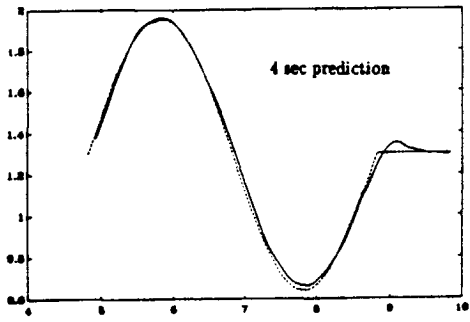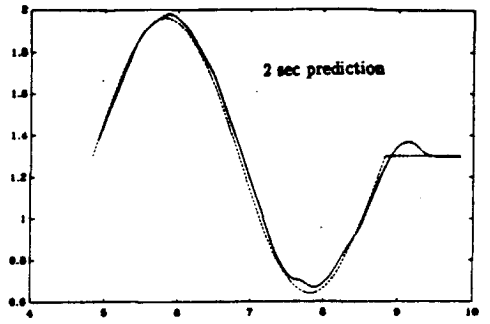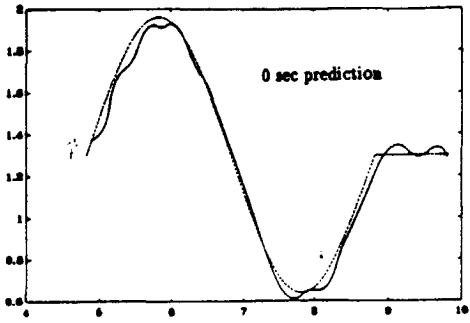
Figure 8.6: *Human tracks.*
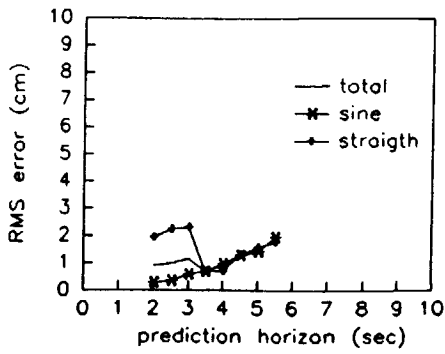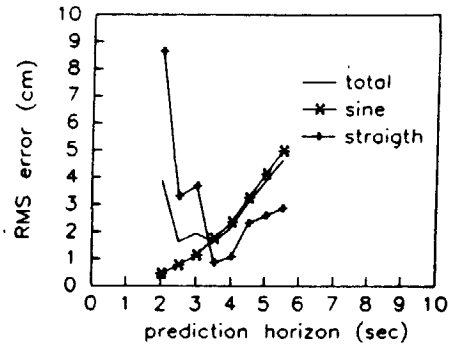
Condition B   Condition C

Figure 8.7: *RMS for conditions B and C in the computer control situation.*
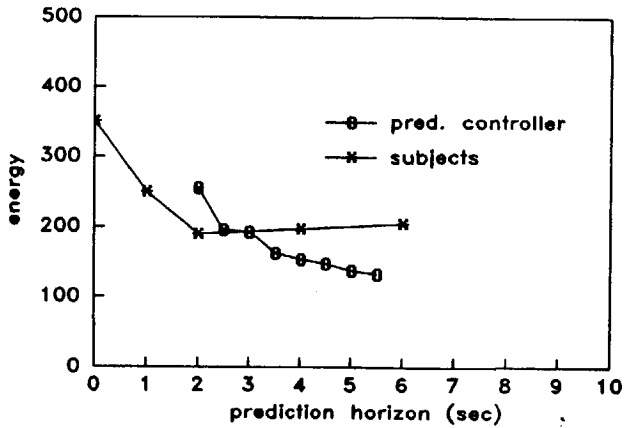
Figure 8.8: *Energy used.*

135

Energy

The results for the energy used are illustrated in Fig. 8.8. For both the computer and the manual control situation it can be seen that increasing the prediction horizon led to less energy consumption. However, in the manual situation the energy used is less sensitive for the length of the prediction horizon, compared to the computer situation.

Subject opinions

The difficulty of the dynamical conditions was, in ascending order, rated as follows: B, C, A. This is the same order as when ordered with respect to the stopping distance and the stopping time. However, note that conditions B and C have the same stopping time.
Subject 1 preferred the longer prediction horizons, whereas subject 2 preferred the shorter ones.

8.6   Discussion

The results for the computer control situation indicate that the optimal prediction horizon equals one time-step. This may be caused by a combination of two facts. Firstly, there was no input weighting present in the cost functional. Secondly, the sine part of the reference trajectory was generated in such a way that no input limitations were effective. Note that input limitations can be considered as an infinite penalty on inputs which are too large. When there is no input weighting in the cost functional it can be proven that the optimal length of the prediction horizon is independent on the system's dynamics, and it equals the length of the control horizon. When the control horizon can be freely chosen, one step ahead control yields the best result. This result is only proven for linear systems, but to a certain extent it might also be true in our case: Every time–step a linearized model can be used.
It must be noted that in practice generally a longer horizon is chosen, because of the robustness desired against parameter variations.

For conditions B and C, the optimal length of the prediction horizon to cope with the critical point seems to be the same (Fig. 8.7). Conditions B and C were characterized by the same stopping time. Therefore, the optimal length seems to be directly related to the stopping time, in the case that unforeseen curves have to be taken. The optimal length of the prediction horizon equaled about half of the stopping time (Table 8.1). How can this factor $\frac{1}{2}$ be explained?
To follow the track without a deviation, the manipulator has to be stopped at the critical point. Therefore, such a bend in the path has to be spotted within the system's stopping distance. Suppose the EE is moving with a constant velocity v. Then, a rough approximation yields:

$$0 = v + a \cdot T_{stop} \Rightarrow a = -v/T_{stop}, \tag{8.8}$$

where a denotes the acceleration and T_{stop} the stopping time. Let P_{stop} denote the stopping

distance. Then, there holds

$$P_{stop} = v \cdot T_{stop} + \frac{1}{2} \cdot a \cdot T_{stop}^2. \tag{8.9}$$

Together with Eq. 8.8 this yields

$$P_{stop} = \frac{1}{2} \cdot v \cdot T_{stop}, \tag{8.10}$$

The length of the predicted trajectory equals

$$P_{pred} = v \cdot T_{pred}. \tag{8.11}$$

In order to spot the critical point in time, so that the manipulator can be stopped, the length of the predicted trajectory has to be equal to the stopping distance: $P_{stop} = P_{pred}$. But then the prediction horizon must be equal to half the stopping time:

$$T_{pred} = \frac{1}{2} \cdot T_{stop}. \tag{8.12}$$

So, because the dynamics of the manipulator are state–dependent, each time–step the maximum stopping time has to be calculated, and then a prediction over half this stopping time has to be calculated.

Although the results for the manual and computer control situation did not exactly fit, they showed a large resemblence. A difference, for instance, was that the performance of the subjects was less dependent on the length of the prediction horizon, compared to the computer control situation. This can be explained by the fact that a human being is more robust for a deviation from the optimal length of the prediction horizon than the computer controller: When a predicted trajectory is too long a human probably ignores the last part of the predicted trajectory, and when it is too short, a human extrapolates the prediction himself.

When considering Fig. 8.8 again, it can be seen that in the computer control situation the energy monotoneously decreased for increasing prediction horizons, whereas the results of the manual control situation suggest the presence of a minimum or dip. The predicted trajectory as calculated in the computer control situation was fully accurate, contrary to the displayed predicted trajectory in the manual control situation. In the manual control situation it is assumed that the inertia matrix and the Jacobian remain constant over the prediction horizon (Appendix D). Moreover, the predicted trajectory consisted of an interpolation between three future points. In the computer control situation the prediction was made less accurate by adding noise on the joint velocities. As can be seen in Fig. 8.9 now also dips occur in the performance. Another explanation can be that too large a length of a predicted trajectory distracts the human operator.

A fundamental problem in this research was the fact that the path to be tracked, as presented to the human operator, has no time–scale attached to it, contrary to the reference

trajectory as used in predictive control theory. This problem was tackled by instructing the subjects to keep the maximum velocity in the horizontal direction, and by generating the reference trajectory according to this instruction. In this way it was expected that both the controllers would use the same time-scale, and so a move–and–wait strategy of the subjects was avoided. As a consequence no weighting on the input was incorporated in the cost functional, which may be questionable.

A different approach would be to use a path planning algorithm for the whole trajectory, and only to instruct the subjects to track the path as well as possible. The influence of this choice still needs to be investigated.

In reality the operator will have to plan a path himself. Then the timing present in the reference trajectory is also generated by the operator. Human planning activities still have to be incorporated in the predictive control model. Such a planning can be based upon several factors, like maintaining a safe distance to obstacles in the environment. This approach was followed in modelling the planning activities of a ship's navigator [Papenhuyzen, Stassen, 1989], and also in determining the best joint combination for redundant manipulators [Das, 1989].
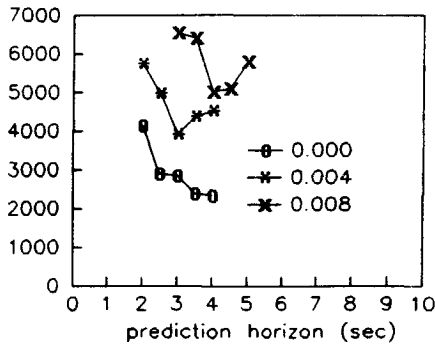
Figure 8.9: *Energy used; inaccurate predictions.*

8.7 Conclusions

Because the research reported in this chapter consisted of only a very preliminary study towards the use of predictive control theory to describe human control behaviour, the following conclusions must be considered as obtained conjectures. The validation of the results needs further research.

To enable the operator to take every possible turn safely, the prediction horizon must be equal to at least half of the maximum stopping time at each time instant.

Predictive control theory can serve as a means to describe human control behaviour.

Chapter 9

Discussion and future research

The starting point of the proposal for this research project was that a human operator had to control a space manipulator from Earth. In the proposal a number of problems was identified for an operator in a manual control situation: time–delays, slow and non-linear dynamics, multivariable character (up to 6 DOF to be controlled), and no direct vision. At the moment the project actually started, it was already known that only in the long term planning the operator will be placed on Earth. Therefore, the three remaining problems were investigated (Chapter 3):

- No direct vision.

- Up to 6 DOF to be controlled.

- Slow and non-linear dynamics.

For the investigation an experimental facility has been developed (Chapters 3 and 4). First-ly, the results of this study will be discussed in a more general setting, leading to future research issues. Then, recommendations will be made with respect to the experimental facility and the experimental design.

When a human operator has to execute a rough positioning task manually, he needs a kind of global view. Such a view can be generated by a camera on the MTFF or even by a camera mounted on the second limb of the manipulator, the elbow camera. If a model of the environment is available, graphical displays can be used to generate a global view. The results of Chapters 5 and 7 indicate that one of the main problems for the operator is the estimation of the distance of the manipulator, and especially of the End–Effector, to objects in the environment. If a model of the environment is available, the End–Effector can be projected on the environment, i.e.reference lines can be provided. The use of reference lines proved to be very useful to the operator. It led to a safer and faster task execution. However, collisions with the environment occur not only with the End–Effector, but also the limbs may hit objects in the environment. Therefore, a collision detection system for the whole manipulator arm may be very desirable, if not necessary for a guaranteed safe task execution. If a model of the environment is available, the system can be based on solving

geometric equations. If such a model is not available, extra sensors have to be provided. The problem of providing an operator with a good three–dimensional perception is also important in a supervisory control situation. A task of the operator is then the monitoring of the task execution. For instance, an incorrectly functioning joint angle encoder leads not only to a deviation of the manipulator from the preprogrammed path, but also inhibits a collision detection system, based on solving geometric equations, from working correctly. Moreover, aids only based on graphics are also improperly functioning in such a situation, because they also use the wrong joint angle information. For instance, suppose that the trajectory to be tracked is displayed on a separate graphical display, together with the position of the POR. Furthermore, suppose that a joint angle encoder shows a static deviation, and that the joint angles are PI controlled. The controller will realize a movement of the manipulator such that the difference between the (wrongly) measured angles and the required angles, of which the trajectory to be tracked consists, are minimized. Then the *measured*, graphically displayed movements of the POR will not show a deviation from the required trajectory, whereas the actual movements of the POR *will* deviate from the trajectory. An operator has to be able to detect such a situation. When reference lines are graphically superimposed on the TV–picture, they might be helpful in detecting such a situation. A reference line from the POR is drawn between the calculated position of the POR and the projection of that point on a base plane. The calculated position of the POR is based upon the wrongly measured angles. Therefore, the reference line will no longer be connnected to the POR in the TV–picture.

The slow and non-linear dynamics only caused real problems for an operator when the time needed to stop the manipulator was larger than 6 seconds or when the stopping distance was larger than 0.3 meter. It must be noted that these numbers are derived by allowing only positioning rate commands in a standard configuration (Fig. 7.4, Section 7.4.1). According to the most recent information the stopping distance for HERA will be less than 0.15 meter. So, the display of the stopping configuration will not be needful in the case of HERA. A display of a predicted trajectory can still be useful, since it led to less energy consumption in the experiments, due to a more calm control behaviour of the operator. The results of Chapter 8 indicate that the length of the prediction horizon should equal at least half of the stopping time at each time instant. Then the operator will be able to take every possible turn safely.

The large number of 6 DOF to be controlled is a limiting factor for an efficient performance, especially when the task becomes critical (Chapters 6 and 7). So, further automation and the development of a supervisory control system are desirable. The task of the operator in a supervisory situation is planning, monitoring and fault management.
To realize a supervisory control system, advanced control schemes, a model of the environment, collision avoidance algorithms, command languages etc. are required. Work has been performed with respect to these separate required items [IEEE trans. on SMC], but mostly the work consisted of a development of (another) new method. To my knowledge a good evaluation and comparison of the different methods has never been done. Moreover, rarely

a complete supervisory control system, where all the items are integrated, has been realized in the area of teleoperation. An application can be found in the control of underwater vehicles [Yoerger, 1990].

Still, research issues are, for instance, how man and computer can interact best in a planning procedure, and the design of fault management (sub)systems. It is expected that knowledge systems can play an important role in planning and fault management activities. In the case of complex systems, a human operator will not find a solution for the problem risen. If he does, Artificial Intelligence (AI) systems will come up much faster with the correct solution, which is important if it is critical to act fastly on a failure [Heer, Lum, 1988]. An inherent problem for knowledge systems is that they are based on knowledge, which must be gathered. Especially with newly designed systems to be controlled, this might yield problems. One can obtain the knowledge by using a (mathematical) model of the system, i.e. create a model based knowledge system. The question which then arises is whether ordinary mathematical techniques will not yield results which are at least as good. Another approach would be to use neural networks, where knowledge can be learned during control.

Since the definition of this research project, the design of HERA has made progress. New problems presented themselves. For instance, in this study the actuators were modelled as systems which can provide instantaneous, constant, but limited torques. No further dynamics, like stiction and friction were taken into account. However, HERA is now relocatable [Schoonejans et.al., 1990]. A consequence is that the actuators in the wrist have to be able to supply the same torques as the actuators in the shoulder. The stiction and friction levels, roughly spoken, are a percentage of the maximum torques which can be applied. So, the wrist joints have a larger stiction/friction level. However, the actuators in the wrist need only to provide small torques, due to the short distance of a payload to the wrist joints. When fine positioning commands are issued, as in the case of an insert task, the required torques are often less than the stiction levels. Then interactions are introduced in the controlled DOF. Personally, I experienced this as a major problem when servicing at Fokker as a subject in preliminary experiments on the HERA Simulation Facility Pilot.

Flexibility effects were not taken into account in this study. Flexibility effects can cause oscillations of the End–Effector. When looking through the End–Effector camera, an operator can experience the picture as unstable. The question is then to what extent these oscillations can or must be compensated. In the most recent design of HERA, flexibility effects may play a more important role than firstly was estimated. The reason is that HERA is now relocatable. When fine positioning commands are issued, as in the case of an insert task, the required torques are often less than the stiction levels. This fact does not only introduce interaction in the controlled DOF, but may also excite the flexibility modes.

Flexibility has also an indirect influence. A predictive display can be used as an aid for coping with both time–delays, when an operator is located on Earth, and the slow and non-linear dynamics. In calculating a prediction, a model of the manipulator is needed. For the application of predictive displays a real-time calculation of such a prediction is ne-

cessary. Therefore, the model may not be too complex. However, incorporating flexibility in the model makes it far more complex, so choices have to be made about which dynamical effects have to be included or not in the model. In general, predictions will always have a certain inaccuracy. The main question is then to what extent inaccuracies in the prediction will influence the behaviour and performance of a human operator.

These considerations led to the definition of a new project, entitled The Role of Flexibility in the Manual Control of a Space Manipulator. The new project is also supported by STW (contract no. DWT00.2208). In the project both the direct influence of flexibility, i.e. an oscillating End–Effector camera, and the indirect influence, i.e. inaccurate predictions, will be investigated.

Work has already been started concerning the calculation of a prediction [Breedveld, 1990]. It will be investigated to what extent different choices about dynamical effects to be included in a prediction model of the manipulator will influence the accuracy of a prediction. Also open loop and closed loop prediction methods will be compared, and it will be investigated how variations in the time–delays have to be handled.

In a supervisory situation there is an extra complication. In order to improve the accuracy of the prediction a closed loop prediction scheme can be used. But for failure detection, correcting the output of the prediction model with measurements can be undesirable. The operator just has to conclude from the difference between the trajectory of the prediction and the (delayed) display of reality that a failure has occurred.

It will be clear from the foregoing that the implementation of a more accurate model for the actuator dynamics should be considered. Also the flexibility of the manipulator should be incorporated in the simulation model.

The tasks to be excuted with the manipulator were split into two subtasks: a rough positioning task and an insert task. Each execution of a subtask required a separate experimental run. This splitting turned out to be very useful to study the possibilities and limitations of a human operator in a manual control situation efficiently. For studying a supervisory control situation it might be desirable to integrate the execution of all subtasks in one experimental run. For instance, when an operator has to decide wether the transition from the rough positioning task to the insert task is allowed, he will probably use both a global view and the End–Effector camera view. This is impossible in the present facility.

In the experiments different starting configurations were used, to avoid that the subjects would automatically execute a predefined control sequence, instead of determining on–line the required commands (Chapter 3). The use of different starting configurations indeed guaranteed a closed loop behaviour, but it required more training. In the case of a 3D rough positioning task, subjects have to face different starting configurations in the training too. These starting configurations do not need to be equal to the ones used in the experiments, but a certain resemblance has to be present.

Chapter 10

Conclusions and recommendations

In this chapter the conclusions of the separate chapters are summarized. The sections or pages between brackets refer to the place were a conclusion is drawn from the results.

Chapter 5: Visibility aspects for a rough positioning task

The presence of reference lines enhanced the three-dimensional perception, which resulted in a tendency towards a safer task execution. (pp. 59, 66)

A split screen facility for displaying two available survey views does not seem a very necessary aid. (p. 68)

The task to be executed was not critical enough for misfits in position estimations by the subjects; the results did not lead to statistically significant conclusions. (p. 66)

Chapter 6: On task allocations between man and computer for a rough positioning task

Referencing the operator's commands to the target frame, instead of to the End–Effector frame did not improve the human operator's control performance. The operator controlled the orientation firstly. In that way the difference between the two reference frames disappeared, before translation commands were issued. (pp. 80, 81, 83)

The reduction of the number of DOF to be controlled by the human operator, led to a more efficient task execution. The 2DOF mode was judged by the subjects to be easier than both End–Effector modes. (pp. 80, 84)

Chapter 7: Non-linear and slow dynamics: aiding the operator with a predictive display

The subjects felt more secure with a predictive display when the time needed to stop the

manipulator was larger than about 5 seconds or when the stopping distance was larger than 0.2 meter. (pp. 94, 110, 111)

The display of the stopping configuration led to a faster task execution when the time needed to stop the manipulator was larger than about 6 seconds or when the stopping distance was larger than 0.3 meter. (pp. 94, 99, 102)

The display of a predicted trajectory always led to less energy consumption, due to a more calm control behaviour of the subjects. (pp. 100, 102, 115)

The results indicate that a collision detection system is very desirable, if not necessary for a guaranteed safe task execution. (p. 113)

In new situations or in an unknown environment the combined problems of the three–dimensional perception and the control of 5 DOF are more serious than the problems due to the slow and non-linear dynamics. (p. 98)

Chapter 8: Describing the operator as a predictive controller

To enable the operator to take every possible turn safely, the prediction horizon must be at least equal to half of the stopping time at each time instant. (pp. 136, 137)

Predictive control theory can serve as a means to describe human control behaviour. (p. 137)

Recommendations

Future research directions should be the supervisory control situation, the effects of flexibility on the performance and behaviour of an operator, and the design of a predictive display to let the operator cope with the time–delays.

References

Anderson R J , Spong M W (1989)
    Bilateral Control of Teleoperators with Time-Delay
    IEEE trans. on Autom. Control, vol. 34, no. 5, pp. 494–501, May.
Andre G , Schoonejans P (1989)
    The Hermes Robot Arm : Teleoperation and Control Concept
    Proc. 2nd Eur. In–Orbit Operations Techn. Symp., Toulouse, France, Sept. 12–14.
Baron S, Berliner G E (1977)
    The Effects of Deviate Internal Representations in the Optimal Model of the Human
    Operator
    Proc. Annual Conf. on Manual Control, Cambridge, MIT, pp. 17–26
Baron S, Muralidharam R, Lancraft R, Zacharias G (1980)
    PROCRU: A Model for Analyzing Crew Procedures in Approach to Landing
    Techn. Report NASA–10035, NASA–Ames, CA
Bejczy A K (1982)
    Manual Control of Manipulator Forces and Torques Using Graphic Display
    IEEE proc. int. conf. cybernetics and society, pp. 691–698
Bejczy A K , Handlykken M (1981)
    Experimental Results with a 6 DOF Force–reflecting Handcontroller
    annual conf. on manual control, USA
Blaauboer W, Brinkman L (1990)
    Analysis and Evaluation of Task Allocation Strategies in a Bottling Line
    proc. 9th Eur. Annual conf. on human deciscion making and manual control, Sept.,
    Varese, Italy, pp. 205–214.
Boomgaard W van den (1986)
    A State–Space Baed Predictive Controller (in Dutch)
    Report A–393, Lab. for Meas. and Contr., Fac. of Mech. Eng. and Marine Techn.,
    Delft UT, The Netherlands
Bos J F T (1988)
    Pilot Experiments on the Manual Control of a Space Manipulator in the Single Joint
    Control Modes
    Report N–293, Lab. for Meas. and Contr., Fac. of Mech. Eng. and Marine Techn.,
    Delft UT, The Netherlands
Bos J F T (1989a)
    Predictive Display an Aid in Controlling Space Manipulators?
    proc. 8th Eur. Annual conf. on human decision making and manual contr., June 12–14,
    Techn. Univ. of Lyngby, Denmark, pp.31–41

146

Bos J F T (1989b)
   The Use of Predictive Displays in the Manual Control of a Space Manipulator: a Pilot
   Experiment
   Report N–317, Lab. for Meas. and Contr., Fac. of Mech. Eng. and Marine Techn.,
   Delft UT, The Netherlands
Bos J F T (1990)
   Man–Machine Research Issues for Teleoperation in Space
   Proc. ESTEC workshop ASTRA, Noordwijk, The Netherlands, June, ESA WPP–018.
Bos J F T , Klashorst F van de (1989)
   Visual Enhancements for Graphical Displays in the Control of Space Manipulators
   proc. 8th Eur. Annual conf. on human decision making and manual contr., June 12–14,
   Techn. Univ. of Lyngby, Denmark, pp.119–132
Bos J F T, Doorenbos H (1990)
   On Task Allocations Between Man and Computer for an Insert Task with a Space
   Manipulator
   proc. 9th Eur. Annual conf. on human deciscion making and manual control, Sept.,
   Varese, Italy, pp. 31–40.
Bos J F T, J.J. van den Bosch (1991)
   Describing the Operator as a Predictive Controller in a Space Telemanipulation
   Task
   proc. 10th Eur. Annual conf. on human deciscion making and manual control, Liege,
   Belgium, Nov. 13–16, to appear.
Bos J F T (1992)
   On Some Possible Aids for an Operator in the Manual Control of a Space Manipulator
   Proc. IFAC Symp. on Analysis, Design, and Evaluation of Man–Machine
   Systems, The Hague, The Netherlands, June 9–11, to appear
Bosch J J van den (1990)
   Voorspellingen toegepast bij regelingen en displays
   Report S–533, Lab. for Meas. and Contr., Fac. of Mech. Eng. and Marine Techn.,
   Delft UT, The Netherlands
Bosch J J van den (1991)
   A Predictive Controller as a Human Operator Model? A Theoretical and Experimental
   Study towards the Optimal Time Horizon of a Prediction Display for a Space Manipulator
   Report A–533, Lab. for Meas. and Contr., Fac. of Mech. Eng. and Marine Techn.,
   Delft UT, The Netherlands
Breedveld P (1990)
   Het Gebruik van Voorspellingsmethoden ter Compensatie van Tijdvertragingen
   bij de Besturing van een Ruimtemanipulator vanaf de Aarde
   Report S–537, Lab. for Meas. and Contr., Fac. of Mech. Eng. and Marine Techn.,
   Delft UT, The Netherlands
Buzan F T , Sheridan T B (1989)
   A Model Based Predictive Operator Aid for Telemanipulators with Time–Delay
   proc. IEEE int. conf. on SMC, nov. 14–17, Cambridge, Massachusetts, pp. 138–143
Clarke D W, Mohtadi C, Tuffs P S (1987a)
   Generalized Predictive Control – Part I. The Basic Algorithm
   Automatica, vol. 23, no. 2, pp. 137–148

Clarke D W, Mohtadi C, Tuffs P S (1987b)
Generalized Predictive Control – Part II. Extensions and Interpretations
Automatica, vol. 23, no. 2, pp. 149–160
Covault C (1981a)
Shuttle Manipulator Tests to Allow Crew Flexibility
Aviation week and space technology, sept. 28, pp. 53–59
Covault C (1981b)
Remote Arm Aids Shuttle Capability
Aviation week and space technology, sept. 7, pp. 57–73
Craig J J (1986)
Introduction to Robotics : Mechanics and Control
Stanford
Das H , Sheridan T B , Slotine J (1989)
Kinematic Control and Visual Display of Redundant Teleoperators
proc. IEEE int. conf. on SMC, nov. 14–17, Cambridge, Massachusetts, pp. 1072–1077
Doorenbos H (1989a)
The Control Side of the MMI of a Manually Controlled Space Manipulator
Report S–439, Lab. for Meas. and Contr., Fac. of Mech. Eng. and Marine Techn.,
Delft UT, The Netherlands
Doorenbos H (1989b)
An Insert Task with a Space Manipulator : Experiments on the Task Allocation
Between Man and Computer
Report A–439, Lab. for Meas. and Contr., Fac. of Mech. Eng. and Marine Techn.,
Delft UT, The Netherlands
Drascic D , Milgram P (1989)
Learning Effects in Telemanipulation with Monoscopic Versus Stereoscopic Remote Viewing
proc. IEEE int. conf. on SMC, nov. 14–17, Cambridge, Massachusetts, pp. 1244–1249
Ellis S R, McGreevy (1987)
Perspective Traffic Display Format and Airline Traffic Pilot Avoidance
Human Factors, vol. 29 (4), pp. 371–382
Ferrell W R (1965)
Remote Manipulation with Transmission Delays
IEEE trans. on Human Factors in Electronics, sept., pp. 24–
Ferrell W R (1966)
Delayed Force Feedback
Human Factors, pp 449–455, okt.
Flatau C R (1973)
The Manipulator as a Means of Extending Our Dexterous Capabilities to Larger
and Smaller Scales
Proc. 21st conf. Remote Syst. Techn., pp. 47–50
Francis B A, Wonham W M (1975)
The Internal Model Principle of Linear Control Theory
Proc. IFAC 6th world congr., Boston MA, paper 43.5
Hamann R J, Bentall R H (1989)
The Hermes Robot Arm, System Description
Proc. 2nd Eur. In–Orbit Operations Techn. Symp., Toulouse, France, Sept. 12–14.

Hannaford B , Kim W S (1989)
      Force Reflection, Shared Control, and Time–Delay in Telemanipulation
      proc. IEEE conf. on SMC, nov. 14–17, Cambridge, Massachusetts, pp. 133–137
Hearn D, Baker M P (1986)
      Computer Graphics
      Prentice Hall
Heer E, Lum H (eds.) (1988)
      Machine Intelligence and Autonomy for Aerospace Systems
      AIAA, ISBN 0–930403–48–7
Heintze J (1988)
      Zicht op Voorspellend Regelen: een Nadere Beschouwing van DMC
      Report A–467, Lab. for Meas. and Contr., Fac. of Mech. Eng. and Marine Techn.,
      Delft UT, The Netherlands
Hess R A (1983)
      Effects of Time–Delays on Systems Subject to Manual Control
      J. Guidance, vol. 7 no. 4, pp.416–421
Hess R A , Modjtahedzadeh A (1990)
      A Control Theoretical Model of Driver Steering Behavior
      IEEE Control Systems Mag., vol. 10, no. 5, August, pp. 3–8
Hill J W (1976)
      Comparison of Seven Performance Measures in a Time– Delayed Manipulation Task
      IEEE trans. on syst., man and cybern., SMC–6, no. 4, pp 286–295, april
Jain A, Gonsalves P, Zacharias G (1989)
      Internal Model Mismatch in the Optimal Control Model
      proc. IEEE int. conf. on SMC, nov. 14–17, Cambridge, Massachusetts, pp. 731–737
Johannsen G , Govindaraj T (1980)
      Optimal Control Model Predictions of System Performance and Attention Allocation
      and their Experimental Validation in a Display Design Study
      IEEE trans. on SMC, vol. 10, no. 5, May, pp. 249–261.
Kalman R E, Bucy R S (1961)
      New Results in Linear Filtering and Prediction Theory
      Trans. ASME J. Basic Eng., vol. 83, pp. 95–107
Kelley C R (1968)
      Manual and Automatic Control
      Bernotat, Gartner (eds.), John Wiley and sons inc.
Kelley C R (1972)
      Adaptive Display Using Prediction in Displays and Controls
      Swets and Zeitlinger, Amsterdam, pp. 61–74.
Keyser D, Cauwenberghe A van (1981)
      A Self–Tuning Multistep Predictor Application
      Automatica, vol. 17, no. 1, pp. 167–174
Kim W S , Tendick F, Ellis S R, Stark L (1987a)
      A Comparison of Position and Rate Control for Telemanipulations with Consideration
      of Manipulator Dynamics
      IEEE journal of Robotics and Automation, vol. 3, no. 5, okt.
Kim W S, Tendick F, Stark L (1987b)

Visual Enhancements in Pick and Place Tasks: Human operators Controlling a Simulated Cylindrical Manipulator
IEEE Journal of Robotics and Automation, vol. 3, no. 5, pp 418–425, oct.
Klashorst F van de (1988)
A Survey of Three–Dimensional Perception Techniques
report S–492, Lab. for Meas. and Contr., Fac. of Mech. Eng. and Marine Techn., Delft UT, The Netherlands (in Dutch)
Klashorst F van de (1989)
3D–perceptie Bepalende Factoren bij het Gebruik van Grafische Displays
Report A–492, Lab. for Meas. and Contr., Fac. of Mech. Eng. and Marine Techn., Delft UT, The Netherlands
Knobloch H W, Kwakernaak H (1985)
Lineare Kontrolltheorie
Springer Verlag, ISBN 3–540–13626–6
Kok J J, Wijk R A van (1978)
Evaluation of Models Describing Human Operator Control of Slowly Responding Systems
PhD. Thesis, dept. of mech. eng., lab. meas. and contr., Delft UT
Kok J J, Stassen H G (1980)
Human Operator Control of Slowly Responding Complex Systems: Supervisory Control
Journ. of Cyb. and Info. Sc., special issue on MMS, 3 (nos. 1–4), pp. 123–174
Kwakernaak, Sivan (1972)
Linear Optimal Control Systems
New York, John Wiley & sons, pp. 389–402
Lambooy P (1988)
Handcontrol of Space Manipulators
Masters Thesis, Fac. of Aircraft and Space Eng. Delft UT, The Netherlands
Lane B (1982)
Stereoscopic Displays
SPIE, vol. 367, pp. 20–31
Leifer L (1983)
Interactive Robotic Manipulation for the Disabled
proc. int. conf. 26th IEEE computer soc. COMPCON, San Francisco, pp.46–49
Levison W H, Kleinman D L, Baron S (1969)
A Model for Human Controller Remnant
IEEE transactions on man machine systems , vol. 10, dec.
Levison W H, Kleinman D L, Baron S (1970)
An Optimal Control Model of Human Response. Part I : Theory and Validation
Automatica , vol.6, pp 357–369
Lunteren A van (1979)
Identification of Human Operator Describing Function Models with One or Two Inputs in Closed–Loop Systems
PhD. thesis, Lab. for Meas. and Contr., Fac. of Mech. Eng. and Marine Techn., Delft UT, The Netherlands
Massimino M J , Sheridan T B (1989)
Variable Force and Visual Feedback Effects on Teleoperator Man/Machine Performance
proc. NASA conf. on space telerobotics, Pasadena, USA

McRuer D T, Jex H R (1967)
    A Review of Quasi–Linear Pilot Models
    IEEE trans. on Human Factors in Electronics, vol. 8, no. 3,pp 231–249
Milgram P, Horst R van de (1980)
    Field–Sequential Colour Stereoscopy with Liquid Crystal Spectacles
    proc. Eurodisplay '84, Sept. 18–20, Paris
Milgram P (1985)
    Control Loops with Human Operator in Space Operations; Part V: Executive Summary
    NLR report TR 84116 L part V; ESA contract 5594/83
Milgram P , Weverinke P (1985)
    Model Analysis of Remotely Controlled Rendezvous and Docking with Display Prediction
    proc. 21st annual conf. on manual control, NASA, CP–2428, Moffet Field
Moray N, King B, Turksen I, Waterton K (1987)
    A Closed Loop Causal Model of Workload Based on a Comparison of Fuzzy and Crisp
    Measurement Techniques
    Human Factors, vol. 29, pp. 339–346
Nguyen A H , Ngo , Stark L (1988)
    Image Model Control of Image Processing
    proc. 33rd IEEE computer societyintl. conf., pp. 539–542, San Francisco
Papenhuijzen R , Stassen H G (1989)
    On the Modelling of Planning and Supervisory Behaviour of the Navigator
    proc. IEEE conf. on SMC, Xian, China, pp. 19-24
Overbeeke C J (1988)
    Space Through Movement : Theory
    PhD.–thesis, Fac. of Indus. Design, TU Delft.
Passenier P O (1989)
    An Adaptive Track Predictor for Ships
    PhD. thesis, Fac. of Elect. Eng., Deflt UT, The Netherlands.
Paul R P (1981)
    Robot Manipulators: Mathematics, Programming and Control
    MIT Press, ISBN 0–262–16082–X
Pennington (1983)
    A Rate–Controlled Teleoperator Task with Simulated Transport Delays
    NASA report TM–85653.
Pepper R, Cole R, Spain E, Sigurdson J (1983)
    Research Issues Involved in Applying Stereoscopic TV to Remote Operated Vehicles
    SPIE vol. 402, pp. 170–173
Pew R , Baron S (1983)
    Perspectives on Human Performance Modelling
    Automatica, vol.19, no. 6,pp.663–676
Prins J, Dieleman P, Jong II de(1989)
    The Real–Time Hermes Robot Arm Simulator: HSFP
    Proc. 2nd Eur. In–Orbit Operations Techn. Symp., Toulouse, France, Sept. 12–14.
Rasmussen J (1983)
    Skills, Rules and Knowledge; Signals, Signs and Symbols; and other Distinction in
    Human Performance Models

IEEE trans. on SMC, vol. 13, no. 3, pp. 257–266
Ravindran R, Doetsch K H (1982)
Design Aspects of the SRMS Control
AIAA, pp. 456–459, further reference unknown
Roode P de (1988)
Performance of Control Strategies Based Upon Simplfied Space Manipulator Models
Report A–408, Lab. for Meas. and Contr., Fac. of Mech. Eng. and Marine Techn.,
Delft UT, The Netherlands
Rouhani R, Mehra R K (1982)
Model Algorithmic Control (MAC); Basic Theoretical Properties
Automatica, vol. 18, no. 4, pp. 401–414
Ruitenbeek J C (1984a)
Inventory on Human Operator Positioning Control Behaviour with Special Emphasis on
Time–Delayed Systems
Report N–227, Lab. for Meas. and Contr., Fac. of Mech. Eng. and Marine Techn.,
Delft UT, The Netherlands
Ruitenbeek J C (1984b)
Pilot Study on Human Operator Positioning Control in Direct Drive Mode with
Delayed Visual Feedback
Report N–229, Lab. for Meas. and Contr., Fac. of Mech. Eng. and Marine Techn.,
Delft UT, The Netherlands
Ruitenbeek J C (1984c)
Invariants in Loaded Goal–Directed Movements
Biological Cybernetics, vol. 51, pp. 11–20
Ruitenbeek J C (1985)
Visual and Proprioceptive Information in Goal Directed Movements: A System
Theoretical Approach
PhD. thesis, Lab. for Meas. and Contr., Fac. of Mech. Eng. and Marine Techn.,
Delft UT, The Netherlands
Sachs L (1982)
Applied Statistics
Springer Verlag, ISBN 0–387–90558–8
Salski A, Noback H (1986)
On the Modelling of the Behaviour of a Navigator. A Fuzzy Set Approach
proc. 6th Eur. Annual conf. on human deciscion making and manual control, Cardiff
Salski A, Noback H , Stassen H G (1987)
A Model of the Navigator's Behaviour Based on Fuzzy Set Theory
In J. Patrick and K. Duncan (eds.) Human Decision Making and Control,
North–Holland Publ. Co.
Schenker P S , Bejczy A K (1990)
Workspace Visualization and Time–Delay Telerobotic Operations
proc. 13th annual AAS Guidance and Control Conf., Febr. , Keystone
Schneider S A, Cannon R H (1989)
Experiments in Cooperative Control: a System Perspective
Proc. NASA conf. on Space Telerobotics
Schoonejans P H M, Andre G, Danan G (1990)

The Hermes Robot Arm: Advances in Concepts and Technologies
Proc. IAF–90–025
Sheppard J S et.al. , (British Aerospace) (1986)
Teleoperation and Control Study, Final Report
ESA Report CR (P) 2413
Sheppard J S et.al. , (British Aerospace) (1989)
Teleoperation and Control Study 2, Final Presentation
ESTEC Conract 6836/86/NL/MAC
Sheridan T B (1989)
Telerobotics
Automatica, vol. 25, no. 4, pp. 487–507
Siegel (1956)
Nonparametric Statistics
McGraw–Hill Book Company, inc.
Smith O J M (1959)
A Controller to Overcome Dead Time
ISAJ, vol. 6, no. 2, pp. 28–33
Soeterboek R (1990)
Predictive Control: A Unified Approach
Ph.D. thesis, Fac. of Electr. Eng., Delft UT, The Netherlands
Stark et.al (1987)
Telerobotics: Display, Control and Communication Problems
IEEE Journal of Rob. and Autom., vol. 3, no. 1, Febr.
Starr G P (1979)
A Comparison of Control Modes for Time–Delayed Remote Manipulation
IEEE trans syst. man and cybern., vol. SMC–9, no. 4, pp. 241–246, april
Starr G P (1981)
Supervisory Control of Remote Manipulation : a Preliminary Evaluation
proc. 17–th Annual Manual USA, pp. 95–107
Stassen H G, Veldt R van de (1982)
Human Operator Models : a Useful Tool in MMif Design ?
Proc. Annual Meeting on Human Factors, Seattle
Stassen H G (1989)
On the Modeling of Manual Control Tasks
Applications of human performance models to system design, McMillan et.al. (eds.),
Plenum Press, ISBN 0–306–43242–0
Stassen H G, Johannsen G, Moray N (1990)
Internal Representation, Internal Model, Human Performance and Mental Workload
Automatica, vol. 26, no. 4, July, pp. 811–820
Stratmann M H (1988)
Raum durch Bewegung : Technology
PhD.–thesis, Fac. of Indus. Design, TU Delft.
Tsang T T C, Clarke D W (1988)
Generalized Predictive Control with Input Constraints
IEE Proc., vol. 135, Pt.D, no. 6, November
Vaart J van de , Hosman R (1988)

Human Performanceand Control Behaviour in Disturbance Compensation Tasks and Target Tracking Tasks
proc. 7th Eur. annual conf. on human decision making and manual control, 18–20 oct., Paris, France, pp.120–125

Vadus J R (1976)
International Status and Utilization of Undersea Vehicles
proc. inter–ocean 76, june, pp. 559–578, Dusseldorf, Germany

Vegte J van de , Milgram P , Kwong R (1990)
Teleoperator Control Models: Effects of Time Delay and Imperfect System Knowledge
IEEE trans. on SMC, vol. 20, no. 6, pp. 1258–1272

Veldhuyzen W (1976)
Ship Manoeuvring under Human Control. Analysis of the Helmsman's Comtrol Behaviour
PhD. thesis, Lab. for Meas. and Contr., Fac. of Mech. Eng. and Marine Techn., Delft UT, The Netherlands

Veldt R van der , Boomgaard W van den (1986)
Predictive Information in the Control Room
Human Decision Making and Manual Control, H.P. Willumeit (editor), Elsevier Science Publ. BV (North–Holland), pp.249–264.

Waard G J de (1987)
User Requirements Document (URD) for the HERA On–Board Software
Fokker Report FSS–N–87–LTPP–048.

Wernli R L (1982)
Robotics Undersea
Mechanical Engineering, aug., pp. 24–31

Weverinke P H (1987)
Model of the Human Observer and Controller of a Dynamic System
Proc. IEEE conf. on system man and cybern., pp. 66–71, further reference unknown

Yoerger D R (1990)
The supervisory Control of Underwater Telerobots
In: Robotics, Control and Society; Moray, Ferrell, Rouse (eds.)
Taylor and Francis, ISBN 0–85066–850–6, pp. 48–59

Zadeh L A (1973)
Outline of a New Approach to the Analysis of Complex Systems and Decision Processes
IEEE trans. on SMC, vol. 3, no. 1, Jan., pp. 28–44

Zadeh L A (1984)
Making Computers Think Like People
IEEE Spectrum, August, pp. 26–32

Appendix A

Kinematics

Notation: $S_i = sin(\theta_i)$ $C_i = cos(\theta_i)$
              $S_{i \cdots j} = sin(\theta_i + \cdots + \theta_j)$ $C_{i \cdots j} = cos(\theta_i + \cdots + \theta_j)$

Kinematics

The A–matrices as mentioned in Section 4.3.1 are equal to [Paul, 1981, p. 60] :

$$A_1 = \begin{bmatrix} C_1 & 0 & S_1 & 0 \\ S_1 & 0 & -C_1 & 0 \\ 0 & 1 & 0 & 0 \\ 0 & 0 & 0 & 1 \end{bmatrix} \tag{A.1}$$

$$A_2 = \begin{bmatrix} C_2 & -S_2 & 0 & a_2 \cdot C_2 \\ S_2 & C_2 & 0 & a_2 \cdot S_2 \\ 0 & 0 & 1 & 0 \\ 0 & 0 & 0 & 1 \end{bmatrix} \tag{A.2}$$

$$A_3 = \begin{bmatrix} C_3 & -S_3 & 0 & a_3 \cdot C_3 \\ S_3 & C_3 & 0 & a_3 \cdot S_3 \\ 0 & 0 & 1 & 0 \\ 0 & 0 & 0 & 1 \end{bmatrix} \tag{A.3}$$

$$A_4 = \begin{bmatrix} C_4 & 0 & -S_4 & a_4 \cdot C_4 \\ S_4 & 0 & C_4 & a_4 \cdot S_4 \\ 0 & -1 & 0 & 0 \\ 0 & 0 & 0 & 1 \end{bmatrix} \tag{A.4}$$

$$A_5 = \begin{bmatrix} C_5 & 0 & S_5 & 0 \\ S_5 & 0 & -C_5 & 0 \\ 0 & 1 & 0 & 0 \\ 0 & 0 & 0 & 1 \end{bmatrix} \tag{A.5}$$

$$A_6 = \begin{bmatrix} C_6 & -S_6 & 0 & 0 \\ S_6 & C_6 & 0 & 0 \\ 0 & 0 & 1 & 0 \\ 0 & 0 & 0 & 1 \end{bmatrix} \tag{A.6}$$

Note that contrary to [Paul, 1981] a_4, the length of the beam segment between the pitch and the yaw joint of the wrist of the manipulator, is zero in our case.
The position and orientation of the wrist, T_6, is equal to :

$$T_6 = A_1 \cdot A_2 \cdots A_6 \tag{A.7}$$

$$= \begin{bmatrix} n_x & o_x & a_x & p_x \\ n_y & o_y & a_y & p_y \\ n_z & o_z & a_z & p_z \\ 0 & 0 & 0 & 1 \end{bmatrix} \tag{A.8}$$

where

$$\begin{aligned} n_x &= C_1 C_{234} C_5 C_6 - S_1 S_5 C_6 - C_1 S_{234} S_6 \\ n_y &= S_1 C_{234} C_5 C_6 - C_1 S_5 C_6 - S_1 S_{234} S_6 \\ n_z &= S_{234} C_5 C_6 + C_{234} S_6 \end{aligned}$$

$$\begin{aligned} o_x &= -C_1 C_{234} C_5 S_6 + S_1 S_5 S_6 - C_1 S_{234} C_6 \\ o_y &= -S_1 C_{234} C_5 S_6 - C_1 S_5 S_6 - S_1 S_{234} C_6 \\ o_z &= -S_{234} C_5 S_6 + C_{234} C_6 \end{aligned}$$

$$\begin{aligned} a_x &= C_1 C_{234} S_5 + S_1 C_5 \\ a_y &= S_1 C_{234} S_5 - C_1 C_5 \\ a_z &= S_{234} S_5 \end{aligned}$$

$$\begin{aligned} p_x &= C_1 \cdot (a_2 C_2 + a_3 C_{23} + a_4 C_{234}) \\ p_y &= S_1 \cdot (a_2 C_2 + a_3 C_{23} + a_4 C_{234}) \\ p_z &= a_2 S_2 + a_3 S_{23} + a_4 S_{234} \end{aligned}$$

Here, a_2 is l_1, the length of the first limb, and a_3 is l_2, the length of the second limb.
The position and orientation of the tip of the End–Effector, T_7, is equal to $T_7 = T_6 \cdot A_7$, where A_7 is a translation along the $\vec{a}$–axis of T_6 equal to the length l_3 of the End–Effector :

$$A_7 = \begin{bmatrix} 1 & 0 & 0 & 0 \\ 0 & 1 & 0 & 0 \\ 0 & 0 & 1 & l_3 \\ 0 & 0 & 0 & 1 \end{bmatrix} \tag{A.9}$$

156

So, the orientation of the frame at the tip is equal to the orientation of the wrist $(\vec{n}, \vec{o}, \vec{a})$ and the position equals $\vec{p} + l_3 \cdot \vec{a}$.

Inverse kinematics

In the inverse kinematics the values of the angles are calculated given T_6, the position and orientation of the wrist. From Eq. A.8 12 equations can be obtained to calculate the 6 joint angles. However, only 6 of those equations are independent, beacuse the $\vec{n}$, $\vec{o}$ and $\vec{a}$ vectors are orthonormal. So, firstly $\vec{n}$ is equal to the cross product of $\vec{o}$ and $\vec{a}$, and secondly the length of the vectors is equal to 1, so that a vector has only 2 independent or free entries. The equations are trigonometric and multiple solutions can exist as is illustrated in Fig. A.1.
In the following algorithm it is assumed that

1. $\theta_1 \in [-\frac{\pi}{2}, \frac{\pi}{2}]$ and $p_x > 0$ (shoulder forward)

2. $\theta_3 < 0$ (elbow down)

3. $\theta_5 \in [-\frac{\pi}{2}, \frac{3\pi}{2}]$

The general formulation is given in [Paul, 1981, p. 78; de Waard, 1988]. Assume $\theta_1 \in [-\frac{\pi}{2}, \frac{\pi}{2}]$ and $p_x > 0$. Then we have that the configuration indicator for the shoulder is forward for sure. Then

$$\theta_1 = atan2(p_x, p_y) \tag{A.10}$$

The next step is to calculate the orientation of link a_4. The projection of $\vec{a}$ on the plane through the x–axis and the y–axis equals

$$C_1 a_x + S_1 a_y$$

The total pitch or elevation angle of a_4, θ_{234}, is the angle between a_z and $C_1 a_x + S_1 a_y$. So

$$\theta_{234} = atan2(a_z, C_1 a_x + S_1 a_y) \tag{A.11}$$
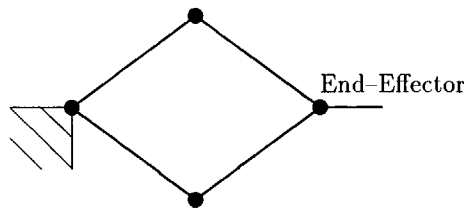
Figure A.1: *Illustration ot the existance of multiple solutions.*

157

With the orientation of link a_4 known, the position of joint 4 in the coordinate frame $X_1Y_1Z_1$, the frame through the two limbs, can now be calculated (Fig. A.2).

$$
\begin{aligned}
p'_x &= C_{23}a_3 + C_2a_2 & \text{(A.12)} \\
&= C_1p_x + S_1p_y - C_{234}a_4 & \text{(A.13)} \\
p'_y &= S_{23}a_3 + S_2a_2 & \text{(A.14)} \\
&= p_z - S_{234}a_4 & \text{(A.15)}
\end{aligned}
$$

Note that a_4 is zero in our case. The angle θ_3 can be derived from the reach of the links a_2 and a_3 :

$$
C_3 = \frac{(p'_x)^2 + (p'_y)^2 - a_2^2 - a_3^2}{2 \cdot a_2 \cdot a_3} \tag{A.16}
$$

It is assumed that $\theta_3 < 0$, so

$$
\begin{aligned}
S_3 &= \sqrt{1 - C_3^2} & \text{(A.17)} \\
\theta_3 &= -atan2(S_3, C_3) & \text{(A.18)}
\end{aligned}
$$

Because of the minus sign C_3 and S_3 have to be recalculated :

$$
\begin{aligned}
C_3 &= cos(\theta_3) \\
S_3 &= sin(\theta_3)
\end{aligned}
$$

The pitch angle of the first limb is determined by

$$
\begin{aligned}
S_2 &= (C_3a_3 + a_2) \cdot p'_y - S_3a_3p'_x & \text{(A.19)} \\
C_2 &= (C_3a_3 + a_2) \cdot p'_x + S_3a_3p'_y & \text{(A.20)} \\
\theta_2 &= atan2(S_3, C_3) & \text{(A.21)}
\end{aligned}
$$

Now

$$
\begin{aligned}
\theta_4 &= \theta_{234} - \theta_2 - \theta_3 & \text{(A.22)} \\
\theta_4 &= \theta_4 + k \cdot 2\pi & \text{(A.23)} \\
\theta_{234} &= \theta_{234} + k \cdot 2\pi & \text{(A.24)}
\end{aligned}
$$

where

$$
k = \begin{cases} 0 & \theta_4 \in (-\pi, \pi] \\ 1 & \theta_4 \in (-3\pi, -\pi] \\ -1 & \theta_4 \in (\pi, 3\pi) \end{cases}
$$

The wrist yaw angle θ_5 is determined by :

$$
\begin{aligned}
S_5 &= C_{234} \cdot (C_1a_x + S_1a_y) + S_{234}a_z & \text{(A.25)} \\
C_5 &= S_1a_x - C_1a_y & \text{(A.26)} \\
\theta_5 &= atan2(S_5, C_5) & \text{(A.27)}
\end{aligned}
$$

158

Because of the allowed range for θ_5 is $[-\frac{\pi}{2}, \frac{3\pi}{2}]$, the solution for θ_5 has to be modified :
IF $\theta_5 \in [-\pi, -\frac{\pi}{2})$ THEN $\theta_5 = \theta_5 + 2\pi$.

The wrist roll angle θ_6 is determined by :

$$
\begin{aligned}
S_6 &= -C_5 \cdot (C_{234} \cdot (C_1 o_x + S_1 o_y) + S_{234} o_z) + S_5 \cdot (S_1 o_x + C_1 o_y) & \text{(A.28)} \\
C_6 &= -S_{234} \cdot (C_1 o_x + S_1 o_y) + C_{234} o_z & \text{(A.29)} \\
\theta_6 &= atan2(S_6, C_6) & \text{(A.30)}
\end{aligned}
$$
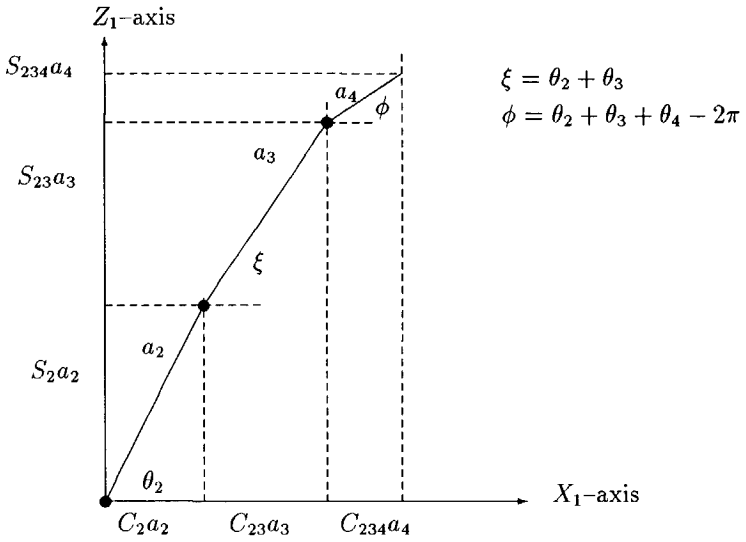
Figure A.2: *The $X_1 Z_1$ plane through the two limbs.*

Appendix B

Calculation inertia matrix

The inertia matrix in Model 2 was derived using the Lagrangian method [Brady, 1982]. There is no gravity in space, so only the kinetic energy E_{kin} has to be taken into account :

$$\frac{d}{dt}(\frac{\delta E_{kin}}{\delta \dot{\theta}_i}) - \frac{\delta E_{kin}}{\delta \theta_i} = T \tag{B.1}$$

As an example for the derivation of the kinetic energy for each mass m_i (Fig. 4.11), the kinetic energy for mass m_1, located at the elbow of the manipulator, will be derived.

Mass m_1 is located at :

$$\begin{bmatrix} x \\ y \\ z \end{bmatrix} = \begin{bmatrix} cos(\theta_1) \cdot cos(\theta_2) \cdot l_1 \\ sin(\theta_1) \cdot cos(\theta_2) \cdot l_1 \\ sin(\theta_2) \cdot l_1 \end{bmatrix},$$

where l_1 denotes the length of limb 1. Let S_i denote $sin(\theta_i)$ and C_i denote $cos(\theta_i)$. Now

$$\begin{bmatrix} \dot{x} \\ \dot{y} \\ \dot{z} \end{bmatrix} = \begin{bmatrix} (-S_1 C_2 \dot{\theta}_1 - C_1 S_2 \dot{\theta}_2) \cdot l_1 \\ (C_1 C_2 \dot{\theta}_1 - S_1 S_2 \dot{\theta}_2) \cdot l_1 \\ C_2 \dot{\theta}_2 l_1 \end{bmatrix} \tag{B.2}$$

$$v_1^2 = \dot{x}^2 + \dot{y}^2 + \dot{z}^2 \tag{B.3}$$

$$= l_1^2 \cdot (C_2^2 \dot{\theta}_1^2 + \dot{\theta}_2^2) \tag{B.4}$$

Now the kinetic energy E_{kin} for mass m_1 equals :

$$E_{kin} = \frac{1}{2} \cdot m_1 \cdot v_1^2 \tag{B.5}$$

$$= \frac{1}{2} \cdot m_1 \cdot l_1^2 \cdot (C_2^2 \dot{\theta}_1^2 + \dot{\theta}_2^2) \tag{B.6}$$

In Model 2 the certripetal and coriolis forces are neglected. This means that the term $\frac{\delta E_{kin}}{\delta \theta_i}$ in Equation B.1 can be neglected, and that in the evaluation of the term $\frac{d}{dt}(\frac{\delta E_{kin}}{\delta \theta_i})$ only the

terms with $\ddot{\theta}_i$ need to be evaluated. Then the inertia matrix D can be derived :

$$
\begin{aligned}
D(1,1) &= m_1 l_1^2 C_2^2 + (C_{23}l_2 + C_2 l_1)^2 \cdot (m_2 + m_3) + 2m_3 \cdot (C_{23}l_2 + C_2 l_1) \cdot S_5 C_{234} l_3 + \\
&\quad m_3 l_3^2 \cdot (C_5^2 + S_5^2 C_{234}^2) \\
D(1,2) &= -m_3 l_3^2 C_5 S_5 S_{234} - m_3 l_1 l_3 S_2 C_5 - m_3 l_2 l_3 S_{23} C_5 \\
D(1,3) &= -m_3 l_3^2 C_5 S_5 S_{234} - m_3 l_2 l_3 S_{23} C_5 \\
D(1,4) &= -m_3 l_3^2 C_5 S_5 S_{234} \\
D(1,5) &= m_3 l_3^2 C_{234} + m_3 l_3 S_5 \cdot (C_{23}l_2 + C_2 l_1) \\
D(1,6) &= 0 \\
D(2,2) &= (m_1 + m_2 + m_3) \cdot l_1^2 + m_2 l_2^2 + m_3 l_2^2 + m_3 l_3^2 S_5^2 + 2m_2 l_1 l_2 C_3 + 2m_3 l_1 l_2 C_3 + \\
&\quad 2m_3 l_1 l_3 S_5 C_{34} + 2m_3 l_2 l_3 S_5 C_4 \\
D(2,3) &= m_2 l_2^2 + m_3 l_2^2 + m_3 l_3^2 S_5^2 m_2 l_1 l_2 C_3 + m_3 l_1 l_2 C_3 + m_3 l_1 l_3 S_5 C_{34} + \\
&\quad 2m_3 l_2 l_3 S_5 C_4 \\
D(2,4) &= m_3 l_3^2 S_5^2 + m_3 l_1 l_3 S_5 C_{34} + m_3 l_2 l_3 S_5 C_4 \\
D(2,5) &= m_3 l_1 l_3 C_5 S_{34} + m_3 l_2 l_3 C_5 S_4 \\
D(2,6) &= 0 \\
D(3,3) &= (m_2 + m_3) \cdot l_2^2 + m_3 l_3^2 S_5^2 + 2m_3 l_2 l_3 S_5 C_4 \\
D(3,4) &= m_3 l_3^2 S_5^2 + m_3 l_2 l_3 S_5 C_4 \\
D(3,5) &= m_3 l_2 l_3 C_5 S_4 \\
D(3,6) &= 0 \\
D(4,4) &= m_3 l_3^2 S_5^2 \\
D(4,5) &= 0 \\
D(4,6) &= 0 \\
D(5,5) &= m_3 l_3^2 \\
D(5,6) &= 0 \\
D(6,6) &= \frac{1}{12} \cdot m_3 \cdot (length^2 + width^2)
\end{aligned}
$$

Note that an inertia matrix is symmetric, so this completes the calculation.

Appendix C

Calculation stopping configuration

The display of the stopping configuration means that it is shown where, or in what configuration, the manipulator will stop, assuming that all rate setpoints are "now" set to zero.

When all End–Effector rate setpoints are set to zero, then all joint rate setpoints $\dot{\theta}_s$ will be zero, independent of the value of the jacobian.

The torques, or in the case of model 1 the accelerations, are almost always scaled, because of the relative large value of the gain of the proportional controller. Suppose that F is the scaling factor. Now it holds that

$$\ddot{\theta}(t) = F(t) \cdot K \cdot (\dot{\theta}_s(t) - \dot{\theta}(t)),$$

where K is the gain of the proportional controller. Because $\dot{\theta}_s$ is the zero vector, the acceleration vector has the opposite direction as the vector of joint rates. In this way the direction of the joint velocity vector remains the same, only the magnitude decreases. It is always the same joint that determines the scaling factor. This implies that all joint rates will become zero at the same moment t_e (Fig. C.1). Note that the product $F(t) \cdot (\dot{\theta}_s(t) - \dot{\theta}(t))$ is the same for almost every t. Only in the very end, when $\dot{\theta} \approx \dot{\theta}_s$ it is not true. However, this effect in the last phase is neglectible. From Fig. C.2 the following can be derived :

$$\ddot{\theta} = \tan(\alpha) = \dot{\theta}_0/t_e \;\Rightarrow\; t_e = \dot{\theta}_0/\ddot{\theta}$$

The joint angles θ increase in t_e seconds with $0.5 \cdot \dot{\theta}_0 \cdot t_e$, which is the surface of the shaded area. So

$$\theta_e = \theta_0 + 0.5 \cdot \frac{\dot{\theta}_0^2}{\ddot{\theta}}$$

The configuration in which the manipulator will stop is derived from the kinematic equations.

162
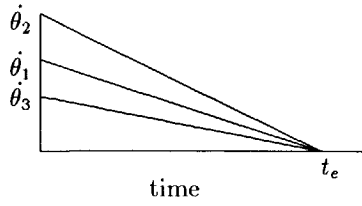
Figure C.1: *All joints velocities become zero at the same time t_e.*
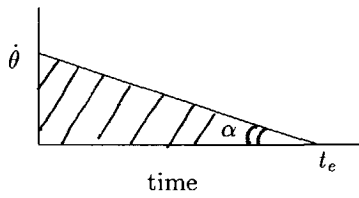
Figure C.2: *Definition of α.*

Appendix D

Calculation prediction over time horizon

In this calculation it is assumed that the End–Effector rate commands remain the same during the time–horizon over which the prediction is made.

First of all, given the End–Effector rate commands, the joint rate setpoints are calculated. The torques, or in the case of model 1 the accelerations, are almost always scaled, because of the relatively large value of K, the gain of the proportional controller. So the evolution of the joint velocities is shown in Fig. D.1 (see also Appendix C). T_1 is defined as the time instant when the required joint velocities are obtained. This is the same time instant for all joints, because of the scaling of the torques.

Suppose $t_0 = 0$ and the prediction horizon is T_{pred}. Then two situations can be distinguished:

1. $T_{pred} \leq t_1$

2. $T_{pred} > t_1$

So, the algorithm becomes :

1. calculate inertia matrix D (Appendix B)
2. calculate joint torques T : $T = K \cdot (\dot{\theta}_s - \dot{\theta})$
   where $K = K_1 \cdot D(\theta)$ in the case of Model 2.
3. calculate scaling factor F for the joint torque vector T
4. $\ddot{\theta} = F \cdot gain \cdot (\dot{\theta}_s - \dot{\theta})$
5. calculate t_1 : $t_1 = (\dot{\theta}_s - \dot{\theta}_0)/\ddot{\theta}$
6. calculate the joint angle values at time T_{pred} :
   IF $T_{pred} \leq t_1$ THEN
   $\quad\quad \theta(T_{pred}) = \theta_0 + \dot{\theta}_0 \cdot T_{pred} + 0.5 \cdot \ddot{\theta} \cdot T_{pred}^2$
   ELSEIF $T_{pred} > t_1$ THEN

$$\theta(t_1) = \theta_0 + \dot{\theta}_0 \cdot t_1 + 0.5 \cdot \ddot{\theta} \cdot t_1^2$$
$$\theta(T_{pred}) = \theta(t_1) + \dot{\theta}_s \cdot (T_{pred} - t_1)$$
ENDIF

7. via the kinematics the configuration of the manipulator can be calculated at time T_{pred}

The joint setpoints are not constant during the prediction time interval, because the jacobian depends on the joint angle values. The question is of course how this fact influences the accuracy of the prediction. In [de Roode, 1988] can be seen that small angle changes have not a large influence on the inverse jacobian. However in our implementation the maximum change in the joint angle values can be specified and in the procedure described above, the joint setpoints are adjusted a number of times, depending on the maximum change in joint angle values.
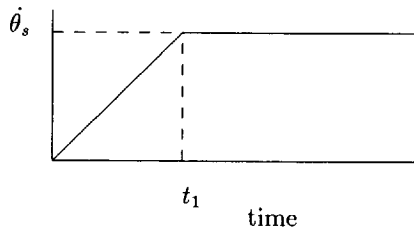
Figure D.1: *Evolution joint velocity.*

Appendix E

Tables Chapter 7

Table E.1: *Significance levels for a smaller completion time with a predictive display compared to the plain situation; 3D; slow situation.*

subject	display	torque factor			
		1	2	3	4
2	stop	0.004	–	–	–
N=12	pred	0.002	–	–	–
3	stop	0.01	–	–	–
N=12	pred	–	–	–	0.008
5	stop	0.002	0.09	–	–
N=12	pred	0.002	0.02	0.004	0.05
7	stop	0.03	–	–	–
N=12	pred	–	–	0.08	–
all	stop	0 (42)	0.04 (31)	– (29)	0.01 (33)
N=48	pred	0 (40)	– (29)	0.006 (34)	0.002 (35)

Table E.2: *Completion times (sec.); 3D situation.*

torque	fast situation				slow situation			
factor		kind of display				kind of display		
	subj	plain	stop	pred	subj	plain	stop	pred
1	2	74.5	67.4	71.7	2	201.9	146.4	145.3
2		57.2	57.3	59.4		116.6	111.9	113.8
3		54.8	54.7	55.3		110.7	106.0	111.7
4		56.2	55.4	55.3		107.7	106.0	100.8
1	4	66.7	63.7	71.0	3	154.9	128.0	138.7
2		61.4	60.6	64.0		111.8	102.4	112.9
3		59.6	55.8	60.8		103.1	99.5	101.4
4		54.8	55.3	63.2		104.3	99.2	92.7
1	6	93.7	84.5	91.6	5	131.9	110.8	101.3
2		77.6	72.4	76.9		99.1	91.4	90.2
3		69.8	70.6	77.9		99.0	90.6	86.6
4		69.8	70.2	68.5		94.9	88.3	85.5
1	8	67.9	65.0	74.8	7	120.3	108.5	117.9
2		60.5	61.3	71.4		96.6	96.6	93.1
3		65.0	60.7	63.2		89.7	86.5	85.7
4		61.2	60.6	65.3		87.3	90.4	87.8

Table E.3: *Significance levels of less energy consumption; 3D situation.*

fast situation					
		torque factor			
subject	comparison	1	2	3	4
2	pred < plain	0.06	0.03	–	0.03
N=12	pred < stop	–	0.02	–	0.10
4	pred < plain	0.07	–	–	–
N=12	pred < stop	–	–	–	0.006
6	pred < plain	–	–	–	–
N=12	pred < stop	–	–	–	–
8	pred < plain	0.06	0.005	0.004	0.003
N=12	pred < stop	0.03	0.008	0.005	0.004
all	pred < plain	0.03 (32)	0.01 (33)	0.006 (34)	0.002 (35)
N=48	pred < stop	– (30)	0.006 (34)	– (30)	0.0003 (37)
slow situation					
		torque factor			
subject	comparison	1	2	3	4
2	stop < plain	0.005	–	–	–
N=12	pred < plain	0.002	0.007	0.004	0.002
	pred < stop	0.05	–	0.01	0.005
3	stop < plain	0.06	0.05	–	–
N=12	pred < plain	0.03	0.02	–	0.02
	pred < stop	–	–	–	0.02
5	stop < plain	–	–	0.04	–
N=12	pred < plain	0.005	0.002	0.002	0.003
	pred < stop	0.003	0.006	0.004	0.003
7	stop < plain	0.01	–	0.003	–
N=12	pred < plain	0.002	0.008	0.004	0.004
	pred < stop	–	0.05	0.02	0.006
all	stop < plain	0.002 (35)	0.06 (31)	0.0003 (37)	– (29)
N=48	pred < plain	0 (43)	0 (39)	0 (41)	0 (43)
	pred < stop	0.006 (34)	0.002 (35)	0.0001 (38)	0 (41)

Table E.4: *Correlation coefficients between the completion times and the energy used; 3D situation. A "–" means that the correlation coefficient is less than 0.60.*

torque factor	fast situation				slow situation			
		kind of display				kind of display		
	subj	plain	stop	pred	subj	plain	stop	pred
1	2	0.88	0.87	0.85	2	0.97	0.98	0.97
2		0.71	0.69	0.66		0.91	0.92	0.88
3		0.61	0.65	–		0.87	0.89	0.83
4		–	–	–		0.90	0.84	0.88
1	4	0.87	0.92	0.78	3	0.94	0.94	0.95
2		0.79	0.89	0.90		0.93	0.97	0.80
3		–	0.80	0.82		0.95	0.96	0.89
4		0.61	0.71	0.84		0.85	0.93	0.84
1	6	0.76	–	0.83	5	0.98	0.97	0.89
2		–	–	0.60		0.93	0.87	0.72
3		–	–	0.65		0.83	–	0.71
4		0.69	–	0.73		0.79	0.82	0.60
1	8	0.98	0.90	0.88	7	0.94	0.88	0.88
2		0.89	–	0.75		0.92	0.85	0.72
3		0.61	–	0.76		0.85	0.72	0.64
4		–	–	–		0.78	0.62	–

Table E.5: *Significance levels of less energy consumption per second when the predicted trajectory is displayed; 3D situation.*

fast situation					
		torque factor			
subject	display	1	2	3	4
2	plain	0.05	0.02	0.08	–
N=12	stop	0.08	0.002	–	–
4	plain	0.06	–	0.04	0.02
N=12	stop	0.02	–	0.02	0.005
6	plain	–	–	0.10	–
N=12	stop	–	–	–	–
8	plain	0.002	0.002	0.02	0.002
N=12	stop	0.006	0.002	0.005	0.002
all	plain	0.0009 (36)	0.0009 (36)	0.0001 (38)	0.0003 (37)
N=48	stop	0.0009 (36)	0.0 (41)	0.0003 (37)	0.0001 (38)
slow situation					
		torque factor			
subject	display	1	2	3	4
2	plain	0.03	0.008	0.005	0.01
N=12	stop	0.004	0.03	0.002	0.04
3	plain	0.07	0.002	–	0.06
N=12	stop	0.03	0.02	–	0.02
5	plain	0.10	0.002	0.002	0.004
N=12	stop	0.005	0.01	0.006	0.003
7	plain	0.002	0.01	0.005	0.002
N=12	stop	0.05	0.10	0.02	0.01
all	plain	0.0009 (36)	0 (44)	0 (42)	0 (42)
N=48	stop	0 (39)	0.0009 (36)	0.0001 (38)	0 (40)

Table E.6: *Significance levels of less commands when the predicted trajectory is displayed; 3D; slow situation.*

subject	display	torque factor 1	2	3	4
2	plain	0.08	–	0.02	0.004
	stop	–	0.05	–	0.04
3	plain	–	0.05	0.08	0.03
	stop	–	–	0.03	0.01
5	plain	0.002	0.002	0.005	0.005
	stop	0.002	0.005	0.006	0.005
7	plain	0.02	0.005	0.01	0.004
	stop	–	0.02	0.01	0.04
all	plain	0.0005 (36)	0 (39)	0.0001 (37)	0 (43)
	stop	0.009 (33)	0.001 (35)	0 (37)	0.0007 (35)

Table E.7: *Significance levels of less commands per second when the predicted trajectory is displayed; 3D.*

fast situation					
subject	display	torque factor 1	2	3	4
all	plain	– (30)	0.002 (35)	– (26)	0.01 (33)
N=48	stop	0.0009 (36)	0.0003 (37)	0.03 (32)	0.002 (35)
slow situation					
subject	display	torque factor 1	2	3	4
2	plain	–	0.10	0.05	0.006
N=12	stop	–	0.02	0.08	0.04
3	plain	–	0.006	0.10	0.07
N=12	stop	0.10	0.03	0.01	0.01
5	plain	0.07	0.002	0.02	0.003
N=12	stop	0.002	0.004	0.004	0.008
7	plain	0.02	0.002	0.02	0.005
N=12	stop	0.03	0.01	0.01	0.03
all	plain	0.11 (30)	0 (42)	0 (39)	0 (40)
N=48	stop	0.0001 (38)	0 (39)	0.0001 (38)	0.0001 (38)

Table E.8: *Correlation coefficients between the number of issued commands and the energy used; 3D situation.*

torque factor	fast situation				slow situation			
		kind of display				kind of display		
	subj	plain	stop	pred	subj	plain	stop	pred
1	2	0.87	0.84	0.68	2	0.73	0.64	0.80
2		0.71	0.85	0.84		0.82	0.90	0.75
3		0.91	0.86	0.80		0.88	0.82	0.76
4		0.89	0.83	0.79		0.94	–	0.87
1	4	0.79	0.90	0.87	3	0.73	0.77	0.77
2		0.75	0.62	0.89		0.86	0.83	0.77
3		–	0.80	0.82		0.68	–	0.83
4		0.90	0.62	0.93		0.72	0.87	0.85
1	6	0.90	0.77	0.84	5	0.72	0.71	0.78
2		0.96	0.72	0.90		–	0.79	0.80
3		–	0.96	0.92		0.62	0.76	0.78
4		0.84	0.87	0.75		0.67	–	0.72
1	8	0.64	0.85	–	7	–	–	–
2		0.78	0.78	0.78		–	0.75	–
3		0.84	0.77	0.78		0.74	0.82	0.79
4		0.67	0.87	0.62		–	–	0.68
1	all	0.78	0.81	0.68	all	–	–	0.71
2		0.81	0.73	0.83		0.65	0.75	0.79
3		0.80	0.85	0.84		0.74	0.77	0.68
4		0.80	0.81	0.80		0.78	0.81	0.87

Summary

Currently the European spacecraft called Hermes, and a space manipulator, the Hermes
Robot Arm (HERA), are being developed. The manipulator will be used for executing tasks
like grasping and moving objects and as a support for extravehicular activities. Although
normally HERA will be controlled under supervisory control, a requirement is that under
all circumstances a human operator must be able to control the manipulator manually.
Our research concerned the design of a Man–Machine Interface for a space manipulator.
The design criteria concerned the safe and economical use of the manipulator. To obtain
realistic characteristics of a space manipulator in this study, the specifications of HERA
were used.
This research deals with the manual control situation. When a human operator has to con-
trol a space manipulator like HERA manually, he is faced with several difficulties. Three
problems were investigated: the lack of direct vision, the control of up to 6 degrees–of–
freedom (DOF), and the influence of the non-linear and slow dynamics.

It was investigated how graphical displays can be used to provide the operator with a good
three–dimensional perception. A task was chosen where global views of the scene have to
be used. The advantage of graphical displays is that they can provide views from any point,
provided a model of the environment is available.
The results showed that the presence of reference lines enhanced the three–dimensional
perception, which resulted in a tendency towards a safer task execution. A split–screen
facility for displaying two available survey views does not seem a very necessary one.

The problem of controlling 6 DOF is most restricting for a task where a large accuracy is
required, such as an insert–task, or a peg–in–hole task. Generally an insert–task has to be
excuted in the End–Effector control mode. The End–Effector frame functions as reference
frame, and the tip of the End–Effector or payload as Point–of–Resolution (POR). When
using the End–Effector frame as reference frame, the direction of a translation depends on
the orientation of the End–Effector. This might cause inefficient and unsafe situations. A
possible solution which was investigated, is the use of the target frame as the reference
frame. Referencing the operator's commands to the target frame, instead of to the End–
Effector frame did not improve the human operator's control performance. The operator
controlled the orientation first. In that way the difference between the two reference frames
disappeared, before translation commands were issued.
Using proximity information, closed-loop control schemes can be designed, which reduce

the number of DOF to be controlled by the human operator. The reduction of the number of DOF to be controlled by an operator from 6 to 2 led to a more efficient task execution. The 2DOF mode was judged by the subjects to be easier than both End–Effector modes.

The motor torques limitations of HERA are such that a space manipulator can be considered as a slowly responding system. The use of two kinds of predictive display were evaluated at our laboratory : a display of the stopping configuration and a display of a predicted trajectory. The displays were evaluated for a rough positioning task in the presence of obstacles.
The display of the stopping configuration did lead to a faster task execution when the time needed to stop the manipulator was larger than 6 seconds, or when the stopping distance was larger than 0.3 meter. The display of the predicted trajectory always did lead to less energy consumption, due to a more calm control behaviour of the subjects.
The results showed that in an unknown environment the combined problems of the three-dimensional perception and the control of 5 DOF are more serious than the problems due to the slow and non-linear dynamics.

An important issue when displaying a predicted trajectory is how to choose the length of the time–horizon over which the prediction has to be calculated. The most effective length will depend on the system dynamics, the task to be executed and the disturbances acting on the system. Experiments with subjects can be performed to investigate this issue, but these experiments will be very time–consuming. Therefore, a first investigation was performed to find out whether predictive control theory can be used to investigate the most effective length of the time–horizon. Herefore, two kinds of experiments were performed: one in which a human acts as a controller, and another in which the control is performed by a predictive controller. The results indicate that predictive control theory can serve as a means to describe human control behaviour. To enable the operator to take every possible turn safely, the prediction horizon must be equal to at least half of the maximum stopping time at each time–instant.

Future research directions are the supervisory control situation, the design of a predictive display to let the operator cope with the time–delays, and the effects of flexibility on the performance and behaviour of an operator.

Samenvatting

Momenteel worden het Europees ruimteveer Hermes, met een bijbehorende ruimtemanipulator, de Hermes Robot Arm (HERA), ontwikkeld. Met behulp van de manipulator zullen taken als het pakken en verplaatsen van objecten worden uitgevoerd, en de manipulator zal een astronaut ondersteunen bij het uitvoeren van activiteiten buiten het ruimteschip. Alhoewel onder normale omstandigheden HERA m.b.v. een supervisie regeling bestuurd zal worden, ligt er een eis dat de arm onder alle omstandigheden ook met de hand bestuurd moet kunnen worden.

Ons onderzoek betreft het ontwerp van een Mens–Machine Interface (MMI) voor een ruimtemanipulator. Ontwerpcriteria zijn het veilige en het economische gebruik van de manipulator. Om realistisch karakteristieken van een ruimtemanipulator te verkrijgen in dit onderzoek, worden de specificaties van HERA gebruikt.

In dit onderzoek wordt de situatie beschouwd waarin een mens de manipulator met de hand moet besturen. In een dergelijke taak, wordt de mens geconfronteerd met verschillende moeilijkheden. Drie probleemgebieden zijn onderzocht: het ontbreken van direkt zicht, het regelen van een groot aantal (maximaal zes) vrijheidsgraden, en de invloed op de bestuurbaarheid van de niet–lineaire en trage dynamica.

Er is onderzocht hoe presentaties op een grafisch beeldscherm het beste gebruikt kunnen worden om de mens te voorzien van een goede drie–dimensionale perceptie. Hierbij is een taak gekozen waarin overzichtsbeelden van de situatie gebruikt dienen te worden. Het voordeel van het gebruik van grafische beeldschermen is dat vanuit elk gezichtspunt een beeld gegenereerd kan worden, mits een model van de omgeving beschikbaar is. De resultaten tonen aan dat het gebruik van zogenaamde referentielijnen de drie–dimensionale perceptie verbetert, wat resulteerde in een snellere en veiliger taakuitvoering. De mogelijkheid om op 1 scherm twee beschikbare overzichtsbeelden, vanuit verschillende aanzichtspunten, tegelijk te presenteren leek niet zo noodzakelijk.

Het probleem om 6 vrijheidsgraden te besturen speelt het meest in een situatie waarin een grote nauwkeurigheid vereist is, zoals in het geval van een zgn. "insert" taak. In het algemeen wordt een insert taak uitgevoerd in de End–Effector control mode. Het End–Effector assenstelsel fungeert als referentie en de tip van de End–Effector is het te besturen punt. Als het End–Effector assenstelsel als referentie gebruikt wordt, dan hangt de richting van een translatie af van de orientatie van de End–Effector. Dit kan leiden tot inefficientie en onveilige situaties. Een mogelijke oplossing is onderzocht, waarbij het assenstelsel van het

175

doel, ofwel het gat, als referentie wordt gebruikt. Dit leidde niet tot een verbetering in de regelprestatie van de mens. Hij regelde eerst de orientatie. Op deze manier verdween echter het verschil tussen de twee assenstelsels voordat translatie commando's gegeven werden.
Door gebruik te maken van nabijheids–informatie kunnen regelalgoritmen ontworpen worden zodanig dat het aantal door de mens te besturen vrijheidsgraden gereduceerd wordt. De reductie van het aantal door de mens te regelen vrijheidsgraden van 6 naar 2 leidde tot een efficientere taakuitvoering. De proefpersonen vonden tevens de situatie waarin ze maar 2 vrijheidsgraden hoefden te besturen veel gemakkelijker.

De koppels die door de motoren van HERA geleverd kunnen worden zijn dusdanig beperkt dat een ruimtemanipulator als een traag reagerend systeem beschouwd kan worden. Het tonen van twee soorten voorspellingen is onderzocht in ons laboratorium: het tonen van de stopconfiguratie, en het tonen van een voorspelde baan. Dit werd geevalueerd voor een grove positioneer taak, terwijl er obstakels in de omgeving aanwezig waren.
Het tonen van de stopconfiguratie leidde tot een snellere taakuitvoering als de stoptijd van de manipulator groter was dan 6 seconden, of als de stopafstand groter was dan 0.3 meter. Het tonen van de voorspelde baan leidde altijd tot een gunstiger energieverbruik, door het rustiger regelgedrag van de proefpersonen.
De resultaten toonden aan dat in een onbekende omgeving het gekombineerde probleem van de drie–dimensionale perceptie en het regelen van 5 vrijheidsgraden groter is dan de problemen die de mens ondervindt vanwege de trage en niet–lineaire dynamica.
Een belangrijk punt bij het tonen van de voorspelde baan is de keuze van de tijd waarover de voorspelling berekend dient te worden. Wat de beste waarde is zal afhangen van de systeem dynamica, de uit te voeren taak en de verstoringen die op het systeem inwerken. Om dit te onderzoeken kunnen er experimenten met proefpersonen worden gedaan, maar die experimenten zullen zeer tijdrovend zijn. Daarom is een eerste studie uitgevoerd om te onderzoeken of voorspellende regeltheorie gebruikt kan worden om de beste waarde voor de voorspellings (tijd) horizon te bepalen. In dit kader zijn er twee experimenten uitgevoerd: één waarin de mens als regelaar optreedt, en één waarin de manipulator bestuurd wordt d.m.v. een voorspellend regelalgoritme. De resultaten geven aan dat voorspellende regeltheorie gebruikt kan worden om het menselijk regelgedrag te beschrijven. Om de mens in staat te stellen elke mogelijke bocht veilig te laten nemen, moet de voorspellings horizon tenminste gelijk zijn aan de helft van de maximale stoptijd op elk ogenblik.

Toekomstig onderzoek dient verricht te worden m.b.t. de supervisie regeling, het ontwerp van een "predictive display" om problemen door tijdvertragingen te ondervangen, en het effect dat de flexibiliteit van de arm zal hebben op de regelprestatie en het gedrag van een menselijke regelaar.

Curriculum Vitae

31 augustus 1962	geboren te Groningen
1974 – 1980	VWO – Ath. B R.S.G. Kamerlingh Onnes te Groningen
1980 – 1986	studie wiskunde aan de Rijks Universiteit Groningen afstudeerrichting : systeemtheorie Het afstudeeronderzoek betrof het modelleren van oneindige tijdreeksen. bijvakken : informatica, differentiaal vergelijkingen
oktober 1986	afgestudeerd bij prof.dr.ir. J.C. Willems
1986 – 1990	Laboratorium voor Meet– en Regeltechniek Faculteit der Werktuigbouwkunde en Maritieme Techniek TU Delft promotieonderzoek m.b.t. mens–machine aspecten van op afstand bestuurde ruimtemanipulatoren promotoren: prof.dr.ir. H.G. Stassen en dr.ir. A. van Lunteren
1991 – heden	Nationaal Lucht– en Ruimtevaartlaboratorium hoofdafdeling Informatica afdeling Wiskundige Modellen en Methoden